

**Exploration of new bioactive
compounds produced by bacteria in
pathogenic lineages**

Toyama Prefectural University

Dandan Li

Feb. 22

CHAPTER 1 Introduction	0
1-1 Background	1
1-2 Natural products as a major source of available drugs.....	1
1-3 Source exploration of natural products.....	3
1-3-1 <i>Burkholderia</i> as a source of natural products.....	6
1-3-2 <i>Vibrio</i> as a source of natural products	8
1-3-3 The objective of this thesis	8
CHAPTER 2 Two new 2-alkylquinolones, inhibitory to the fish skin ulcer pathogen <i>Tenacibaculum maritimum</i>, produced by a rhizobacterium of the genus <i>Burkholderia</i> sp.	13
2-1 Background	14
2-2 Results and Discussion.....	16
2-2-1 Fermentation and isolation	16
2-2-2 Structure Determination.....	16
2-2-3 Bioactivity	19
2-3 Conclusion	20
2-4 Experimental.....	21
2-4-1 General experimental procedures	21
2-4-2 Collection of <i>Burkholderia</i> strains and broth screening	21
2-4-3 Fermentation, extraction, and isolation	21
2-4-4 Evaluation of antimicrobial activity	23
2-5 Spectral data	27
CHAPTER 3 4-Hydroxy-3-methyl-2(1<i>H</i>)-quinolone, originally discovered from a <i>Brassicaceae</i> plant, produced by a soil bacterium of the genus <i>Burkholderia</i> sp.: determination of a preferred tautomer and antioxidant activity	38
3-1 Background	39
3-2 Results and Discussion.....	41
3-2-1 Fermentation and isolation	41
3-2-2 Structure Determination.....	41
3-2-3 Synthesis of 9.....	43
3-2-4 Bioactivity	45
3-3 Conclusion	46
3-4 Experimental.....	47
3-4-1 General experimental procedures	47
3-4-2 Microorganism.....	47
3-4-3 Fermentation and isolation	48
3-4-4 Evaluation of Fe ³⁺ binding activity.....	48
3-4-5 Antibacterial assay	49
3-5 Spectral data	53
CHAPTER 4 Three new <i>O</i>-isocrotonyl-3-hydroxybutyric acid congeners produced by a sea anemone-derived marine bacterium of the genus	

Vibrio	74
4-1 Background	75
4-2 Results and Discussion.....	77
4-2-1 Fermentation and isolation	77
4-2-2 Structure Determination.....	77
4-2-3 Absolute Configuration	80
4-4 Experimental.....	82
4-3 Conclusion.....	82
4-4-1 General experimental procedures	83
4-4-2 Biological material	83
4-4-3 Fermentation and isolation of 19-22	83
4-4-4 Preparation of (<i>S</i>)- and (<i>R</i>)-Phenylglycine Methyl Ester Amides	85
4-4-5 Antibacterial Assay	86
4-4-6 Cytotoxicity Assay	86
4-5 Spectral data	90
CHAPTER 5 Conclusion	127
Acknowledgements	132
Publication List	133

CHAPTER 1

Introduction

1-1 Background

Increased longevity is a significant symbol of human progress. The life expectancy had been extended 24 years from the year 1950 to the year 2017 [1]. Some countries have projects to exceed life expectancy over 85 and large numbers of people are now living into their ninth decades [2]. These advances reflect the decline of disease mortality. However, the world continues to face the challenges from diseases such as bacterial infectious diseases, allergy, and lifestyle diseases based on the day to day habits of people [3-5]. According to the WHO, more than 10 million people for each year die from lifestyle diseases caused by smoking of tobacco, alcohol use, or a simple lack of physical activity and cholera caused by bacterium *V. cholerae* killed tens of millions of people in the last seven outbreaks [6, 7]. In addition, allergy such as allergic rhinitis, food allergy, atopic dermatitis, and asthma have always given a serious damage on our life.

1-2 Natural products as a major source of available drugs

Natural products have been studied as medicines for hundreds of years in our history. On account of the fact of excellent pharmacological activity and good biocompatibility of natural products, over 30% clinical drugs come from natural products [8]. Although the synthetic drugs take a quite large proportion in clinical therapy, the inspirational sources of many of them almost came from structure diversities and various biological activities of natural products.

Natural products, especially those from microorganisms, have served as a rich and indispensable resource of medicines. Penicillin G (Figure 1-1), the first antibiotic, isolated from a fungus *Penicillium* in the middle of the 19th century, dramatically improved the prognosis of infectious diseases. It is well known that penicillin has saved millions of lives in World War II. Subsequent researches showed that penicillin

contained a characteristic four-membered β -lactam ring and this ring can be used to inhibit the formation of new cell wall. This is the reason why penicillin kills pathogenic bacteria. The application of penicillin has effectively controlled a number of bacterial infectious diseases such as pneumonia, syphilis, cellulitis and so on.

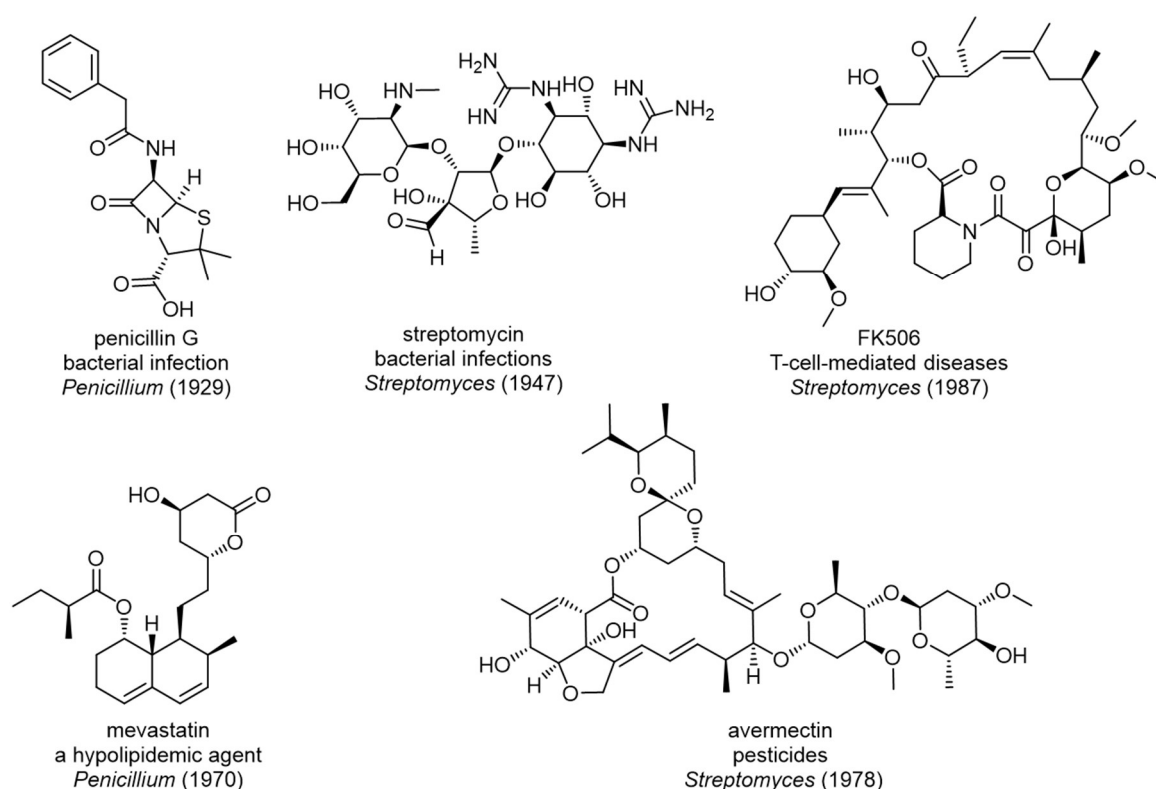


Figure 1-1. Microbial metabolites used as clinical medicines or drug leads.

Streptomycin, discovered from *Streptomyces*, is the first antibiotic to treat tuberculosis, which at that time was a thought as deadly illness. Because the benefit brought by these two antibiotics were so huge, Fleming and Waksman, the discoverers of these antibiotics, received Nobel Prizes. In addition to these, a hypolipidemic agent mevastatin, an immunosuppressant FK506, and anthelmintic avermectin all provided new remedies, which were not available before these drugs were discovered.

The implementation of NMR, high performance liquid chromatography, and mass spectrometry in the mid-1980s at natural product chemistry research accelerated the

discovery of new natural products (Figure 1-2) [9]. However, in contrast to this, the number of novel natural products, as judged by Tanimoto similarity scores, are declining year by year. In addition, no antibiotics based on natural products with novel molecular skeletons were approved over the near 30 years. To our disappointment, new antibiotics that have recently entered the market, such as daptomycin and ticacumicin B1, have their discovery origins back in the 1980s [9].

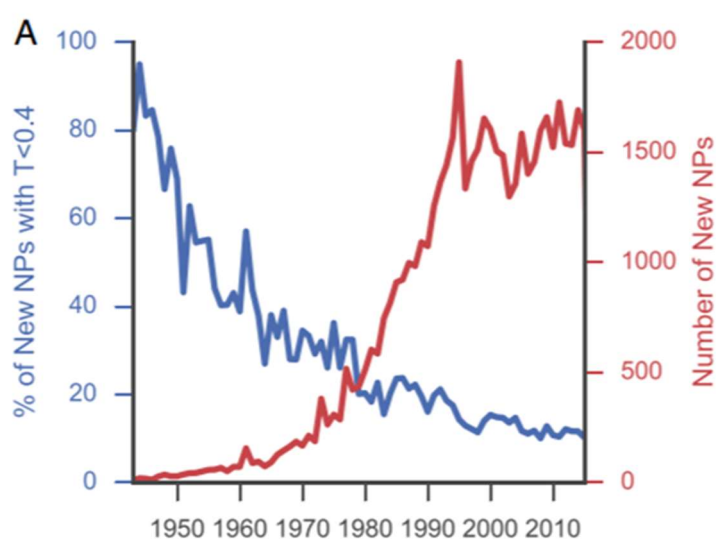


Figure 1-2. The relative data about the number of new compound isolation (red line) and the rate of novel compound isolation (blue line) were relisted.

The decline in the ratio of discovering new molecular scaffolds is mainly because the major traditional sources, fungi and actinomycetes, have been exploited so extensive that the room for discovering molecules with new skeletons becomes quite limited. Thus, to address this problem, exploring new resource would be a necessary option to be taken.

1-3 Source exploration of natural products

Because so many species are present in the domain Bacteria and Fungi, selection

of the taxa should directly determine the output of natural product discovery. Exploring those closely related to the already proven taxa is a conceivable choice, which has especially been often attempted in plant product research [10]. For example, the plants of producing alkaloids, terpenoids, sinapyl alcohols, and sinapyl alcohol derivatives were rather continuous at the morphological characteristics [10].

Another choice is to find taxa which are phylogenetically distant but have similar life history. So far, nearly three-quarters of the total antibiotics have been isolated from actinomycetes and fungi [11]. There are many traits that are common to the both groups, such as energy metabolism, filamentous growth, spore formation, ability to degrading persistent plant-derived biopolymers, etc. these traits are shared by bacteria of the class *Ktedonobacteria* within phylum *Chloroflexi*, and several new natural products were reported from this group [12].

Another important trait is the high incidence of pathogenic and symbiotic species in these microbes. For example, potato scab, a common and disfiguring disease of potato tubers that affect potatoes and other root vegetables, are caused by actinomycetes of the genus the *Streptomyces*. Green mold, a noxious postharvest disease of citrus, was caused by *Penicillium digitatum* within the kingdom *Fungi*. Furthermore, many of them also play important roles in nature as symbionts like ant symbiotic actinobacteria *Pseudonocardia*, which protected the ants' fungal garden and plant root symbiotic fungus *Arbuscular mycorrhiza*, which enhanced host plant acquisition of mineral nutrients, as shown in Figure 1-3.

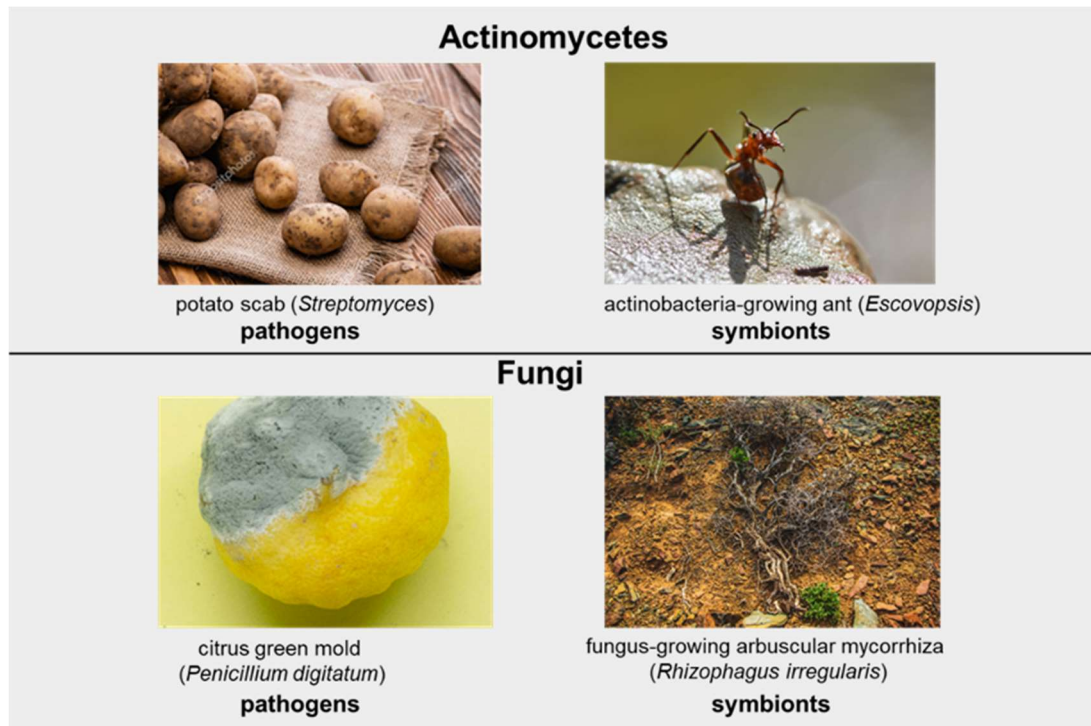


Figure 1-3. The pathogenicity and symbiotic life forms shared by actinomycetes and fungi.

Recent studies have shown that these relationships are maintained through the production of low-molecular weight compounds (Figure 1-4). For example, thaxtomin A, produced by the potato pathogen *Streptomyces* spp., showed a positive correlation between their pathogenicity and thaxtomin production. Tryptoquialanine A, isolated from the pathogen of citrus fruits *Penicillium digitatum*, was shown to completely inhibit the citrus seed germination. Dentigerumycin, a bacterial mediator, and lipochitoooligosaccharide, a symbiotic signal, were produced by the symbiotic actinobacteria *Pseudonocardia* and symbiotic fungus *Arbuscular mycorrhiza*, respectively.

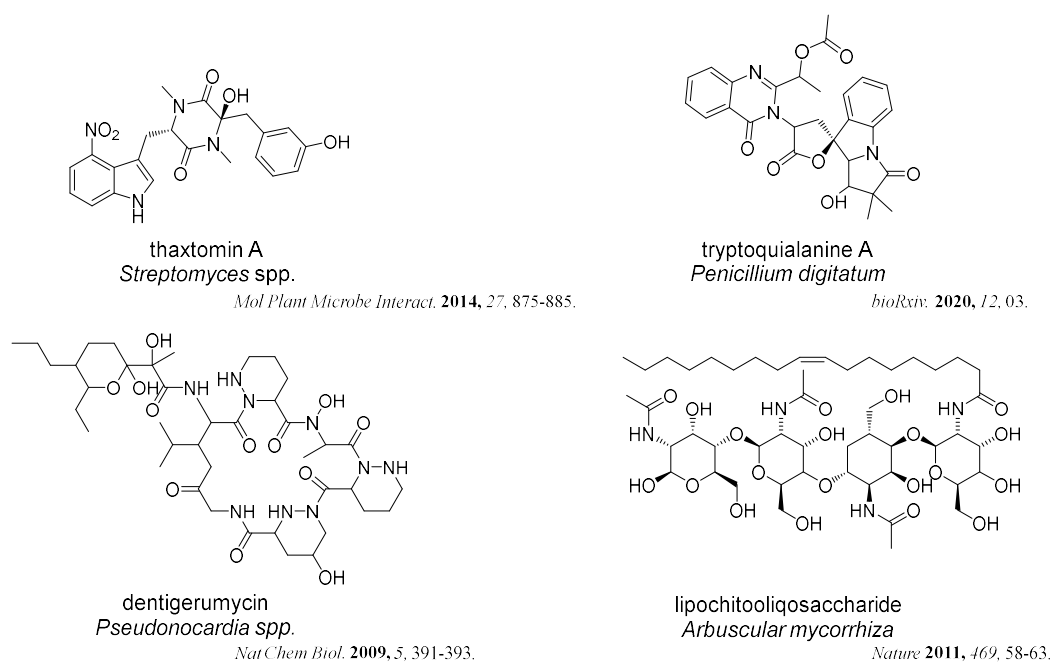


Figure 1-4. Natural products from host-symbionts/pathogens interaction.

Considering that the evolutionary origin of symbiosis is pathogenic infection [13], there is no wonder if symbiotic and pathogenic species are co-classified in the same taxon or a symbiotic species sometimes shows pathogenicity to other host organisms. Thus, bacteria in pathogenic lineages are expected to have the larger capacity to produce natural products than free-living organisms.

Most of the microbial natural products were found from Gram-positive bacteria, and chemical studies on Gram-negative bacteria has not been carried out extensively [14]. Based on these backgrounds, Gram-negative proteobacteria in pathogenic lineages are expected to be promising, and two genera *Burkholderia* and *Vibrio*, were especially noted, as described below.

1-3-1 *Burkholderia* as a source of natural products

The genus *Burkholderia*, belonging to the class *Betaproteobacteria*, occupies a vast niche in terrestrial ecosystems as free-living organisms or in association with eukaryotic hosts such as humans, animals, plants, and fungi. In recent years,

Burkholderia has specifically grabbed our attention because some species in this genus are confirmed as human pathogens, such as *B. cepacia* complex causing lung infections in immunocompromised people and *B. mallei* leading to glanders [15-17].

Some *Burkholderia* species are beneficial to the host organisms. For instance, *B. ambifaria* and *B. caribensis* can promote the grain crop amaranth growth through nitrogen fixation [18]. In addition, some natural products have been discovered (Figure 1-5), which seem to be involved in the interaction with their hosts such as toxoflavin, one of the key virulence factors produced by the plant pathogen *B. gladioli* [19], malleilactone, a virulence factor from *B. pseudomallei* [20], and burkholdine, a potent antifungal peptide from *B. ambifaria* [21].

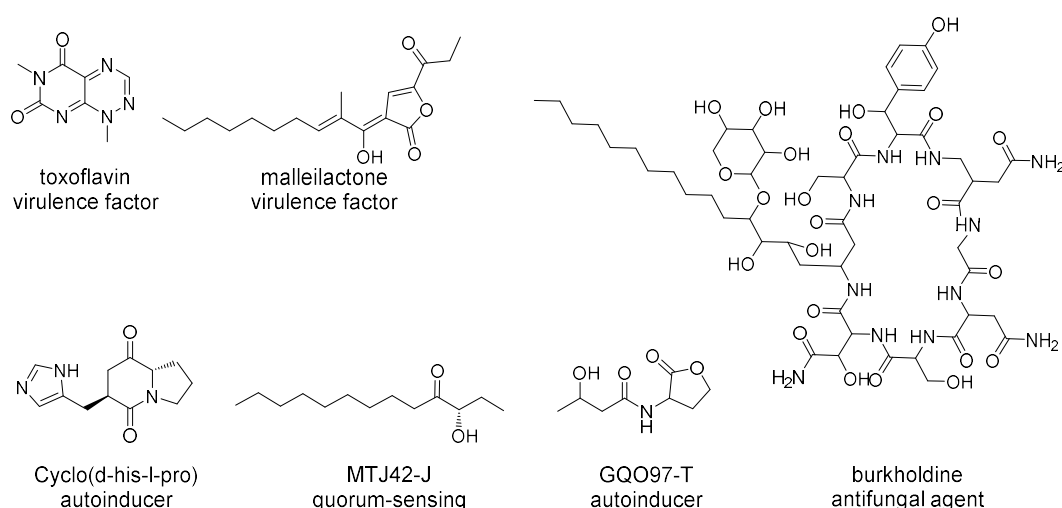


Figure 1-5. Natural products from hosts-*Burkholderia/Vibrio* interaction.

The gene mining technology has confirmed that *Burkholderia* genomes encode a plethora of natural products with potential therapeutic relevance and biotechnological applications. It is thought as one of the emerging, gifted producers of natural products because of the metabolically diverse multifaceted traits [22-24].

1-3-2 *Vibrio* as a source of natural products

The genus *Vibrio*, belonging to the class *Gammaproteobacteria*, is a genetically and metabolically diverse group of heterotrophic bacteria that are ubiquitously distributed in the oceans and represents a large fraction (0.5–5%) of the total bacterial community in major oceans around the world [25]. *Vibrio* is an emerging health threat linked to increasing seawater temperatures [26]. Although less well-known, the interactions between *Vibrio* and ocean planktons play a major role for the coastal ecology and human infection potential.

The genus *Vibrio* have cataloged 128 species at the time of writing and more than 12 are associated with food poisoning [27-29]. Among these species, *Vibrio cholerae* are the most feared and the most extensively studied pathogen [30, 31]. Thus, other related species such as *V. parahaemolyticus*, *V. vulnificus*, *V. alginolyticus*, *V. damsela*, *V. fluvialis*, *V. furnissii*, *V. hollisae*, *V. metschnikovii*, and *V. mimicus* have drawn special attention in the last decade [31]. It is reported that 70% food poisoning in Japan are caused by seafood such as fish and shellfish, contaminated with *V. parahaemolyticus* [32].

On the other hand, studies have shown that some symbiotic species of *Vibrio* have the capacity of fixing nitrogen/phototrophy/producing plant hormone [33-35]. Meanwhile, some natural products were produced because of the interaction between the genus *Vibrio* and host in Figure 1-5 like autoinducers, GQO97-T and cyclo (d-his-1-pro), which can regulate the virulence and fitness [36-38].

1-3-3 The objective of this thesis

As discussed already, exploitation of new drug resources, following to actinomycetes and fungi, are requested, and Gram-negative proteobacteria in pathogenic lineages were proposed as one of the promising candidates.

To validate this project, acquisition of new bioactive metabolites from three

species, two from the genus *Burkholderia* and one from the genus *Vibrio*, each representing those of terrestrial and marine origins, were attempted in this thesis, which will be detailed in the following chapters.

References

1. United Nations Department of Economic and Social Affairs PD World Population Prospects: The 2017 Revision, DVD Edition.
2. Foreman, K. J., Marquez, N., Dolgert, A., Fukutaki, K., Fullman, N., McGaughey, M. *Lancet*. **2018**, 392, 2052–2090.
3. Tabish, S. A. *J Cardiol Curr Res*. **2017**, 9, 326.
4. Byrne, J. P. Encyclopedia of Pestilence, Pandemics, and Plagues: A–M. ABC-CLIO. p. 99.
5. McConnell, T. H. The Nature of Disease: Pathology for the Health Professions. 2007, p. 159.
6. WHO. **2017**. Noncommunicable diseases. Fact Sheet.
7. Ali, M., Nelson, A. R., Lopez, A. L., Sack, D. *PLOS*. **2015**, 9, 3832-3845.
8. Newman, D. J., Cragg, G. M. *J. Nat. Prod.* **2012**, 75, 311–335.
9. Pye, C. R., Bertin, M. J., Lokey, R. S., Gerwick, W. H., Linington, R. G. *PNAS*. **2017**, 114, 5601–5606.
10. Nagano, H., Hanai, R., Yamada, H., Matsushima, M., Miura, Y., Hoya, T., Kuroda, C. *Chem. Biodivers*. **2012**, 9, 789–805.
11. Ding, T., Yang, L. J., Zhang, W. D., Shen, Y. H. *RSC Adv*. **2019**, 9, 21964–21988.
12. Igarashi, Y., Yamamoto, K., Ueno, C. Yamada, N., Xiaohanyao, Ye., Zhou, T., Harunari, E., Oku, N. *J Antibiot*. **2019**, 72, 653–660.
13. Nishiguchi, M. K., Hirsch, A. M., Devinney, R., Vedantam, G., Riley, M. A., Mansky, L. *M. Vie Milieu Paris*. **2008**, 58, 87–106.

14. Buijs, Y., Bech, P. K., Vazquez-Albacete, D., Bentzon-Tilia, M., Sonnenschein, E. C., Gram, L., Zhang, S.D. *Nat. Prod. Rep.* **2019**, *36*, 1333-1350.
15. Parke, J. L., Gurian-Sherman, D. *Annu. Rev. Phytopathol.* **2001**, *39*, 225–258.
16. Mahenthiralingam, E., Baldwin, A., Dowson, C. G. *J. Appl. Microbiol.* **2008**, *104*, 1539–1551.
17. Larsen, J. C., Johnson, N. H. *Mil. Med.* **2009**, *174*, 647–651.
18. Parra-Cota, F. I., Peña-Cabriales, J. J., de los Santos-Villalobos, S., Martínez-Gallardo, N. A., Delano-Frier, J. P. *PLoS One.* **2014**, *9*, e88094.
19. Li, X., Li, Y., Wang, R., Wang, Q., Lu, L. *Appl. Environ. Microbiol.* **2019**, *3*, 106-119.
20. Klaus, J. R., Deay, J., Neuenswander, B., Hursh, W., Gao, Z., Bouddhara, T., Chandler, J. R. *J. Bacteriol.* **2018**, *200*, 8-18.
21. Tawfik, K. A., Jeffs, P., Bray, B., Dubay, G., Falkinham, J. O., Mesbah, M., Schmidt, E. W. *Org. Lett.* **2010**, *12*, 664–666.
22. Pidot, S. J., Coyne, S., Kloss, F., Hertweck, C. *Int. J. Med. Microbiol.* **2014**, *304*, 14–22.
23. Baltz, R. H. *J. Ind. Microbiol. Biotechnol.* **2017**, *44*, 573–588.
24. Liu, X., Cheng, Y. Q. *J. Ind. Microbiol. Biotechnol.* **2014**, *41*, 275– 284.
25. Takemura, A. F., Chien, D. M. Polz, M. F. *Front Microbiol.* **2014**, *5*, 38.
26. Diner, R. E., Rabines, A. J., Zheng, H., Steele, J. A., Griffith, J. F., Allen, A. E. *General Microbiology* **2020** (in press). doi: 10.21203/rs.2.18876/v1
27. Parte, A. C. *Int. J. Syst. Evol. Microbiol.* **2018**, *68*, 1825–1829.
28. Mohamad, N., Amal, M. N. A., Yasin, I. S. M., Zamri Saad, M., Nasruddin, N. S., Al-

- saari, N., Mino, S., Sawabe, T. *Aquaculture* **2019**, *512*, 734289
29. Ceccarelli, D., Amaro, C., Romalde, J. L., Suffredini, E., Vezzulli, L. *Food Microbiology: Fundamentals and Frontiers*. 2019, p. 347–388.
30. Kaper, J.B., Morris, G.J., Levine, M. M. *Clin Microbiol Rev.* **1995**, *8*, 48–86.
31. Chakraborty, S., Nair, G. B., Shinoda, S. *Rev Environ Health*. **1997**, *12*, 63–80.
32. Kaneko, T., Colwell, R. R. *J. Bacteriol.* **1973**, *113*, 24-32.
33. Kang, S. R., Srinivasan, S., Lee, S. S. *Int. J. Syst. Evol. Microbiol.* **2015**, *65*, 3552–3557.
34. Gómez-Consarnau, L., Akram, N., Lindell, K., Pedersen, A., Neutze, R., Milton, D. L., González, J. M., Pinhassi, J. *PLoS Biol.* **2010**, *8*, e1000358.
35. Gutierrez, C. K., Matsui, G. Y., Lincoln, D. E., Lovell, C. R. *Appl. Environ. Microbiol.* **2009**, *75*, 2253–2258.
36. Al-Zereini, W., Laatsch, H., Anke, H. *Antibiotics* **2010**, *63*, 297–301.
37. Sandy, M., Han, A., Blunt, J., Munro, M., Haygood, M., Butler, A. *J. Nat. Prod.* **2010**, *73*, 1038–1043.
38. Motomasa, K., Shunji, A., Gato, K. *Chem Pharm Bull.* **1994**, *42*, 2449–2451.

CHAPTER 2

Two new 2-alkylquinolones, inhibitory

to the fish skin ulcer pathogen

***Tenacibaculum maritimum*, produced**

by a rhizobacterium of the genus

***Burkholderia* sp.**

2-1 Background

As discussed in Chapter 1, a higher capability of producing bioactive molecules is expected from bacteria in pathogenic lineages, which is exemplified by actinomycetes and fungi that include many pathogenic or symbiotic species. To examine this prospect, the genera *Burkholderia* and *Vibrio*, representing terrestrial- and marine-inhabiting pathogenic lineages, respectively, were chosen as the subjects of this study.

As the first project of this thesis, *Burkholderia* strains, of vegetable rhizosphere origin, were examined in this chapter. These strains were provided by Associated Professor Masafumi Shimizu at Gifu University, who studies the beneficial effect of rhizobacteria for *Alliaceae* plants on the growth *Cucurbitaceae* plants, which is applied to companion planting of Melon and Welsh onion in Hokkaido and calabash (*L. siceraria*) and the same in Tochigi [1-4].

Using *Pseudomonas* agar supplemented with C-F-C, *Burkholderia* strains were selectively collected from rhizosphere soils of Welsh onion (*Allium fistulosum*), Chinese chive (*Allium tuberosum*), and cucumber (*Cucumis sativus*). In total, 38 strains were cultured in four different media, which were designed by Ms. Atsumi Hasada of this laboratory based on the known recipes for fermentation of plant pathogenic bacteria, to give 144 broth extracts. These extracts were screened against a panel of 9 pathogenic microorganisms consisted of four Gram-negative bacteria, one yeast, and four fungi, which results in the detection of antimicrobial activity from most of the extracts. Among these, the fermentation product of strain MBAF1239, identified as *Burkholderia* sp. within the *B. cepacia* complex based on the 16S rRNA gene sequence, showed wide antimicrobial spectrum with high potency. Intrigued by this result, the responsible constituents were pursued in the following study.

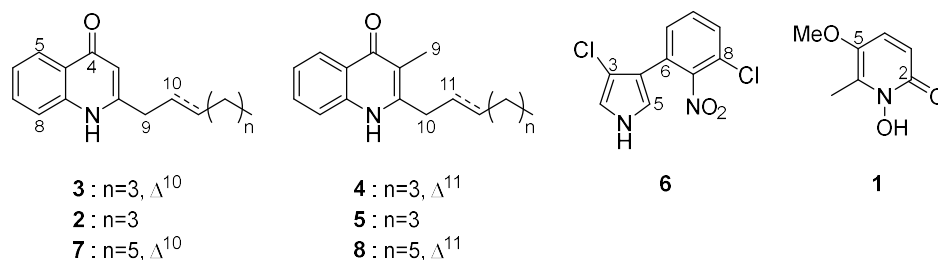


Figure 2-2. Structures of 1-8.

2-2 Results and Discussion

2-2-1 Fermentation and isolation

The seed culture V22 medium was used for the growth of the strain MBAF1239 for 2 days. Then the production medium IMM-HS, which was designed based on the composition of IMM [5] and HS media [6] for metabolite production, was prepared and cultured for 4 days. After fermentation, the *n*-BuOH was added to the fermented liquid cultures for extraction of metabolites. Then the combined butanol layer was dried and fractionated successively by solvent-partitioning to give *n*-hexane, 90% aqueous MeOH, and 60% aqueous MeOH-soluble fractions. The antimicrobial testing showed that the second fraction was the most potent against *Rhizopus oryzae* (fungal pathogen of rice seedling blight), *Trichophyton rubrum* (dermatophytosis pathogen), and *Tenacibaculum maritimum* (skin ulcer of marine fish). Then the second fraction was fractionated by ODS flash chromatography and purified by HPLC to give eight metabolites 1-8 (Scheme 2-1).

2-2-2 Structure Determination

Compound 7 was isolated as colourless liquid and gave a molecular formula of $C_{18}H_{23}NO$ based on a HRESITOFMS ion peak ($[M+H]^+$ m/z 270.1855, Δ +0.3 mmu). The spectra of 1H , ^{13}C , and HSQC showed that the existence of five aromatic (δ_H/δ_C 8.34/126.3, 7.57/131.9, 7.32/123.6, 7.26/116.8, and 6.18/109.5) and two olefinic (δ_H/δ_C

5.79/137.7 and 5.54/123.0) methines, six aliphatic methylenes ($\delta_{\text{H}}/\delta_{\text{C}}$ 3.37/37.4, 2.12/32.5, 1.43/29.1, 1.33/28.9, 1.31/22.6, and 1.30/31.7), and a methyl ($\delta_{\text{H}}/\delta_{\text{C}}$ 0.89/14.1) group, leaving one carbonyl (δ_{C} 179.0) and three aromatic resonances (δ_{C} 149.9, 139.4, and 125.3) as quaternary carbons (Table 1). Based on the rest of two unsaturation degrees, two rings constituting a fused bicycle were confirmed by the number of available aromatic carbons (=eleven). In addition, UV spectrum showed an absorption around the 340-320 nm region, corresponding to a 4-quinolone substructure [7]. Additionally, 2D NMR spectra also supported this assignment. The ^{13}C NMR spectrum showed weak resonances at the chemical shifts 157.6, 150.8, 134.6, and 118.4 ppm and the ^1H NMR spectrum showed a broaden secondary amine proton signal (δ 8.07). The HMBC correlation from H3 to C9 supported a 2-nonenyl group (C9~C17) at C2 (Figure 2-3).

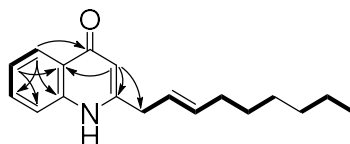


Figure 2-3. Key COSY (bold line) and HMBC (arrow) correlations for **7**.

The ^1H NMR spectrum showed a blunt signal shape during the olefinic protons H10 and H11 and the geometry of double bond at C10 cannot be determined due to the amphibolous coupling constant. However, a literature survey found that an *E*-isomer, burkholone has a chemical shift of 32.5 ppm at C12 while a *Z*-isomer, haplacutine F exhibited the same at 27.7 ppm (Figure 2-4). Because C12 of **7** resonate at 32.5 ppm, Thus, the geometry at C12 was concluded as *E* and this compound **7** was determined to be (*E*)-2-(non-2-en-1-yl)quinolin-4(1*H*)-one.

Table 2-1: NMR data for compound **7** in CDCl₃ (δ in ppm).

pos.	¹³ C	¹ H, mult. (<i>J</i> in Hz), integration	COSY	HMBC (¹ H to ¹³ C)
1		8.07, br, 1H		
2	149.9			
3	109.5	6.18, s, 1H		2, 4a, 9
4	179.0			
4a	125.3			
5	126.3	8.34, d (7.9), 1H	6	4, 7, 8a
6	123.6	7.32, t, 7.5, 1H	5, 7	4a, 8
7	131.9	7.57, brs, 1H	6	
8	116.8	7.26, ov ^a		
8a	139.4			
9	37.4	3.37, brs, 2H	10	
10	123.0	5.54, m, 1H	9, 11	
11	137.7	5.79, m, 1H	10, 12	
12	32.5	2.12 ddd (7.2, 6.5, 6.3), 2H	11, 13	10, 11, 13, 14
13	29.1	1.43, m, 2H	12, 14	
14	28.9	1.33, m, 2H		
15	31.7	1.30, m, 2H		
16	22.6	1.31, m, 2H	17	
17	14.1	0.89, t (6.5), 3H	16	15, 16

^aSignal overlapped by a residual solvent peak.

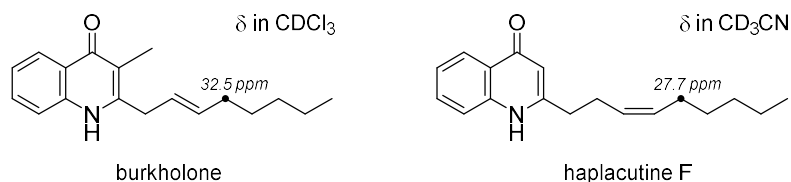


Figure 2-4. Referential ¹³C chemical shifts of an allylic carbon in burkholone [8] and haplacutine F [9].

Compound **3** was isolated as colorless solid and gave a molecular formula of C₁₆H₁₉NO based on the ESITOFMS ion peak *m/z* 242 and *m/z* 240 in the positive and negative modes, respectively. Compound **3** and **7** showed the similar ¹H NMR spectra except for the intensity of the methylene resonances between 1.48 and 1.23 ppm: which amounted for eight protons in **7**. This result implied that compound **3** is a congener of compound **7** having a two-methylene shorter aliphatic chain. Further structure analysis by 2D NMR experiments confirmed the expected structure. The geometry of the double bond was similarly determined as discussed for **7**. Based on the above analysis about

the double bond, compound **3** was determined as (*E*)-2-(hept-2-en-1-yl) quinolin-4(*1H*)-one.

The other isolated metabolites were determined to be known compounds based on 1D, 2D NMR data and MS spectra: **1** as 2-heptylquinolin-4(*1H*)-one [10], **2** as (*E*)-2-(hept-2-en-1-yl)-3-methylquinolin-4(*1H*)-one [6], **4** as PSC-C or 2-heptyl-3-methylquinolin-4(*1H*)-one [10], **5** as PSC-D or (*E*)-3-methyl-2-(non-2-en-1-yl)quinolin-4(*1H*)-one [11], pyrrolnitrin (**6**) [12], and BN-227 (**8**) [22] (Figure 2-2).

The biological source of 4-quinolone is abundantly distributed in nature, including *Rutaceae* plants [15], Gram-positive [16, 17] and Gram-negative bacteria [18-20], and a marine sponge [21]. In addition, 4-quinolone is a common core of synthetic antibactericides [14] and among of them, 2-alkyl-4-quinolones are the classics of antibiotics. Previous studies of bioactivity suggested that the substituted 4-quinolones play an important role as antibacterial, antifungal, iron-chelating, and autoinducer agents to improve the competition and survival of the producers [22]. Additionally, drug discovery assays have verified 5-lipoxygenase inhibitory activity [23], plant-growth promoting activity [22, 24], and IGF dependent cell-specific cytotoxicity [8]. Recent metabolomics approach revealed the presence of more than 50 analogs in this group [25] for 4-quinolone derivatives. Compounds **3** and **7** have been detected by MS spectrometry in previous studies [19, 26-28], although detailed structure characterization was not made. In this study, compounds **3** and **7** were isolated for the first time, which enabled rigorous structure characterization by spectroscopic method. In addition, their bioactivity (see below) was evaluated for the first time.

2-2-3 Bioactivity

Antimicrobial test showed that some of the 2-alkyl-4-quinolones are inhibitory against fungal pathogens *R. oryzae* and *T. rubrum*. Compounds **1-6** have a stronger activity than compounds **7** and **8** for the test strain *T. maritimum*. In addition, 2-heptenyl-3-methyl congener **3** exhibited the strongest activity. Because *T. maritimum* is a cause active agent of fatal skin ulcers in marine fish, compounds **1-8** offer new

scaffolds to develop new medicines for the treatment of this economically devastating epizootic [29].

Table 2-2: Antimicrobial activity of **1-8** (10 µg/6 mm disc)

	<i>Tenacibaculum maritimum</i>	<i>Trichophyton rubrum</i>	<i>Rhizopus oryzae</i>
1	33 ^a	0	0
2	24	0	0
3	55	34	10
4	25	30	10
5	22	20	30
6	25	30	15
7	20	-- ^b	--
8	7	--	--

^aSize of inhibitory zone in mm. ^bNot tested.

2-3 Conclusion

In this study, 9 human/fish/plant pathogenic microbes were used to screen 144 extracts from 38 *Burkholderia* strains in 4 different media. The result showed that most of the strains (35 out of 38) proved to be promising as a resource of antibiotics.

To date, more than 100 secondary metabolites have been isolated from *Burkholderia* strains. According to the large genome size recorded in NCBI genome database, much higher capacity in secondary metabolism is expected this bacterial genus. This study, two new alky quinolones were isolated along with six known compounds G1549 (**1**), 2-heptyl-4(1*H*)-quinolone (**2**), 2-heptyl-4(1*H*)-quinolone (**4**), PSC-D (**5**), pyrrolnitrin (**6**) and BN-227 (**8**) from strain *B. cepacia* MBAF1239, which confirmed this production capacity of the *Burkholderia* strains.

In the previous study, we have known that compounds **1**, **2**, **4-6**, and **8** have a variety of bioactivities including antibacterial, antifungal, anticancer, antiallergenic activities and quorum-sensing signaling. This is the first report on the antibiotic property of alkyl quinolones against the fish pathogen *Tenacibaculum maritimum*, a main etiological agent of fish ulcer disease “tenacibaculosis” with high mortalities. This result demonstrated that alkyl quinolones are promising as a new treatment for fish

infective disease.

2-4 Experimental

2-4-1 General experimental procedures

The UV spectrum was recorded on a Hitachi U-3210 and IR spectrum was recorded on a Perkin Elmer Spectrum 100 spectrophotometer. NMR spectra were recorded on a Bruker AVANCE 500 spectrometer and using solvent CDCl_3 ($\delta_{\text{H}}/\delta_{\text{C}}$ 7.26/77.0 ppm) and CD_3OD ($\delta_{\text{H}}/\delta_{\text{C}}$ 7.26/77.0 ppm) as solvent. HR-ESI-TOFMS spectra were obtained on a Bruker micrOTOF focus mass spectrometer.

2-4-2 Collection of *Burkholderia* strains and broth screening

Collection of *Burkholderia* strains were done by Assoc. Prof. Masafumi Shimizu using Cfc-medium at Gifu University in 2010, while fermentation and broth screening of the collection bacteria were done by Ms. Atsumi Hasada in 2013. *Burkholderia* strains were isolated from the rhizosphere soil of Welsh onion and cucumber at an experimental farming of Mie University. Those collected strains were cultured in 4 different media to give 144 extracts and then tested against test microbes including 9 human/fish/plant pathogens (*Edwardsiella ictaluri* NBRC105724^T, *T. maritimum* NBRC16015, *Trichophyton rubrum* NBRC5467, *Candida albicans* NBRC0197, *R. oryzae* NBRC4705, *Glomerella cingulata* NBRC5907, *Ralstonia solanacearum* SUPP1541, *Rhizobium radiobacter* NBRC13263 and *Athelia rolfsii* NBRC30071). In this study, the strain MBAF1239 was considered as a candidate and identified as *Burkholderia cepacia* by an analysis of 16S rRNA gene sequence, demonstrated an impressively high incidence of antagonistic strains in this genus.

2-4-3 Fermentation, extraction, and isolation

The strain MBAF1239 was seed-cultured in 100 mL V22 (soluble starch 1%, glucose 0.5%, NZ-case 0.3%, yeast extract 0.2%, Tryptone 0.5%, K_2HPO_4 0.1%, $\text{MgSO}_4 \cdot 7\text{H}_2\text{O}$ 0.05%, and CaCO_3 0.3%, pH 7.0) for 2 days. After seed-culture, a three-

mL resulting culture was transferred into 500 mL K-1 flasks each containing 100 mL production medium IMM-HS (glucose 1%, K₂HPO₄ 0.36%, KH₂PO₄ 0.41%, MgSO₄·7H₂O 0.02%, CaCl₂·2H₂O 0.01%, FeSO₄·7H₂O 0.002%, NH₄Cl 0.1%, biotin 0.0001%, and L-histidine 0.4%) for metabolite production. After 4 days production culture at 30 °C, 1-butanol was added to each flask for the extraction of secondary metabolites as a ratio 1:1. Then the mixture was shake for 1 h and the 1-butanol layer was collected by centrifuge at 6000 rpm for 10 min. Evaporation of 1-butanol layer gave a crude extract 5.35 g from a 2 L production culture. The extraction was first partitioned between 60% MeOH (250 mL) and CH₂Cl₂ (250 mL x 3). Then CH₂Cl₂ layer was evaporated and was successively partitioned between 90% aqueous MeOH (150 mL) and *n*-hexane (150 mL x 3). In the antibacterial activity against *Tenacibaculum maritimum*, the most active MeOH layer was subjected to ODS flash chromatography (ϕ 3 x 7 cm) eluted with a stepwise gradient of 25, 40, 55, and 85% (v/v) MeCN in 50 mM NaClO₄. The third fraction showed the strongest activity for the test strain *T. maritimum*, which was subjected to the reversed phase HPLC on a Cosmosil AR-II column (ϕ1 x 25 cm), using a linear gradient elution program [eluent: MeOH (A), 1:1 CH₃CN/H₂O (B); 0–5 min 100% B, 5–45 min 100% B to 0% B, 45–65 min 0% B; flow 3 mL min⁻¹ and UV detection at 210 nm to afford two new 2-alkyl quinolones **3** (0.5 mg) and **7** (0.7 mg), together with four known 2-alkyl quinolones, Pyo Ib or 2-heptylquinolin-4(1*H*)-one **1** (2.3 mg), (*E*)-2-(hept-2-en-1-yl)-3-methylquinolin-4(1*H*)-one **2** (2.5 mg), PSC-C or 2-heptyl-3-methylquinolin-4(1*H*)-one **4** (2.5 mg), PSC-D or (*E*)-3-methyl-2-(non-2-en-1-yl)quinolin-4(1*H*)-one **5** (0.8 mg), pyrrolnitrin **6** (0.5 mg), and BN-227 **8** (0.8 mg).

(*E*)-2-(Hept-2-en-1-yl)quinolin-4(1*H*)-one (**3**): UV (MeCN) λ_{max}, nm (ε): 328 (29887), 322 (27568), 316 (29828), 292 (10689), 288 (10901), 260 (6599), 240 (51173); IR ν_{max} (ATR) cm⁻¹: 2927, 2873, 1636, 1595, 1553, 1505, 1473, 1445, 1355, 1322, 1275, 1104, 1028, 969, 841, 762, 676; ¹H NMR δ_H (CD₃OD): 6.21 (s, 1H, H3), 8.20 (d, *J*=8.1 Hz, 1H, H5), 7.39 (brt, *J*=6.9 Hz 1H, H6), 7.68 (brs, 1H, H7), 7.57 (brs, 1H, H8), 3.42 (brs, 2H, H9), 5.61 (brd, *J*=13.9 Hz, 1H, H10), 5.71 (m, 1H, H11),

2.09 (dt, $J=6.3$ and 6.2 Hz, 2H, H12), 1.38 (m, 2H, H13), 1.34 (m, 2H, H14), 0.90 (t, $J=6.9$ Hz, 3H, H15); ^{13}C NMR δ_{C} (CD_3OD): 155.7 (C2), 108.9 (C3), 180.8 (C4), 125.5(C4a), 126.0 (C5), 125.1 (C6), 133.5 (C7), 119.1 (C8), 141.6 (C8a), 37.8 (C9), 125.3 (C10), 136.5 (C11), 33.2 (C12), 32.6 (C13), 23.2 (C14), 14.2 (C15); HRMS-ESITOF (m/z) $[\text{M} + \text{H}]^+$ calcd for $\text{C}_{16}\text{H}_{20}\text{NO}$, 242.1539; found: 242.1539.

(*E*)-2-(Non-2-en-1-yl)quinolin-4(1*H*)-one (**7**): UV (MeCN) λ_{max} , nm (ϵ): 328 (18600), 322 (16800), 316 (18200), 292 (8000), 288 (8400), 260 (5300), 240 (23,200); IR ν_{max} (ATR) cm^{-1} : 2923, 2853, 1730, 1635, 1593, 1554, 1500, 1471, 1443, 1354, 1320, 1247, 1137, 1028, 965, 836, 759, 672; HRMS-ESITOF (m/z): $[\text{M} + \text{H}]^+$ calcd for $\text{C}_{18}\text{H}_{24}\text{NO}$, 270.18524; found: 270.1855.

2-4-4 Evaluation of antimicrobial activity

In this study, 6 mm paper disk were first used to evaluate the activities. Then the 10 $\mu\text{g}/\text{disc}$ for each compound was prepared and a certain amount test pathogen contained: *T. maritimum*, *R. oryzae* and *T. rubrum* were used to detect the anti-activities of compounds 1-8 and the paper-disc agar diffusion method described in our previous study [30]. *Flexibacter maritimus* medium (0.5% peptone and 0.05% yeast extract in sea water) solidified with 10% agar was used to test against *T. maritimum*.

References

1. Igarashi, C., Asano, Y., Nishioka, T., Suga, H., Hyakumachi, M., Shimizu, M. *Japanese Jpn. J. Phytopathol.* **2017**, *83*, 87–94.
2. Zhang, H., Mallik, A., Zeng, R. S. *J Chem Ecol.* **2013**, *39*, 243–252.
3. Kapoulas, N., Koukounaras, A., Ilić, Z. S. *Scientia Horticulturae.* **2017**, *219*, 310–318.
4. Suzuki, Y., Simizu, M. *IOBC/WPRS Bull.* Hyakumachi, M. **2013**, *86*, 187–188.
5. Ballio, A., Barra, D., Bossa, F., DeVay, E. J., Grgurina, I. Iacobellis, N. S., Marino, G., Pucci, P., Simmaco, M., Surico, G. *Physiol. Mol. Plant Pathol.*, **33**, 493-496.
6. Hoitink, H. A. J., Sinden, S. L. *Phytopathol.* **1970**, *60*, 1236-1237.
7. Hashimoto, M., Hattori, K. *Chem. Pharm. Bull.* **1967**, *15*, 718-720.
8. Mori, T., Yamashita, T., Furihata, K., Nagai, K., Suzuki, K., Hayakawa, Y., Shin-ya, K. *J. Antibiot.* **2007**, *60*, 713-716.
9. Staerk, D., Kesting, J. R., Sairafianpour, M., Witt, M., Asili, J., Emami, S. A., Jaroszewski, J. W. *Phytochem.* **2009**, *70*, 1055-1061.
10. Wells, I. C. *J. Biol. Chem.* **1952**, *196*, 331-340.
11. Moon, S. S., Kang, P. M., Park, K. S., Kim, C. H. *Phytochem.* **1996**, *42*, 365-368.
12. Gerth, K., Trowitzsch, W., Wray, V., Höfle, G., Irschik, H., Reichenbach, H. *J. Antibiot.* **1982**, *35*, 1101-1103.
13. Itoh, J., Amano, S., Ogawa, Y., Kodama, Y., Ezaki, N., Yamada, Y. *J. Antibiot.* **1980**, *33*, 377-382.
14. Bisacchi, G. S. *J. Med. Chem.* **2015**, *58*, 4874-4882.
15. (a) Michael, J. P. *Nat. Prod. Rep.* **2008**, *25*, 166–187; (b) Michael, J. P. *Nat. Prod. Rep.*

- 2007**, 24, 223–246; (c) Michael, J. P. *Nat. Prod. Rep.* **2005**, 22, 627–646; (d) Michael, J. P. *Nat. Prod. Rep.* **2003**, 20, 476–493; (e) Michael, J. P. *Nat. Prod. Rep.* **2001**, 18, 543–559.
16. Dekker K. A., Inagaki, T., Gootz, T. D., Huang, L. H., Kojima, Y., Kohlbrenner, W. E., Matunaga, Y., McGuirk, P. R., Nomura, E., Sakakibara, T., Sakemi, S., Suzuki Y., Yamauchi Y., Kojima N. *J. Antibiot.* **2008**, 51, 145-152.
17. Cheng, C., Othman, E. M., Reimer, A., Grüne, M., Kozjak-Pavlovic, V. *Tetrahedron Lett.* **2016**, 57, 2786-2789.
18. Kunze, B., Höfle, G., Reichenbach, H. *J. Antibiot.* **1987**, 40, 258-265.
19. Vial, L., Lepine, F., Milot, S., Groleau, M.-C., Dekimpe, V., Woods, D. E., Deziel, E. J. *Bacteriol.* **2008**, 190, 5339-5352.
20. Long, R. A., Qureshi, A., Faulkner, D. J., Azam, F. *Appl. Environ. Microbiol.* **2003**, 69, 568-576.
21. Hertiani, T., Edrada, R., van Soest, R. W. M., Sudarsono, Proksch, P. *J. Pharm.* **2008**, 19, 128-136.
22. Heeb, S., Fletcher, M. P., Chhabra, S. R., Diggle, S. P., Williams, P., Cámara, M. *FEMS Microbial. Rev.* **2011**, 35, 247-274.
23. Kitamura, S., Hashizume, K., Lida, T., Miyashita, E., Shirahata, K., Kase, H. *J. Antibiot.* **1986**, 60, 1160-1166.
24. Moon, S. S., Myung, E. J., Cho, S. C., Park, J. B., Chung, B. J. *Korean J. Pest. Sci.* **2002**, 6, 64-71.
25. Lépine, F., Milot, S., Déziel, E., He, J., Rahme, L. G. *J. Am. Soc. Mass Spectrom* **2004**,

- 15, 862-869.
26. Okada, B. K., Wu, Y., Mao, D., Bushin, L. B., Seyedsayamdostet, M. R. *ACS Chem. Biol.* **2016**, *11*, 2124-2130.
27. Wang B., Waters, A. L., Sims, J. W., Fullmer, A., Ellison, S., Hamann, M. T. *Microbial. Ecol.* **2013**, *65*, 1068-1075.
28. Depke, T., Franke, R., Broenstrup, M. *J. Chromatogr. B*, **2017**, *1071*, 19-28.
29. Avendaño-Herrera, R., Toranzo, A. E., Magariños, B. *Dis. Aquat. Organ.* **2006**, *71*, 255–266.
30. Oku, N., Matsumoto, M., Yonejima, K., Tansei, K., Igarashi, Y. *Beilstein J. Org. Chem.* **2014**, *10*, 1808-1816.

2-5 Spectral data

Table of contents

(*E*)-2-(hept-2-en-1-yl) quinolin-4(*1H*)-one (**3**)

¹H NMR spectrum (CH₃OD, 500 MHz)

¹³C NMR spectrum (CH₃OD, 125 MHz)

COSY spectrum (CH₃OD, 500 MHz)

HSQC spectrum (CH₃OD, 500 MHz)

HMBC spectrum (CH₃OD, 500 MHz)

(*E*)-2-(non-2-en-1-yl) quinolin-4(*1H*)-one (**7**)

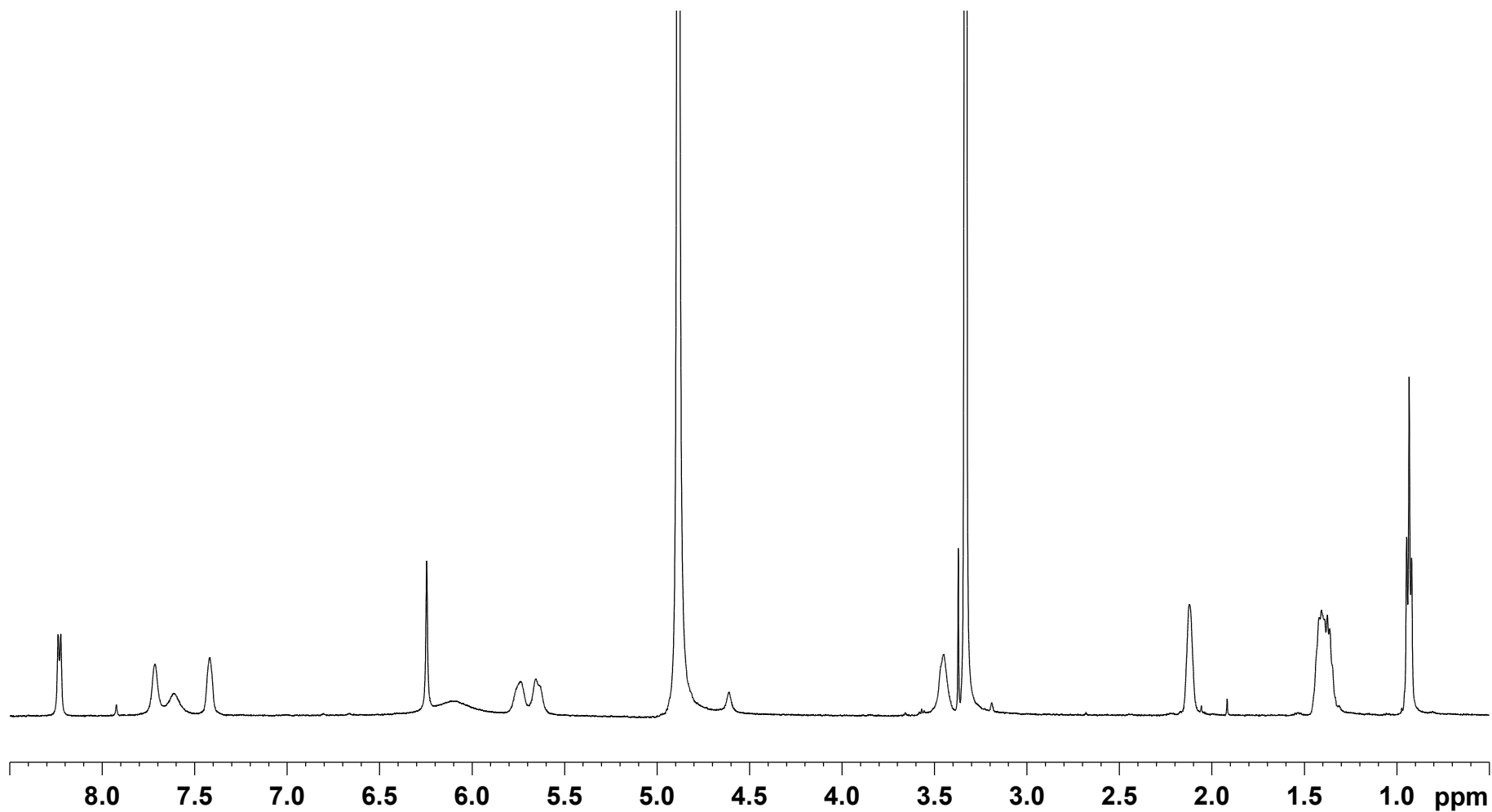
¹H NMR spectrum (CDCl₃, 500 MHz)

¹³C NMR spectrum (CDCl₃, 125 MHz)

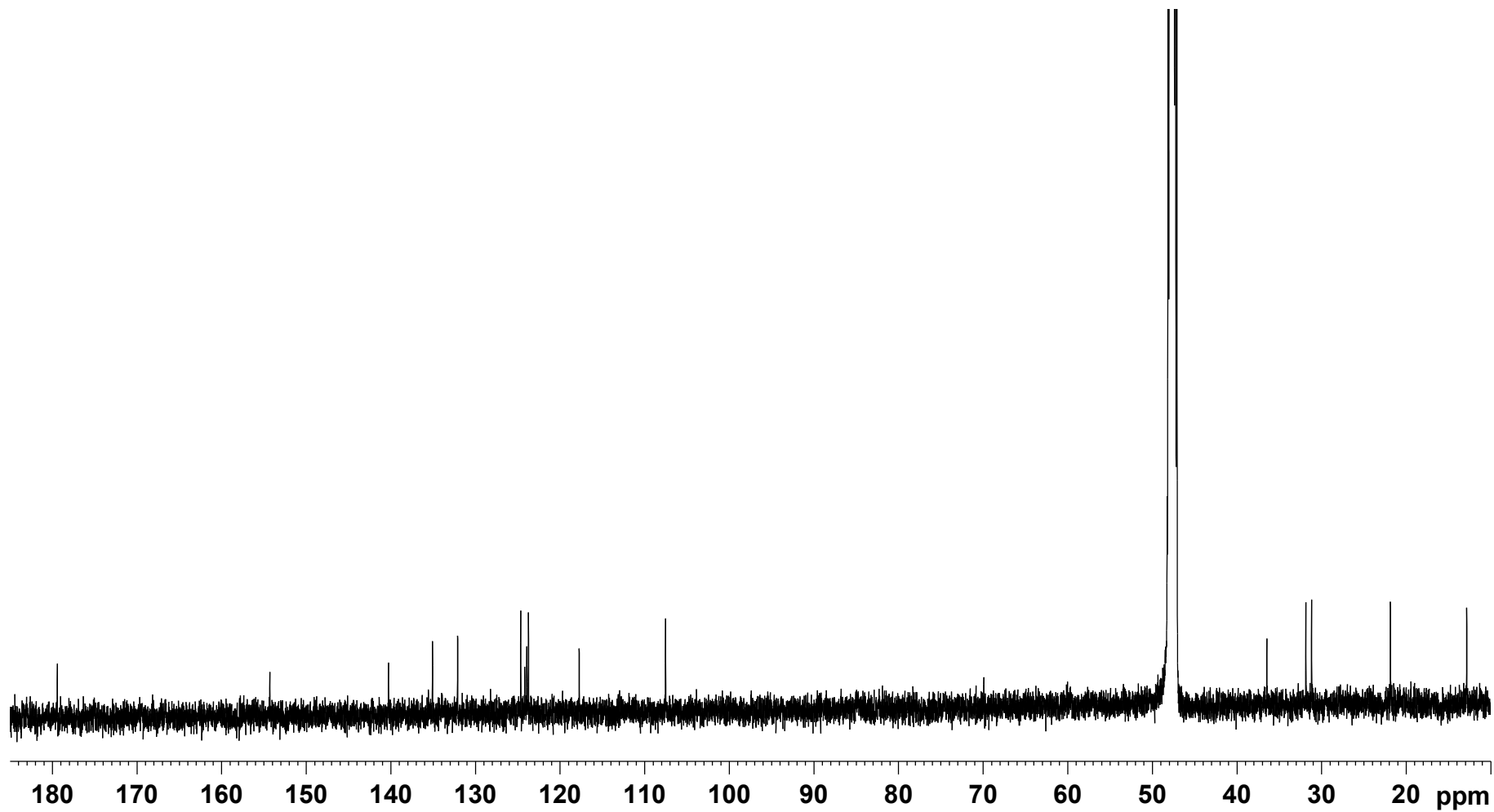
COSY spectrum (CDCl₃, 500 MHz)

HSQC spectrum (CDCl₃, 500 MHz)

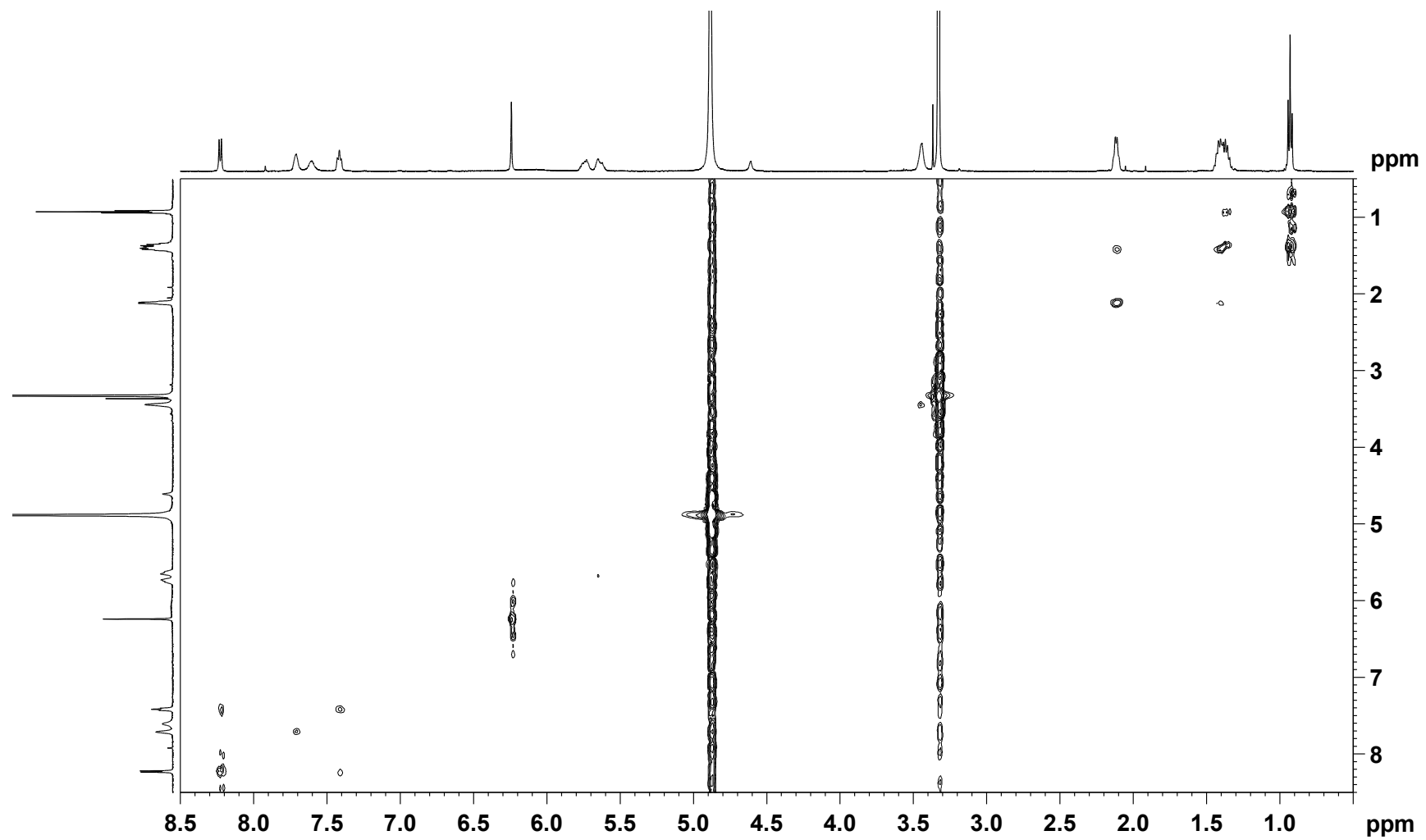
HMBC spectrum (CDCl₃, 500 MHz)



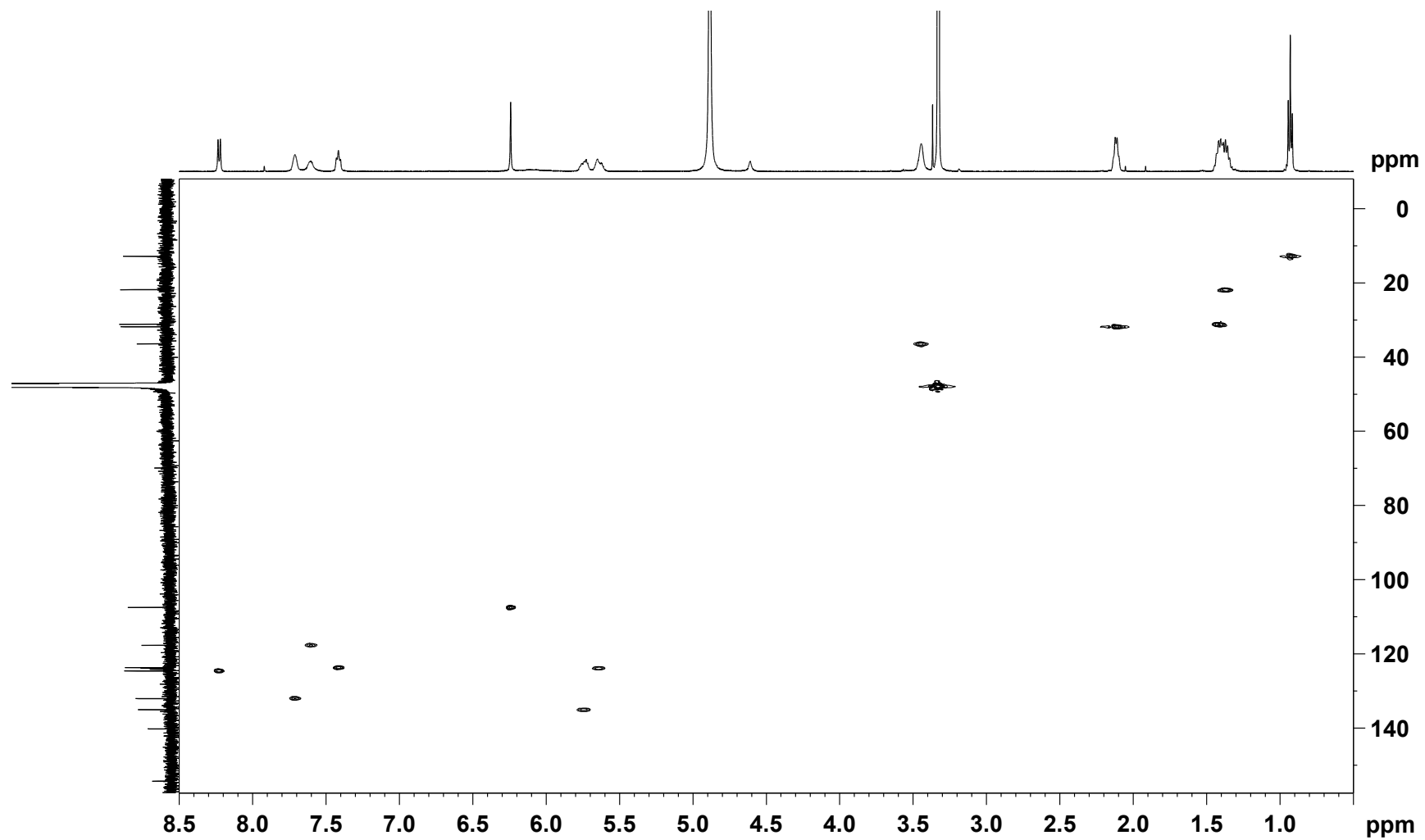
¹H NMR spectrum of (*E*)-2-(hept-2-en-1-yl)quinolin-4(1*H*)-one (**3**) (500 MHz, CH₃OD)



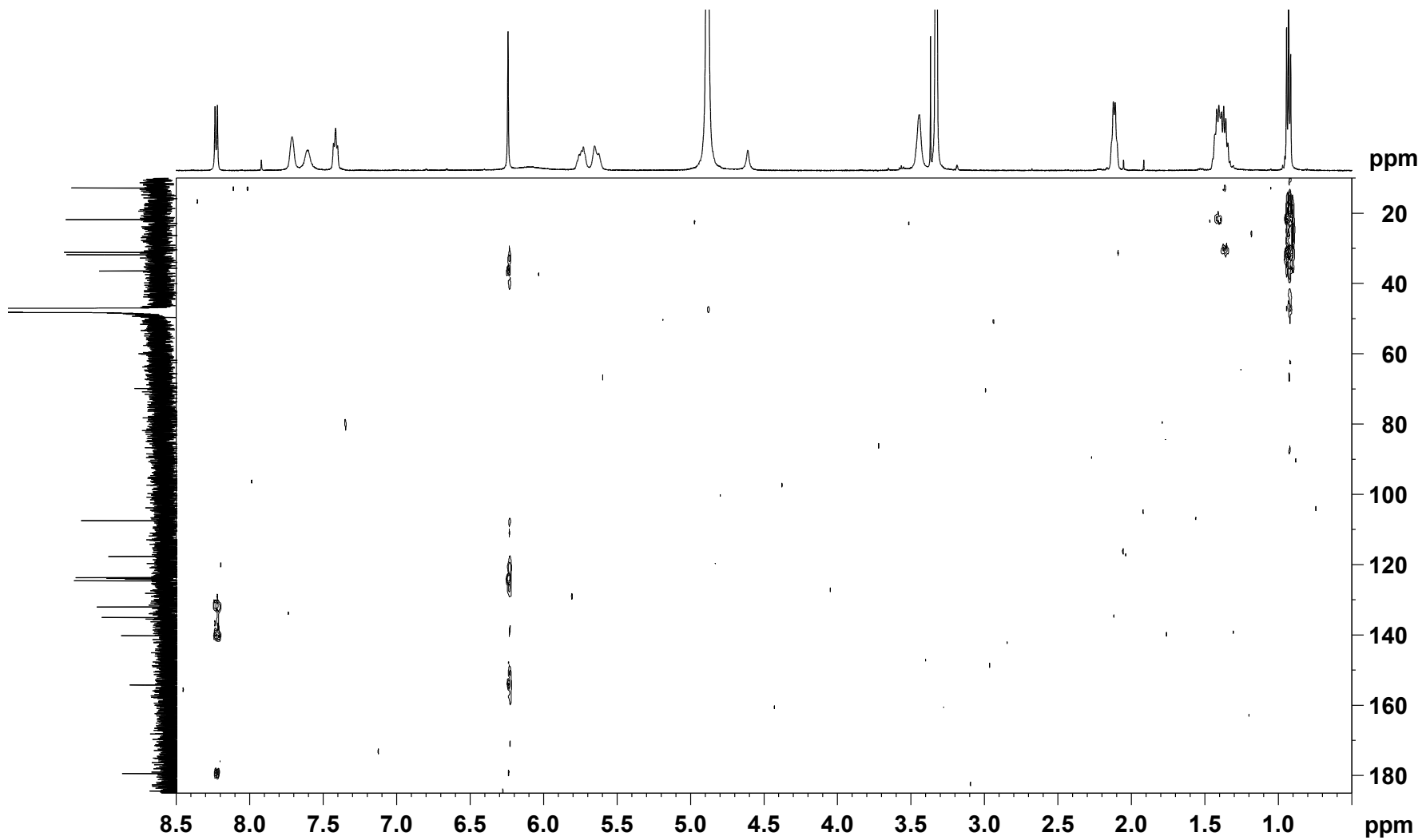
¹³C NMR spectrum of (*E*)-2-(hept-2-en-1-yl)quinolin-4(1*H*)-one (**3**) (125 MHz, CH₃OD)



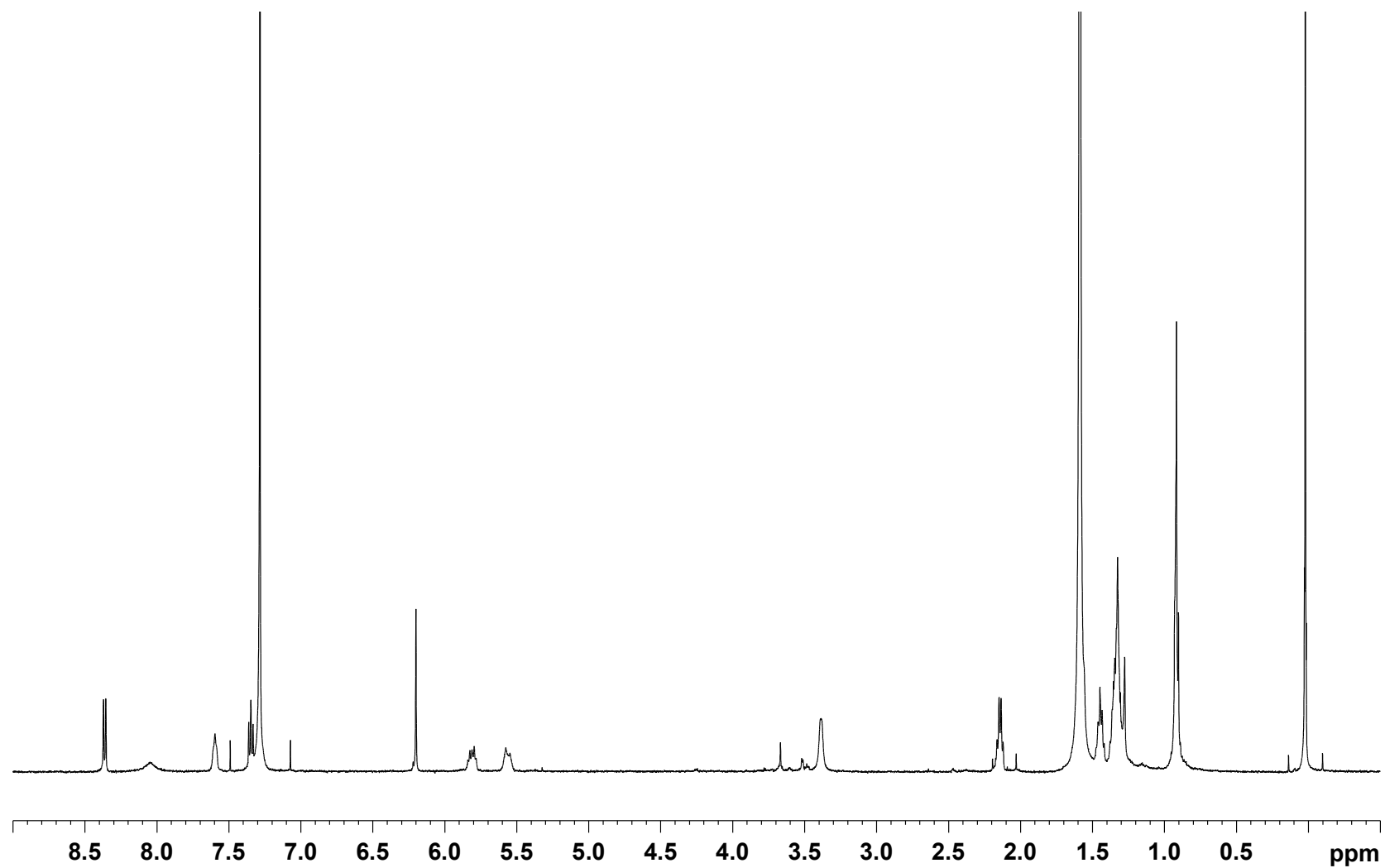
COSY spectrum of (*E*)-2-(hept-2-en-1-yl)quinolin-4(1*H*)-one (**3**) (500 MHz, CH₃OD)



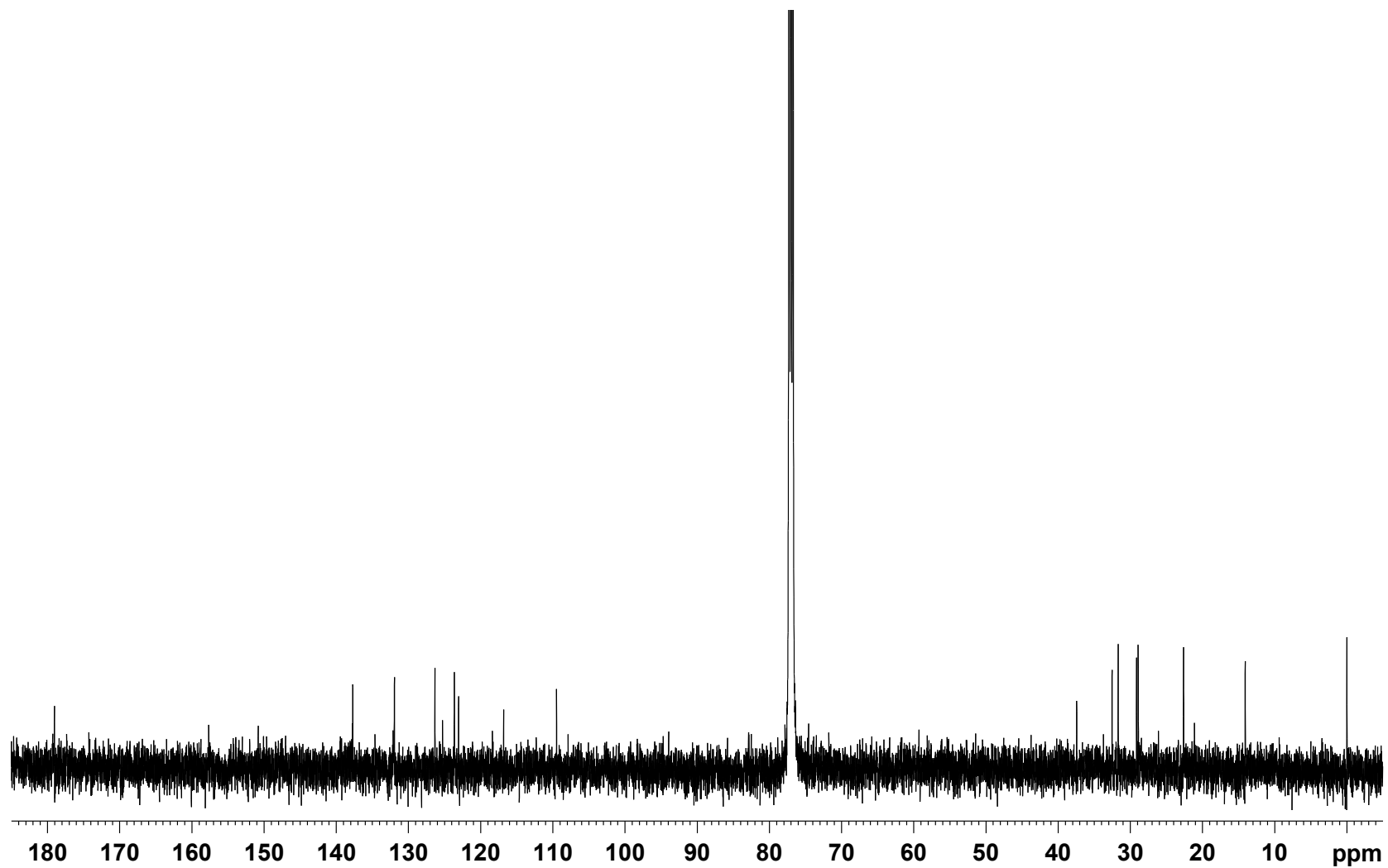
HSQC spectrum of (E)-2-(hept-2-en-1-yl)quinolin-4(1H)-one (**3**) (500 MHz, CH₃OD)



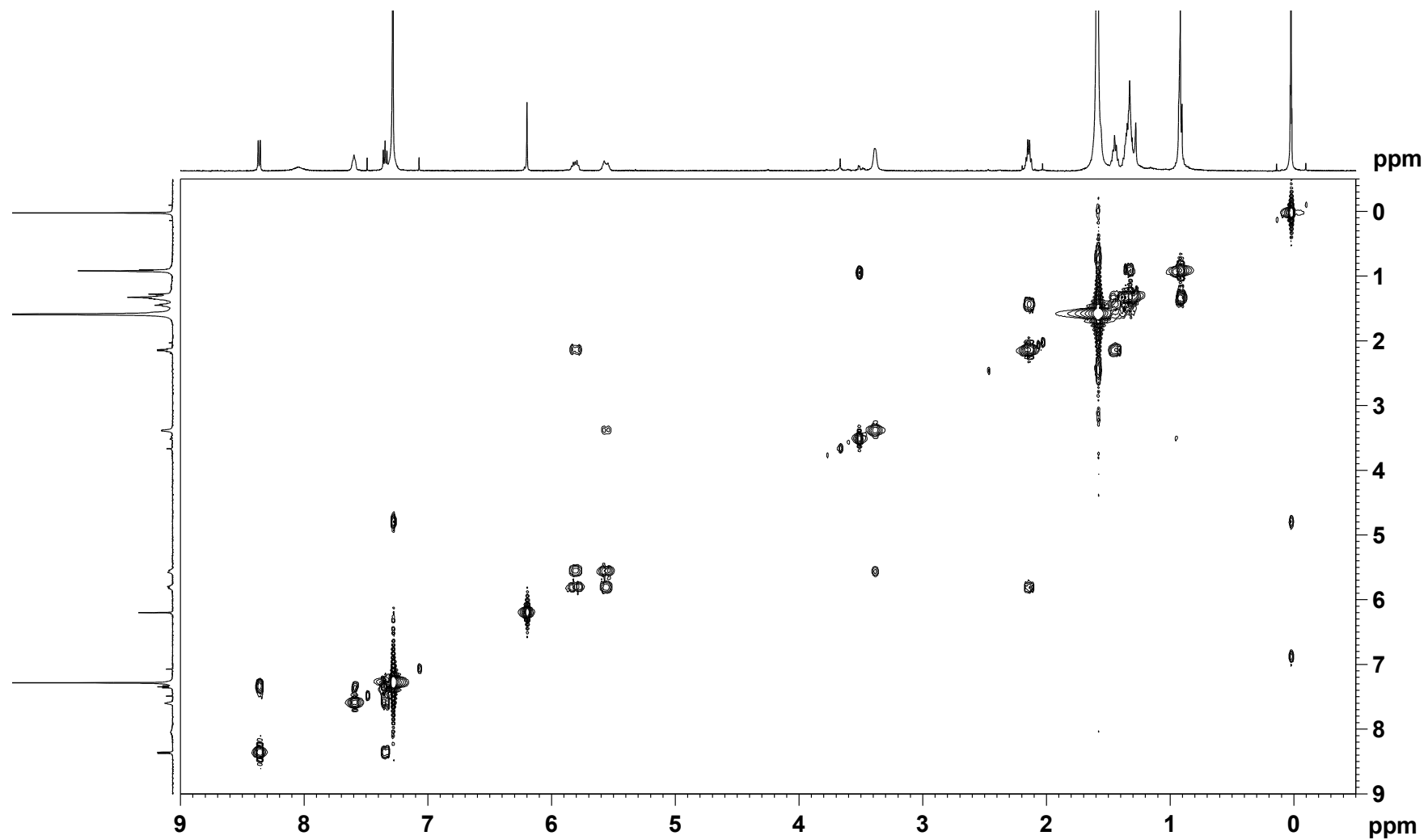
HMBC spectrum of (*E*)-2-(hept-2-en-1-yl)quinolin-4(1*H*)-one (**3**) (500 MHz, CH_3OD)



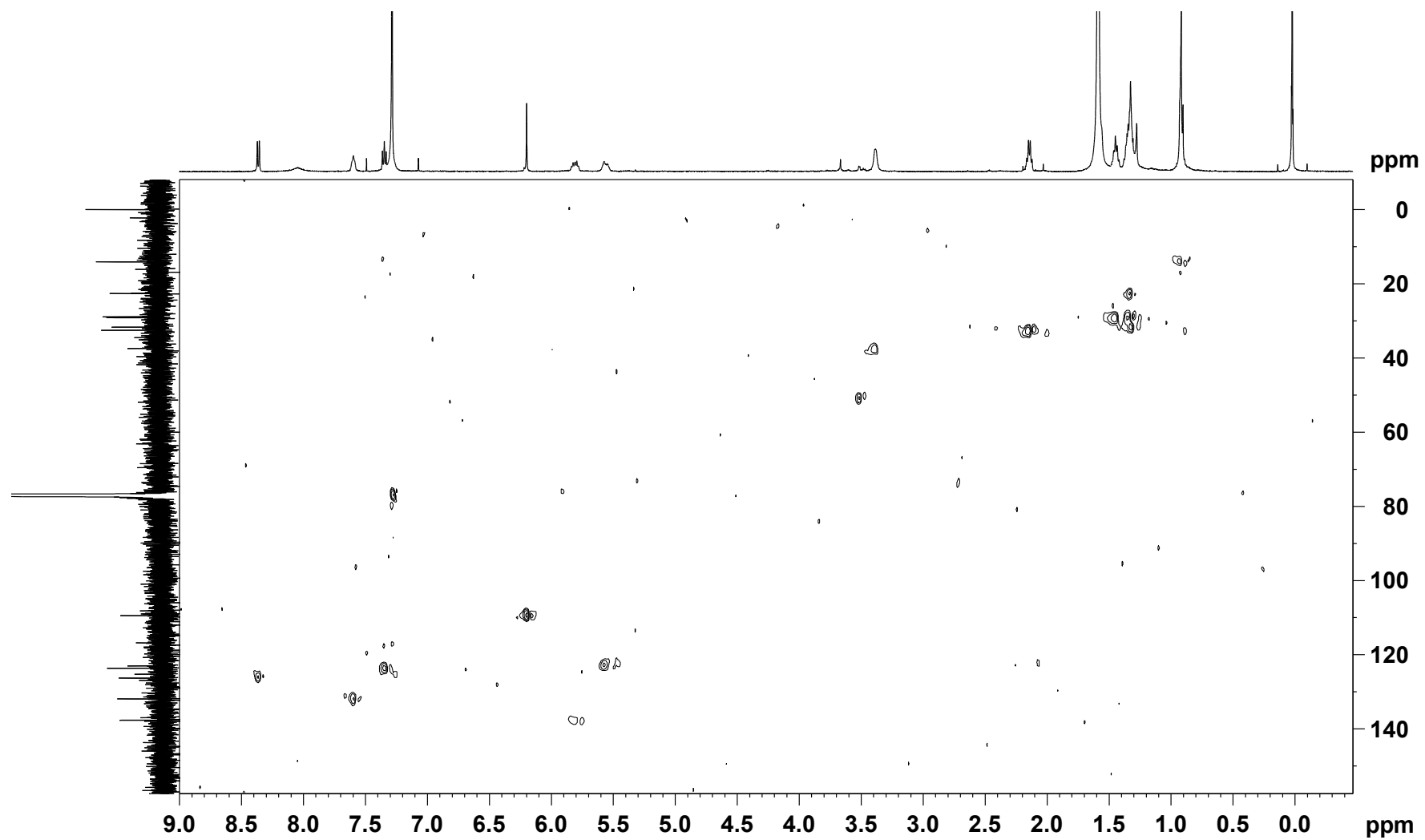
¹H NMR spectrum of (*E*)-2-(non-2-en-1-yl)quinolin-4(1*H*)-one (**7**) (500 MHz, CDCl₃)



¹³C NMR spectrum of (*E*)-2-(non-2-en-1-yl)quinolin-4(1*H*)-one (**7**) (125 MHz, CDCl₃)



COSY spectrum of (*E*)-2-(non-2-en-1-yl)quinolin-4(1*H*)-one (**7**) (500 MHz, CDCl₃)



HSQC spectrum of (*E*)-2-(non-2-en-1-yl)quinolin-4(1*H*)-one (**7**) (500 MHz, CDCl₃)

CHAPTER 3

4-Hydroxy-3-methyl-2(1*H*)-quinolone,
originally discovered from a
Brassicaceae plant, produced by a soil
bacterium of the genus *Burkholderia*
sp.: determination of a preferred
tautomer and antioxidant activity

3-1 Background

In Chapter 2, two new 2-alkylquinolones, **3** and **7**, along with 6 known metabolites, were discovered from a *Burkholderia* strain isolated from a rhizosphere soil sample. To further explore the structural diversity of secondary metabolites from *Burkholderia*, a strain with a different isolation background was chosen as the subject of this chapter. The strain coded as 3Y-MMP (Figure 3-1), was isolated from a soil sample of rice pad collected in Toyama by Associate Professor Yukiko Shinozaki at National Institute of Technology, Toyama College, based on an enrichment culture technique using 1 mM ZnCl₂ as a selection pressure. Strain 3Y-MMP showed a 99.9% similarity to *Burkholderia cepacia* N1_1_43 by a molecular phylogenetic analysis of 16S rRNA gene sequence.



Figure 3-1. *Burkholderia* sp. 3Y-MMP on YM agar.

Strain 3Y-MMP was cultured in three different media and resulting fermentation products were analyzed using an HPLC-DAD system, which exhibited the good production of the strain 3Y-MMP in medium King's B. Among of them, three major peaks around 15-20 min were determined to be the known spoxazomicin C and pyochelin based on the UV analysis [1-3]. In addition, A new metabolite **9** without the similar UV spectrum in our in-house UV-database (Figure 3-2) were found.

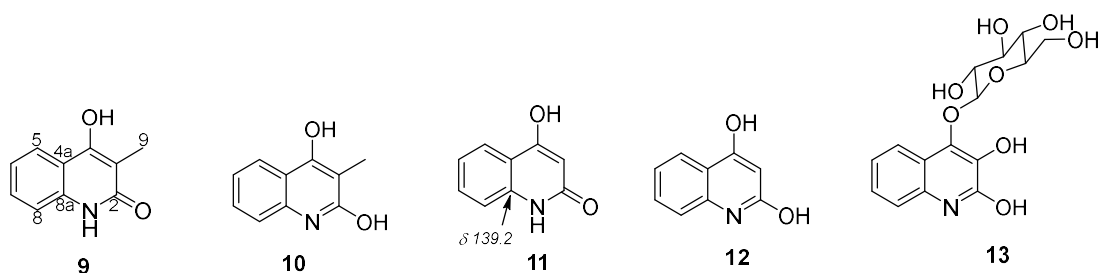


Figure 3-3. Structures of 9-13 [4-10].

3-2 Results and Discussion

3-2-1 Fermentation and isolation

The strain 3Y-MMP was recovered on YM agar then transferred with agar substratum directly into production King's B medium (peptone 2%, glycerin 1%, K_2HPO_4 0.41%, $MgSO_4 \cdot 7H_2O$ 0.15%) for 4 days with reciprocal shaking at 200 rpm. The fermented products were extracted with 1-BuOH, and then partitioned between CH_2Cl_2 and 60% MeOH. Then 60% MeOH fraction was further fractionated by ODS flash chromatography and purified by elution with 16% aq. MeCN-0.1% HCOOH HPLC to give the 4-hydroxy-3-methyl-2-(1H)-quinolinone (**9**, 5.2 mg, Scheme 3-1).

3-2-2 Structure Determination

Compound **9** was isolated as white power and gave a molecular formula of $C_{10}H_9NO_2$ based on a HRESITOFMS ion peak ($[M+Na]^+$ obsd m/z 198.0525, calcd 198.0526). Broad absorption around 3364 cm^{-1} and strong absorption at 1580 cm^{-1} in the IR spectrum indicated the existence of hydroxy and amino groups.

The 1H and ^{13}C NMR data in $DMSO-d_6$ are shown in Table 1. Analysis of the 1H NMR coupling constants and COSY and HSQC revealed the existence of four coupled aromatic methines (δ_C 122.7/ δ_H 7.85 dd, $J=7.9, 1.0$ Hz; 121.2/7.12 ddd, $J=7.9, 7.2, 0.7$ Hz; 129.8/7.41 ddd, $J=8.1, 7.2, 1.2$ Hz; 115.0/7.23 d, $J=8.1$ Hz), two heteroatom-substituted non-protonated sp^2 carbons (δ 164.0 and 157.4), three sp^2 non-protonated

carbons (δ_c 137.4, 115.8, and 106.9), methyl proton at 1.98 ppm and a singlet exchangeable proton at 11.23 ppm; Further analysis of HMBC spectrum in DMSO displayed the correlations from H-5 to C-8a, C-4, and from H-7 to C-8a, and H-6 to C-4a, and H-8 to C-4a to form a disubstituted benzene ring. However, the remaining parts were assembled into a C₄ enol-amidyl or enol-imidic acyl unit because of the correlations from the proton H₃9 to the C-4, C-3 and C-2. In addition, the correlations of HMBC from the H₃-9 to C-4a of the benzene ring implied the connection and the correlations from the exchangeable proton to C-4a and C-3 supported this connection as well as hydroxylation at the benzylic position.

Finally, by comparing the chemical shift with the known compounds 4-methoxy-1,3-dimethyl-2(1*H*)-quinolone **14** with a chemical shift of 138.4 ppm [11], *N*-methyl-2-pyridone **15** with a chemical shift of 139.5 ppm [12], 2,4-dimethoxy-3-methylquinoline **16** with a chemical shift of 147.0 ppm and 2-methoxypyridine **17** with a chemical shift of 147.2 ppm [13, 14], the structure of **9** was assigned to have a 2-quinolone form but not 2-quinolinol [15] (Figure 3-4). The same structure with 4-hydroxy-3-methyl-2 (1*H*)-quinolinone was synthesized from diethyl malonate and aniline and the assignment was further substantiated as below.

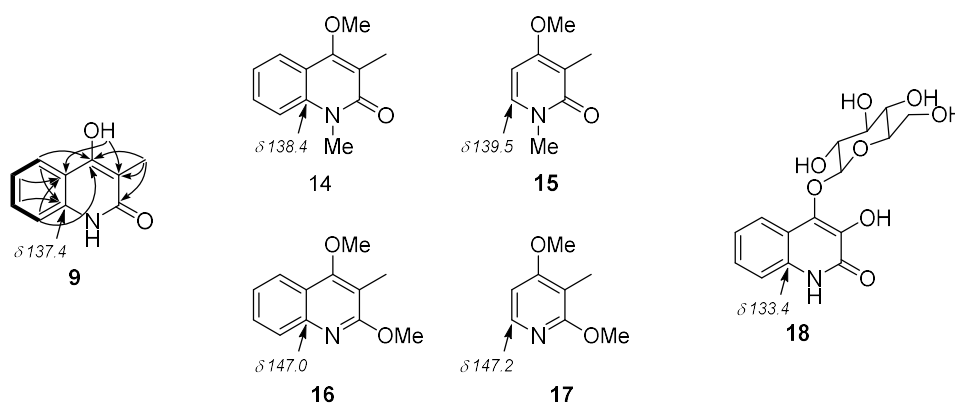


Figure. 3-4. COSY-deduced spin-system (bold lines) and key HMBC correlations (arrows) for **9**, and structures of compounds **14-18** with a ¹³C chemical shift at C-8a position.

Table 3-1: NMR data of **9** in DMSO-*d*₆ (297 K)

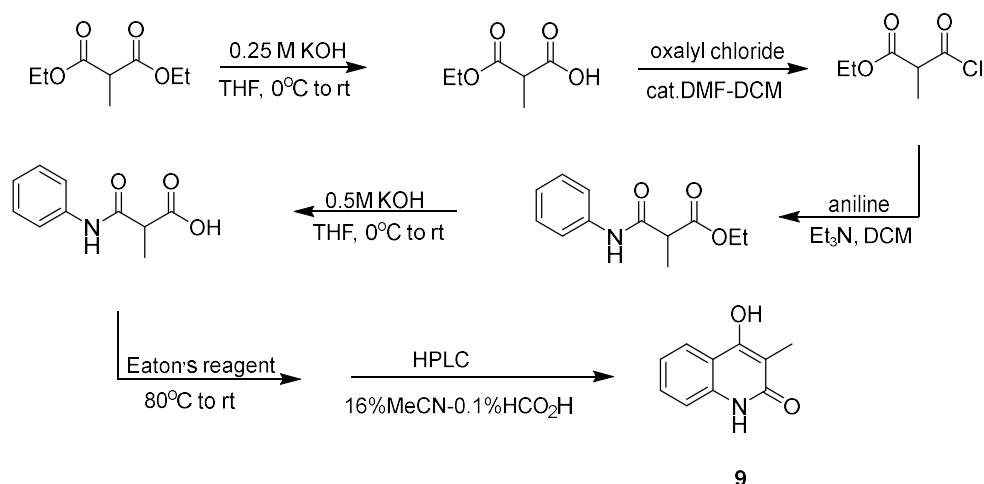
9			
No.	¹³ C	¹ H mult. (<i>J</i> in Hz), integration	HMBC (¹ H to ¹³ C)
1 ^a			
2	164.0		
3	106.9		
4	157.4		
4-OH		11.30 brs, 1H	3, 4a
4a	115.8		
5	122.7	7.85 dd (7.9, 1.0), 1H	4, 7, 8a
6	121.2	7.12 ddd (7.9, 7.2, 0.7), 1H	4a, 5, 7, 8, 8a
7	129.8	7.41 ddd (8.1, 7.2, 1.2), 1H	5, 8, 8a
8	115.0	7.23 d (8.1), 1H	4, 4a, 6, 7, 8a
8a	137.4		
9	9.6	1.98 s, 1H	2, 3, 4, 4a

^aSignal for amide proton not observed.

3-2-3 Synthesis of **9**

In an effort to increase the amount of **9** to evaluate by bioassay, total synthesis was conducted according to the procedure (Scheme 3-2) established by Kawada and coworkers [16].

First, diethyl methyl malonate was hydrolyzed to 2-methyl-1-ethyl ester-propanedioic acid with the action of 0.25 M KOH and then converted to acid chloride by *N,N*-dimethylformamide, which was acylated aniline to give ethyl 2-methyl-3-oxo-3-(phenylamino) propanoate. Treatment with 0.5 M KOH, *N*-phenyl-2-methylmalonamic acid, which was cyclized with Easton's reagent, gave **9** (Scheme 3-2). The total yield was 18.8%.



Scheme 3-2. Synthetic preparation of **9** [16].

Although compound **9** has been synthesized several times [17] and the chemical shifts of ^1H and ^{13}C resonances were enumerated [16], one-on-one assignments of the resonances to each structural part are first done in this work. In addition, the correlations of enol proton and the comparison of chemical shift with the known compounds confirmed 2-quinolone as a preferred tautomer. In addition, correction of the structures of known compounds **12** (139.2 ppm) and **13** (133.4 ppm) were made to 4-hydroxy-2(1*H*)-quinolone (4HQ, **11**) and 4-*O*- β -D-glucopyranosyl-3,4-dihydroxy-2-quinolone (**18**) respectively, based on the chemical shift of C-8a [18,10].

Compared with the known compound **10**, structural similarity between **9** and **11** implied that **9** also belongs to a member of 2-alkyl-4-quinolone class signaling molecules/antibiotics known from *Pseudomonas aeruginosa* and some *Burkholderia* species [19, 20]. Compound **9** with a 3-methyl group are exclusively produced by *Burkholderia* species [21]. These metabolites are biosynthesized by head-to-head condensation of anthranilate and β -ketoacylate precursors, followed by a modification at C3 or nitrogen by putative monooxygenases or methyltransferase [20]. The biosynthesis of compound **11** is proposed based on malonate as the acylate precursor in this pathway. Thus, the same mechanism should be adopted by **9** with an additional methylation on C3.

3-2-4 Bioactivity

In the previous studies, the compound **9** showed inhibitory activities against *Mycobacterium tuberculosis* H37Ra and weak cytotoxicity against MRC-5 human lung-derived fibroblasts [22]. Meanwhile, an assay using RAW 264.7 murine macrophage-like cells showed that **9** could not inhibit the production of nitric oxide [23]. In this study, antimicrobial testing showed that **9** was inactive against *Rhizobium radiobacter* NBRC14554, *Ralstonia solanacearum* SUPP1541, *Tenacibaculum maritimum* NBRC16015 (Gram-negative bacteria), *Staphylococcus aureus* FDA209P JC-1 (Gram-positive bacterium), *Candida albicans* NBRC0197, and *Saccharomyces cerevisiae* S100 (yeasts).

The luminol chemiluminescence extinction assay was used to evaluate the antioxidant activity of **9** [24, 25] which quantifies the presence of the most detrimental ROS, hydroxy radical [26, 27], as intensity of luminescence emitted by oxidation of luminol. The result showed that 10 μ M of compound **9** decreased luminescence to 14% of the control reaction (Figure. 3-4). At first, the compound **9** was thought to entrap catalyst Cu^{2+} as the mechanism of chemiluminescence inhibition because the Cu^{2+} was used to catalyze Fenton reaction to yield hydroxy radical. However, as far as checked by CAS assay [28], this speculation about entrapment of Cu^{2+} were overthrown based on the weak activity of metal-chelation in specified concentration. Thus, **9** was found to be another example of the antioxidants from *Burkholderia*.

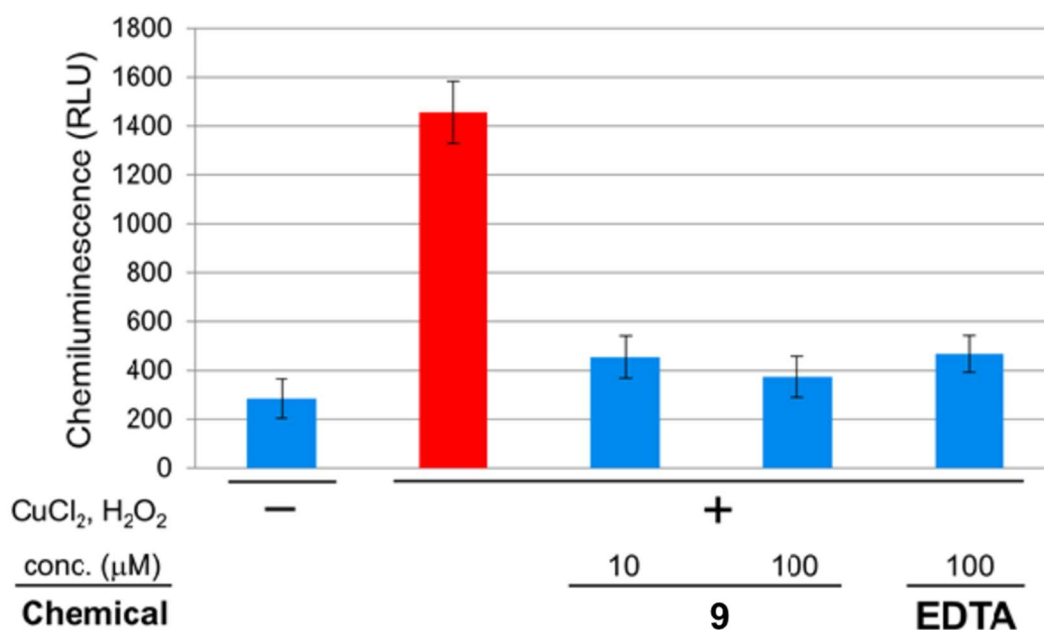


Figure 3-4. Extinction of luminol chemiluminescence by **9**.

3-3 Conclusion

In summary, 4-hydroxy-3-methyl-2(1*H*)-quinolone (**9**), an old synthetic molecule and recently discovered from a plant without providing abundant evidence to support the structure, was isolated from a fermentation extract of *Burkholderia* sp. 3Y-MMP. The structure of compound **9** was determined by the first full spectroscopic analyses using MS and NMR. According to the comparison of ¹³C chemical shift with the related compounds and synthetic compound **9**, the compound **9** was determined as to have a 2-quinolone form.

Burkholderia strain 3Y-MMP, isolated in a Zn²⁺ enrichment culture, was chosen for metabolite analysis. While the activity of compound **9** was insignificant in the metal-chelating assay, the luminol chemiluminescence extinction assay showed that the compound **9** has a strong antioxidant activity. Even though the mechanisms of antioxidant are unclear, the compound **9** was considered as a new antioxidant from the

Burkholderia.

On the one hand, the discovery of compound **9** from the *Burkholderia* indicated the high production capacity of *Burkholderia*, on the other hand, even though more than 100 compounds isolated from this genus, new compound discovery has proven the genus *Burkholderia* as a promising resource of new bioactive metabolites.

3-4 Experimental

3-4-1 General experimental procedures

UV and IR spectra were collected on a Hitachi U-3210 and a Perkin Elmer Spectrum 100, respectively. NMR spectra were collected on a Bruker AVANCE 500 spectrometer in DMSO-*d*₆ or CDCl₃ using referencing solvent signals at $\delta_{\text{H}}/\delta_{\text{C}}$ 2.5/39.5 and 7.27/77.0, respectively. HR-ESI/TOFMS were recorded on a Bruker micrOTOF focus mass spectrometer. Chemiluminescence was measured on a Molecular Devices SpectraMax M2 microplate reader.

3-4-2 Microorganism

Burkholderia sp. 3Y-MMP was isolated from a soil sample Toyama City, June 2015, by a similar procedure described in reference [29]. In the initial screening of strain, 1 mM of ZnCl₂ was added to the medium as selection pressure for strains. Then taxonomy of strain 3Y-MMP was determined by a 16S rRNA sequence analysis using a primer set 10F (5'-GTTTGATCCTGGCTCA-3') and 800R (5'-TACCAGGGTATCTAATCC-3'). The result showed a 99.9% similarity of to *Burkholderia cepacia* strain N1_1_43 based on the DNA Data Bank of Japan (DDBJ) website. This strain will be deposited in NBRC once it resumes services, which is currently suspended due to a nation-wide State of Emergency regarding COVID-19 declared on Apr. 16 by the Government of Japan.

3-4-3 Fermentation and isolation

Burkholderia sp. 3Y-MMP was recovered and the colony was transferred into 100 mL production medium King's B medium composed of peptone 2%, glycerin 1%, K₂HPO₄ 0.41%, and MgSO₄·7H₂O 0.15%. Then 500 mL K-flasks containing above medium were rotary shaken at 200 rpm at 30 °C for 4 days. After fermentation, 1-butanol was used to extract the fermentation broth with the ratio 1:1 under the 6000 rpm centrifugation. The supernatant was collected and dried in vacuo to give a solid (2.7g) from a 2 L culture. 60% MeOH layer separated from CH₂Cl₂ was subjected to ODS with a step gradient of MeCN-0.1% HCOOH (20%, 30%, 40%, 50%, 60%, 70% and 80%). Fraction 2 (30% MeCN) was evaporated to provide 69.4 mg, and then the purification was achieved by reversed-phase HPLC (Cosmosil AR-II column, 1 × 25 cm) with an isocratic elution of 16% MeCN-0.1% HCOOH, yielding **9** (5.2 mg, 31.3 min) with sufficient purity for NMR-based structure characterization.

4-Hydroxy-3-methyl-2(1H)-quinolone (9): UV (MeOH) λ_{\max} nm (ϵ): 312 (2300), 226 (12000); IR (ATR) ν_{\max} 3268, 3186, 2958, 2927, 1595, 1486, 1387, 1354, 1243, 1026, 772, 761, 692, 664 cm⁻¹; HR-ESITOFMS m/z 198.0525 [M+Na]⁺ (calcd for C₁₀H₉NNaO, 198.0526); ¹H and ¹³C NMR data are shown in Table 1.

3-4-4 Evaluation of Fe³⁺ binding activity

The iron-binding activity was evaluated by the CAS assay developed by Schwyn and Neilands [21]. Two-point five mg of compound **9** was first dissolved in 20 μ L DMSO. Then, add above mixture to the 50 μ L blue-colored CAS stock solution and bring volume up to 100 μ L with H₂O (final concentration of **9**: 160 mM). After incubation for 10 min, the solution changed color from deep blue to orange caused by the removed of Fe³⁺ from the indicator CAS dye and implied the compound **9** had chelating ability.

3-4-5 Antibacterial assay

Antibacterial and antifungal assay were performed against strains *Tenacibaculum maritimum* (NBRC16015), *Rhizobium radiobacter* (NBRC14554), *Ralstonia solanacearum* (SUPP1541), *Staphylococcus aureus* (FDA209P JC-1), *Candida albicans* (NBRC0197) and *Saccharomyces cerevisiae* (S100). The activity was evaluated by MIC method using 96-well plates with concentrations of 0.049, 0.098, 0.2, 0.4, 0.8, 1.6, 3.2, 6.4, 12.5, 25, 50, 100 µg/mL. After incubation at 30 °C for 2 days, the MIC value was the lowest drug concentration of no strain growth.

Antioxidant assay

The method of antioxidant activity was described in reference [30]. Ten µM of luminol, 1000 µM of H₂O₂ and a vehicle solvent with or without compound **9** were mixed in 50 mM boric acid-sodium hydroxide buffer at pH 9.0. Then 100 µM of CuCl₂ was added to the above mixture to initiate Fenton reaction. After incubation for 5 min, chemiluminescence at 500 nm was recorded on a microplate reader. The above experiments were repeated 3 times and the mean ratio of light extinction was expressed as the potency of antioxidant activity.

References

1. Inahashi, Y., Iwatsuki, M., Ishiyama, A., Namatame, M., Nishihara-Tsukashima, A., Matsumoto, A., Shiomi, K. *J. Antibiot.* **2011**, *64*(4), 303–307.
2. Cox, C. D., Rinehart, K. L., Moore, M. L., Cook, J. C. *Proc Natl Acad Sci.* **1981**, *78*, 4256–4260.
3. Sokol, P. A. *FEMS Microbiol. Lett.* **1984**, *23*, 313–317.
4. Shang, X. F., Susan, L., Natschke, M., Liu, Y. Q., Guo, X., Xu, X. S., Goto M., Li, J. C., Yang, G. Z., Lee, K. H. *Med. Res. Rev.* **2018**, *38*, 775–828.
5. Shang, X. F., Susan, L., Natschke, M., Yang, G. Z., Liu, Y. Q., Guo, X., Xu, X. S., Goto, M., Li, J. C., Zhang, J. Yu., Lee, K. H. *Med. Res. Rev.* **2018**, *38*, 1614–1660.
6. Arndt, F., Ergener, L. and Kutlu, O. *Chem. Ber.* **1953**, *86*, 951-957.
7. Hebanowska, E., Tempczyk, A., Łobocki, L., Szafranek, J., Szafranek, A., Urbanek, Z. H. *J. Mol. Struct.* **1986**, *147*, 351-361.
8. Luis García Ruano, J., Pedregal, C., Rodríguez, J. H. *Heterocycles* **1991**, *32*, 2151–2159.
9. Lépine, F., Dekimpe, V., Lesic, B., Milot, S., Lesimple, A., Mamer, O. A., Rahme, L. G., Déziel, E. *Biol. Chem.* **2007**, *388*, 839–845.
10. Yang, X., Yang, J. *Acta. Pharm. Sin.* **2008**, *43*, 1116–1118.
11. Reisch, J., Mester, I. *Arch. Pharm. (Weinheim, Ger.)* **1980**, *313*, 751–755.
12. Still, I. W. J., Plavac, N., McKinnon, D. M., Chauhan, M. S. *Can. J. Chem.* **1976**, *54*, 280–289.
13. Osborne, A. G., Warmesley, J. F., Dimitrova, G. T. *J. Nat. Prod.* **1992**, *55*, 589–595.

14. Chambers, R. D., Parsons, M., Sandford, G., Skinner, C. J., Atherton, M. J., Moilliet, J. S. J. *Chem. Soc., Perkin Trans. 1* **1999**, 803–810.
15. Moon, B. S., Lee, B. S., Chi, D. Y. *Bioorg. Med. Chem.* **2005**, *13*, 4952–4959.
16. Kawada, M., Inoue, H., Ohba, S., Hatano, K., Abe, H., Hayashi, C., Watanabe, T., Igarashi, M. PCT Int. Appl. WO 2014/132902 A1.
17. Gabriel, S., Gerhard, W. *Ber. Dtsch. Chem. Ges B.* **1921**, *54B*, 1067–1078.
18. AIST Spectral Database for Organic Compounds. SDBS No. 15669.
https://sdb.sdb.aist.go.jp/sdb/cgi-bin/direct_frame_top.cgi (accessed Feb 23, 2020).
19. Heeb, S., Fletcher, M. P., Chhabra, S. R., Diggle, S. P., Williams, P., Cámara, M. *FEMS Microbiol. Rev.* **2011**, *35*, 247–274.
20. Coulon, P. M. L., Groleau, M. C., Déziel, E. *Front. Cell. Infect. Microbiol.* **2019**, *9*, 33.
21. Vial, L., Lépine, F., Milot, S., Groleau, M. C., Dekimpe, V., Woods, D. E., Déziel, E. *J. Bacteriol.* **2008**, *190*, 5339–5352.
22. de Maced, M. B., Kimmel, R., Urankar, D., Gazvoda, M., Peixoto, A., Cools, F., Torfs, E., Verschaeve, L., Lima, E. S., Lyčka, A., Milićević, D., Klásek, A., Cos, P., Kafka, S., Košmrlj, J., Cappoen, D. *Eur. J. Med. Chem.* **2017**, *138*, 491–500.
23. Aoki, S., Ye, Y., Higuchi, K., Takashima, A., Tanaka, Y., Kitagawa, I., Kobayashi, M. *Chem. Pharm. Bull.* **2001**, *49*, 1372–1374.
24. Paejo, I., Petrakis, C., Kefalas, P. *J. Pharm. Toxicol. Methods* **2000**, *43*, 183–190.
25. Georgetti, S. R., Casagrande, R., Di Mambro, V. M., Azzolini, A. E., Fonseca, M. J. *AAPS PharmSci.* **2003**, *5*, E20.
26. Sakihama, Y., Cohen, M. F., Grace, S. C., Yamasaki, H. *Toxicology* **2002**, *177*, 67–

80.

27. Stadtman, E. R., Berlett, B. S. *J. Biol. Chem.* **1991**, *266*, 17201–17211.

28. Schwyn, B., Neilands, J. B. *Anal. Biochem.* **1987**, *160*, 47–56.

29. Shinozaki, Y., Kitamoto, H., Sameshima-Yamashita, Y., Kinoshita, A., Nakajima-Kambe, T. *J. Gen. Appl. Microbiol.* **2019**, *65*, 273–276.

30. Parejo, I., Petrakis, C., Kefalas, P. J. *Pharmacol. Toxicol. Methods* **2000**, *43*, 183–190.

3-5 Spectral data

Table of contents

4-Hydroxy-3-methyl-2(1*H*)-quinolone (**9**)

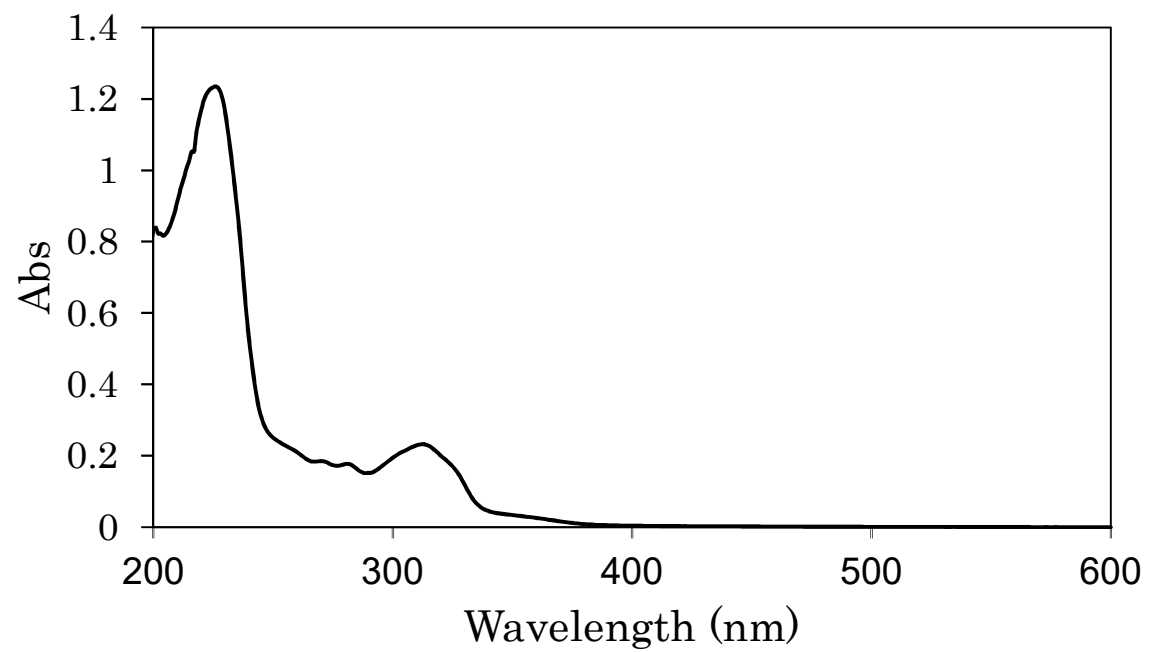
- UV spectrum of natural **9**
- IR spectrum of natural **9**
- UV spectrum of synthetic **9**
- IR spectrum of synthetic **9**
- ¹H NMR of natural (upper) and synthetic (lower) **9** (DMSO-*d*₆, 297 K, 500 MHz)
- ¹³C NMR of natural (upper) and synthetic (lower) **9** (DMSO-*d*₆, 297 K, 125 MHz)
- COSY spectrum of natural **9** (DMSO-*d*₆, 297 K, 500 MHz)
- HSQC spectrum of natural **9** (DMSO-*d*₆, 297 K, 500 MHz)
- HMBC spectrum of natural **9** (DMSO-*d*₆, 298 K, 500 MHz)
- COSY spectrum of synthetic **9** (DMSO-*d*₆, 298 K, 500 MHz)
- HSQC spectrum of synthetic **9** (DMSO-*d*₆, 299 K, 500 MHz)
- HMBC spectrum of synthetic **9** (DMSO-*d*₆, 298 K, 500 MHz)

Ethyl 2-methyl-3-oxo-3-(phenylamino) propanoate

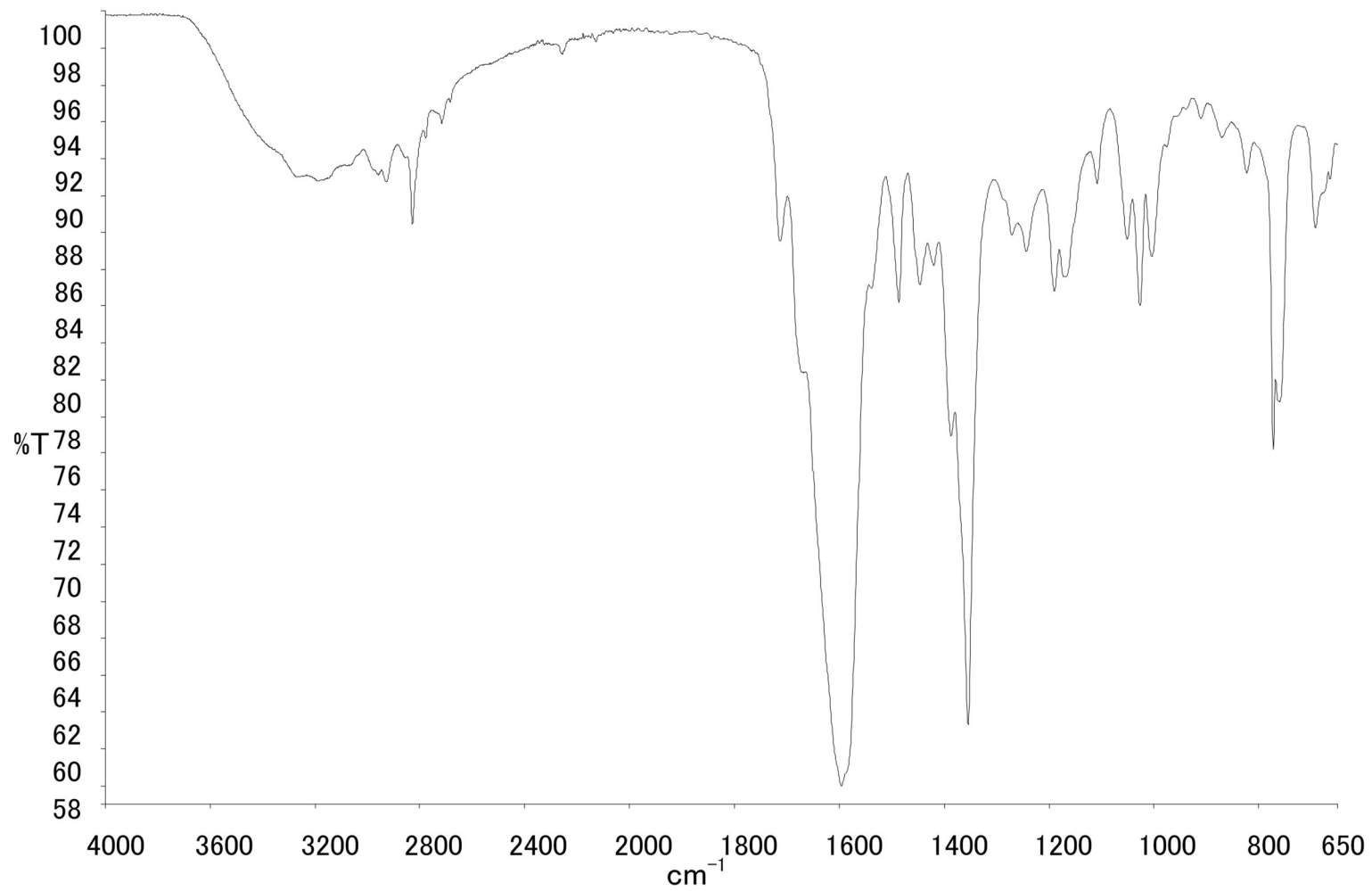
- UV spectrum
- IR spectrum
- ¹H NMR spectrum (CDCl₃, 500 MHz)
- ¹³C NMR spectrum (CDCl₃, 125 MHz)

N-Phenyl-2-methylmalonamic acid

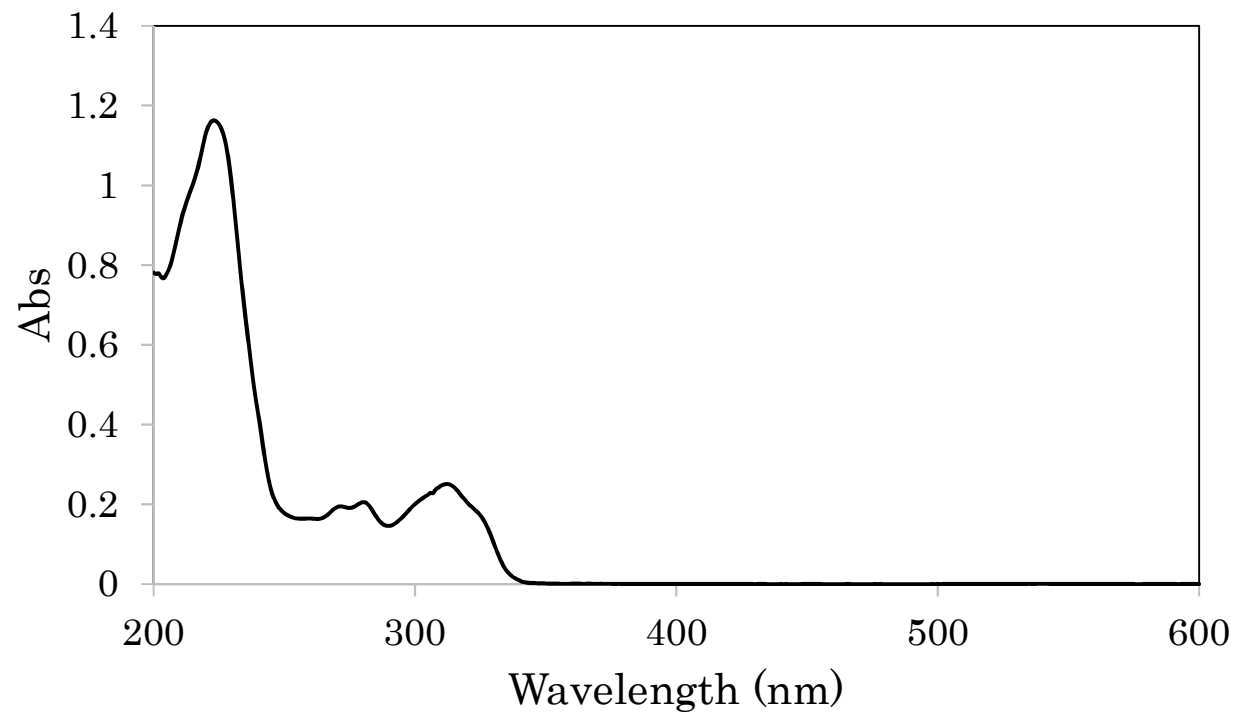
- UV spectrum
- IR spectrum
- ¹H NMR spectrum (DMSO-*d*₆, 500 MHz)
- ¹³C NMR spectrum (DMSO-*d*₆, 125 MHz)



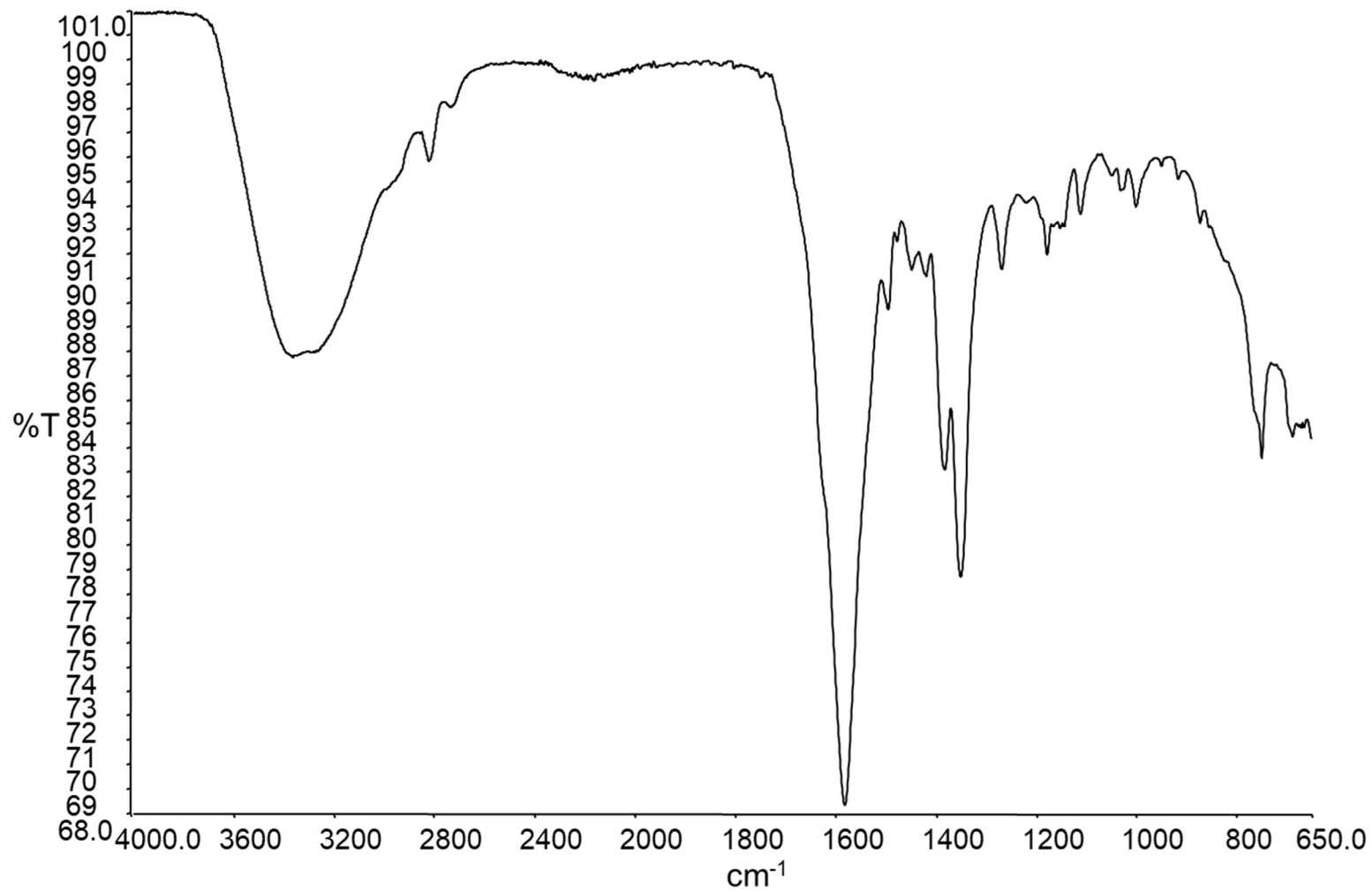
UV spectrum of natural **9**



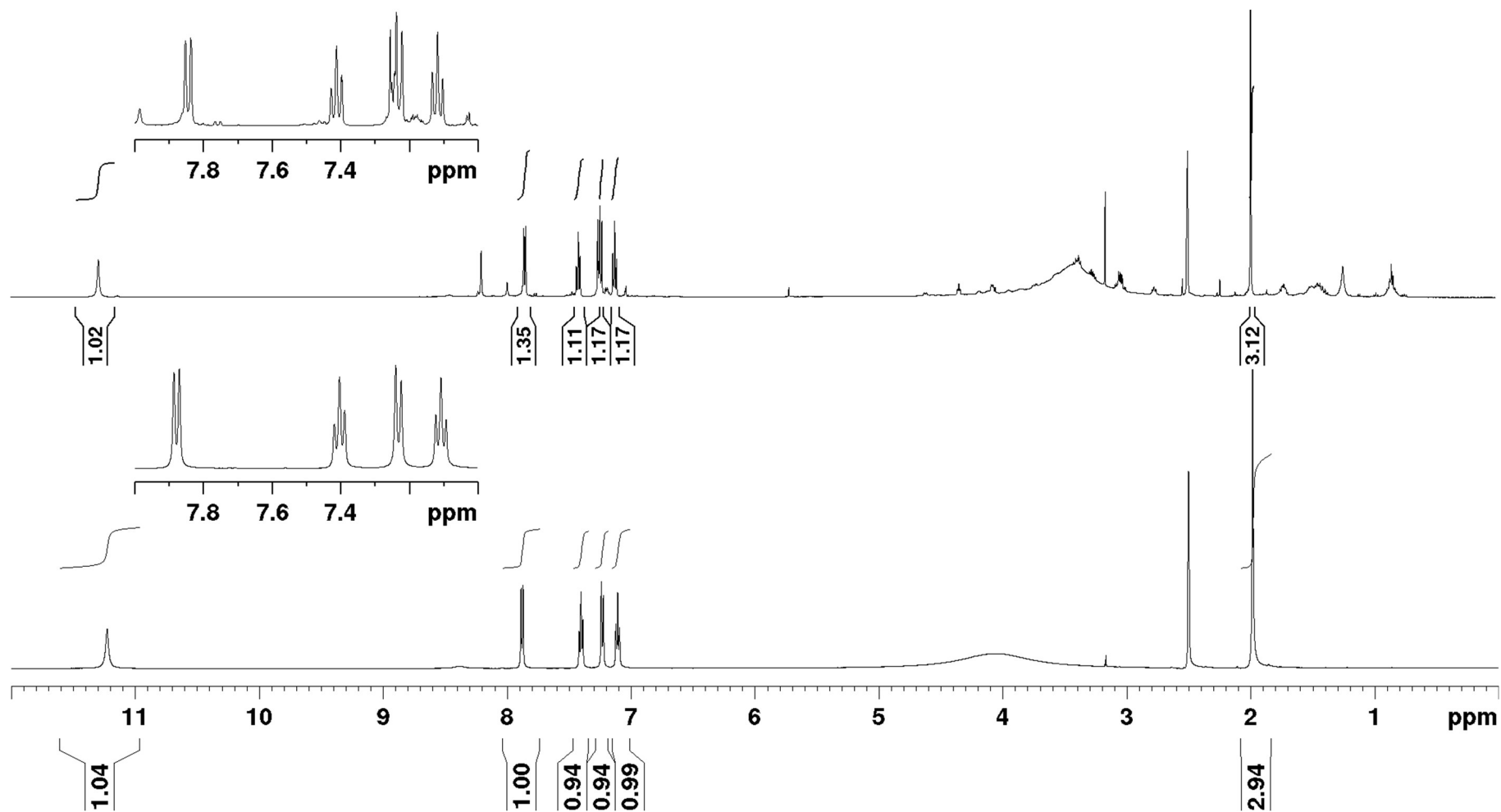
IR spectrum of natural **9**



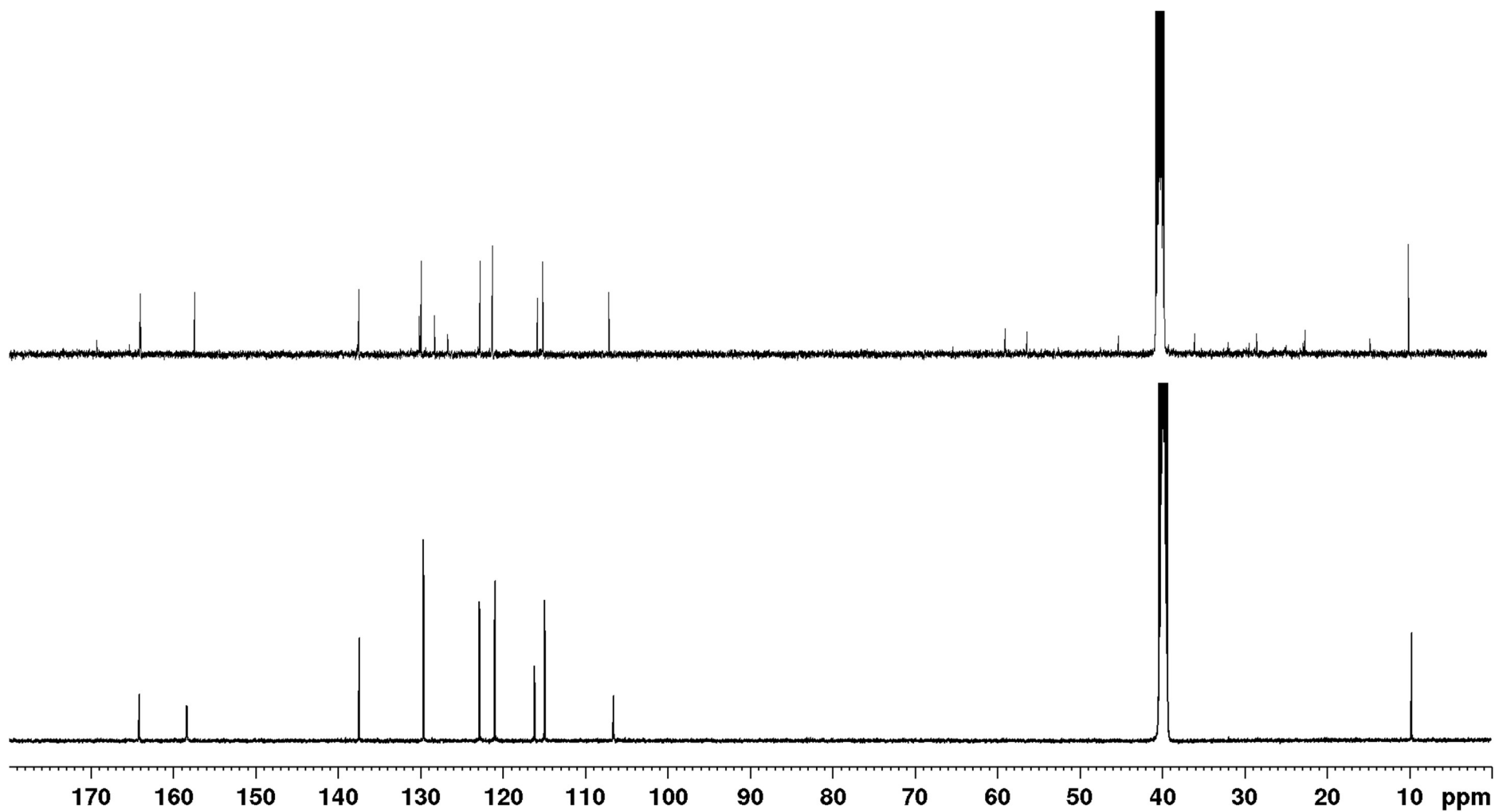
UV spectrum of synthetic **9**



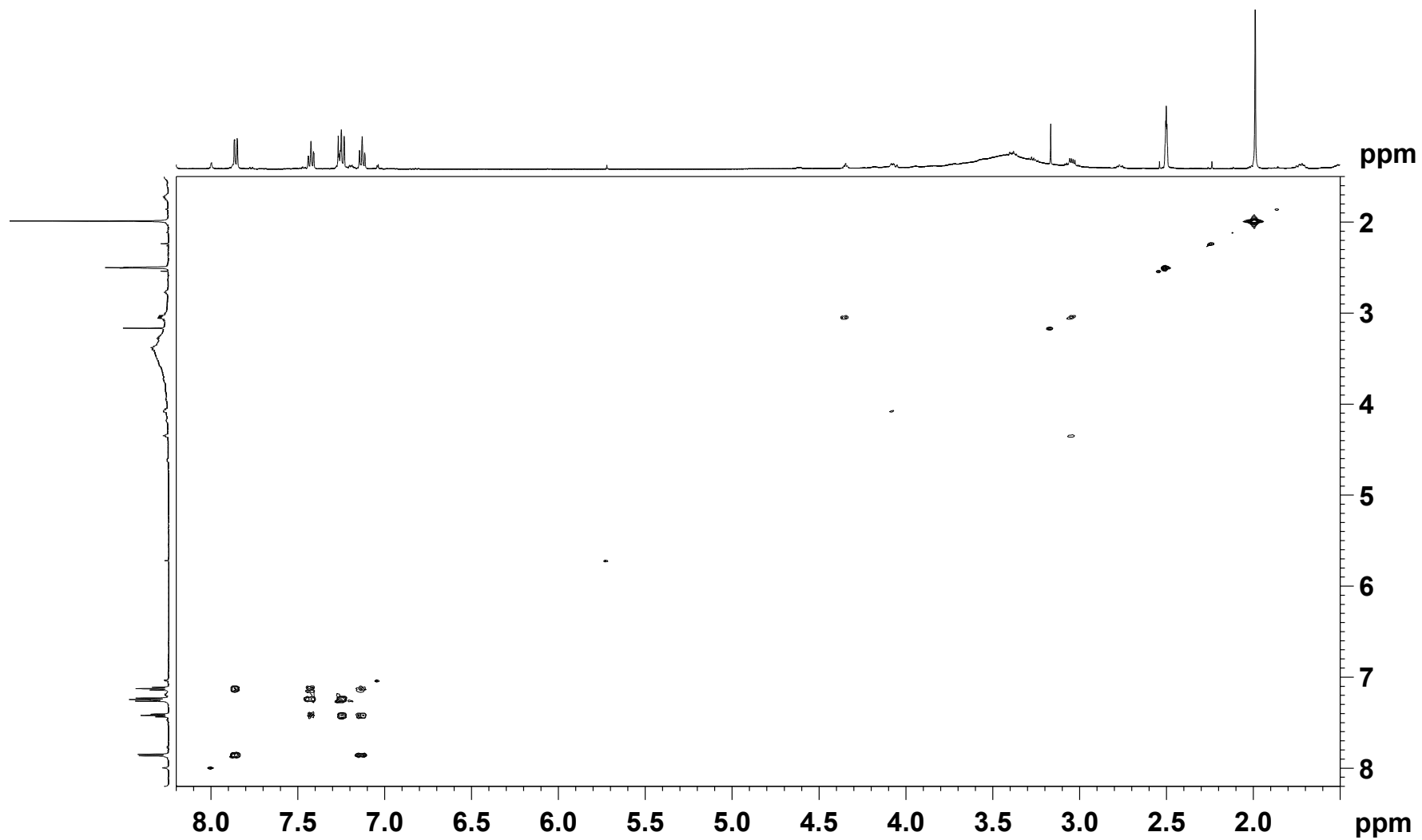
IR spectrum of synthetic **9**

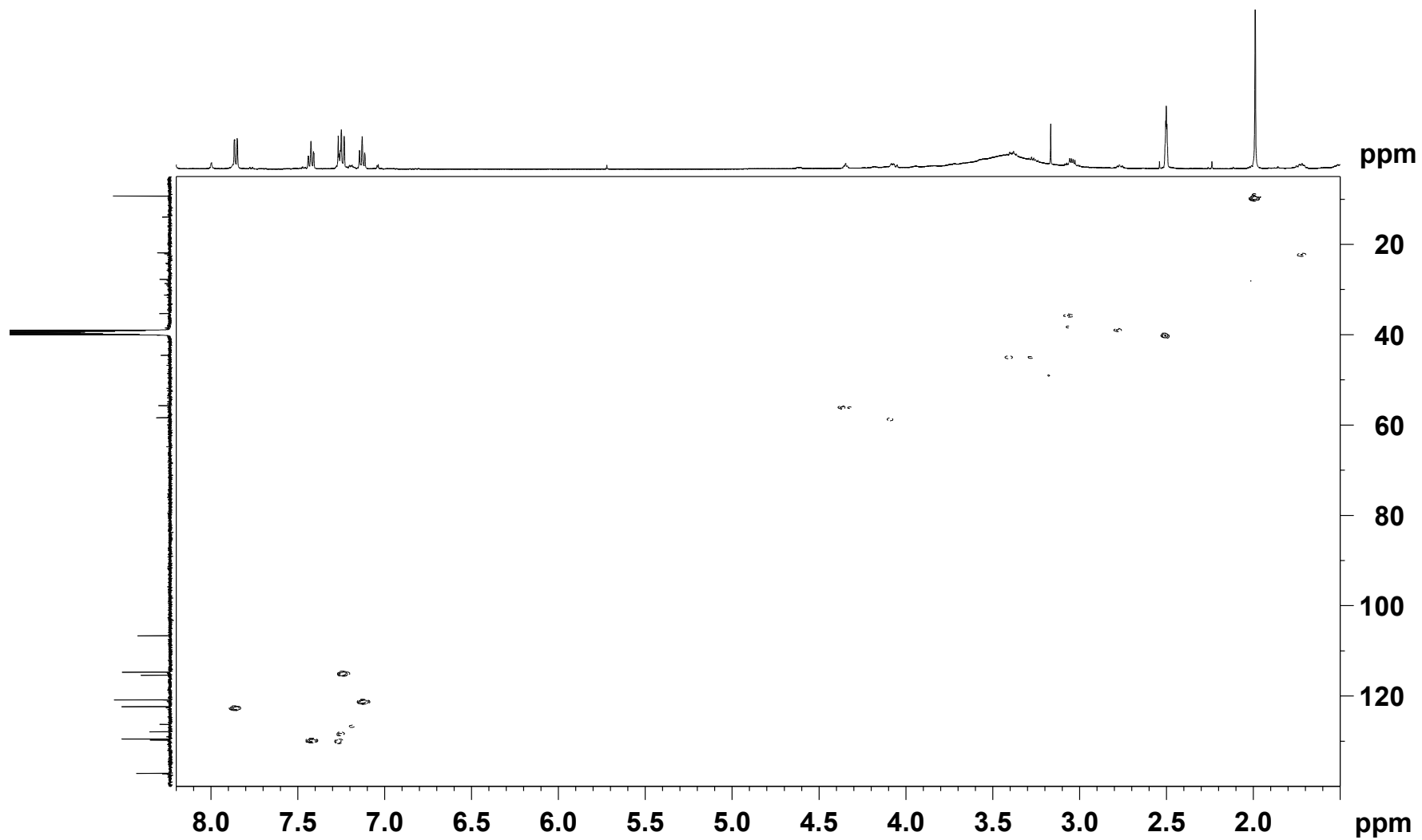


^1H NMR spectra of natural (upper) and synthetic (lower) **9** (500 MHz, 297 K, $\text{DMSO-}d_6$)

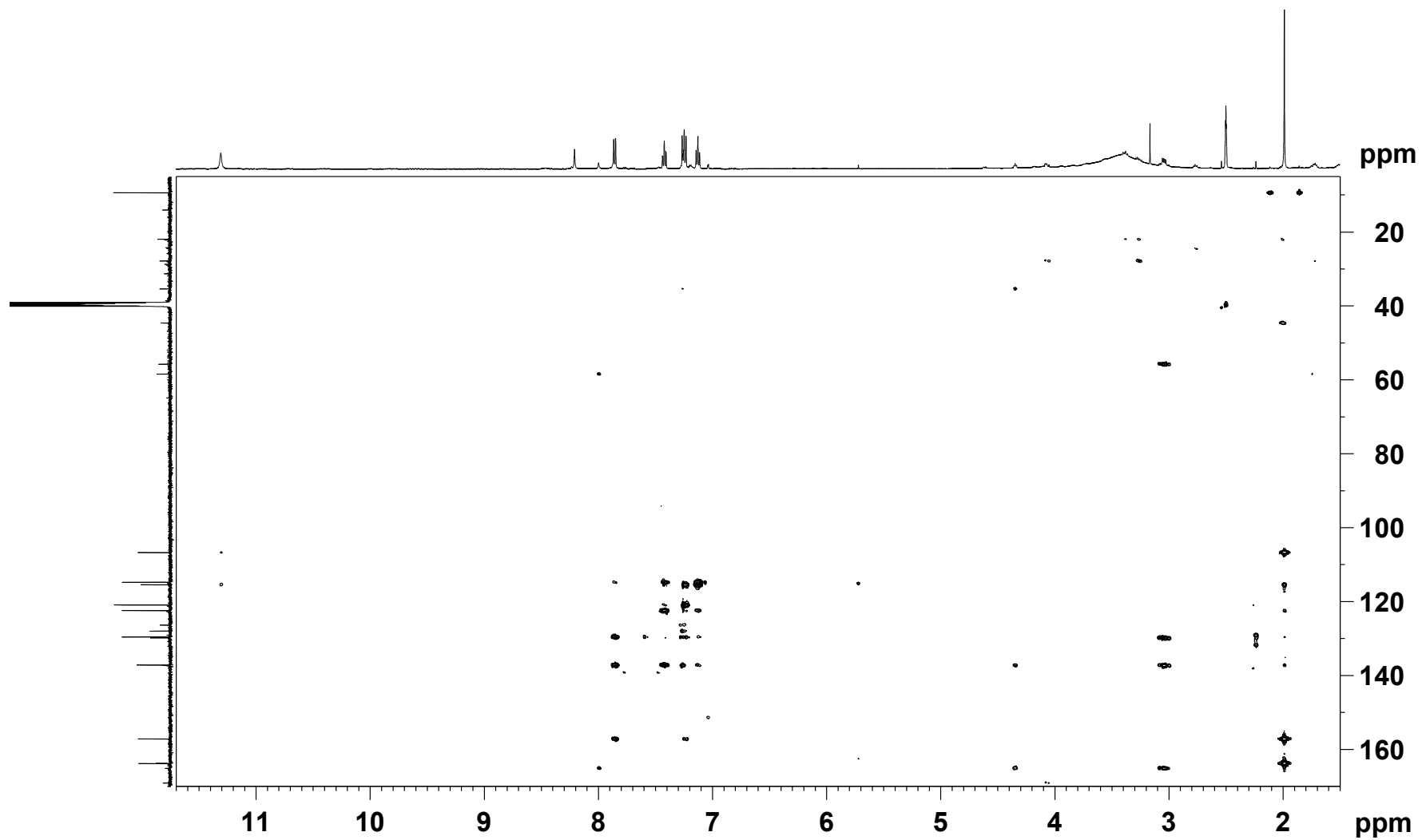


^{13}C NMR spectra of natural (upper) and synthetic (lower) **9** (125 MHz, 297 K, $\text{DMSO-}d_6$)

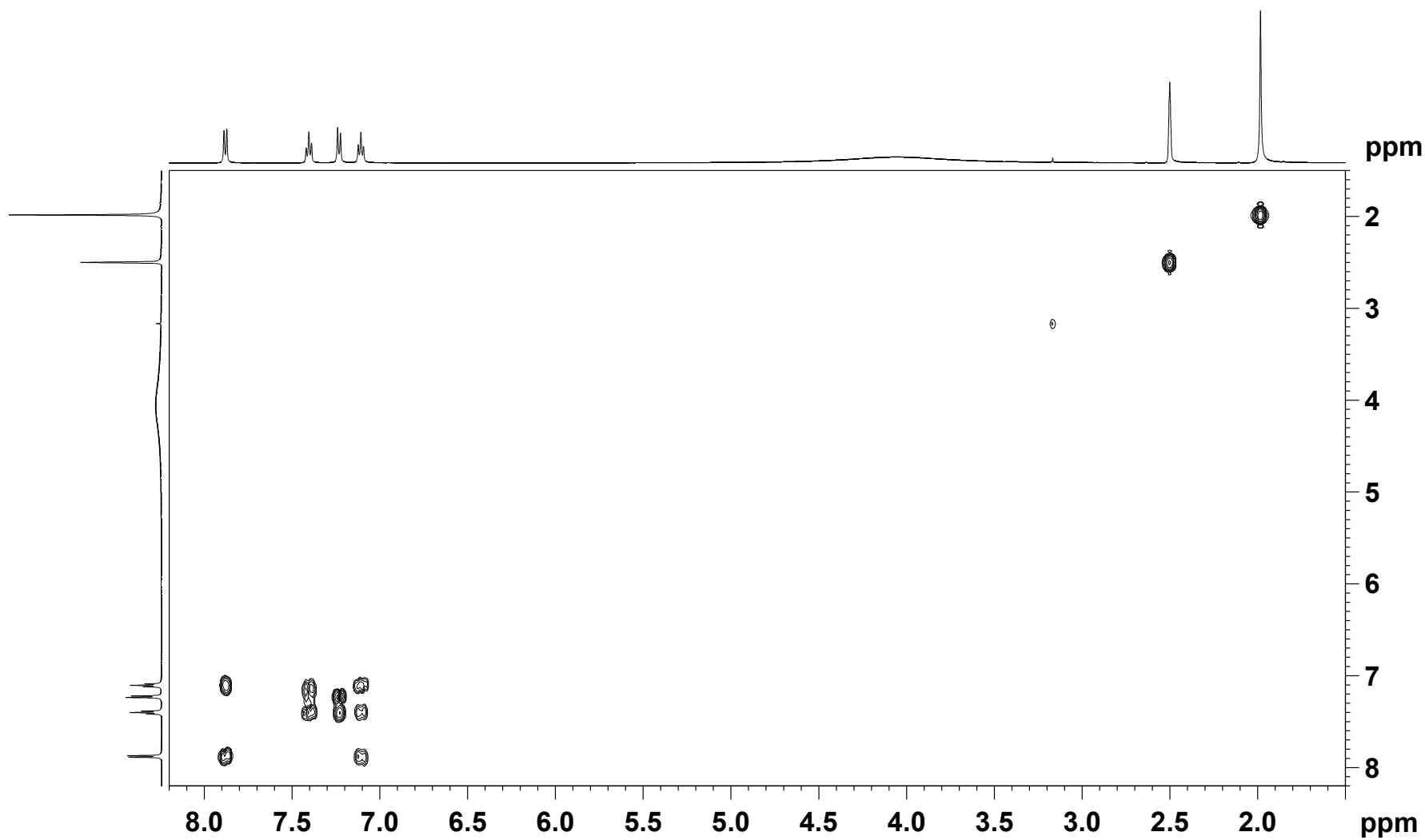


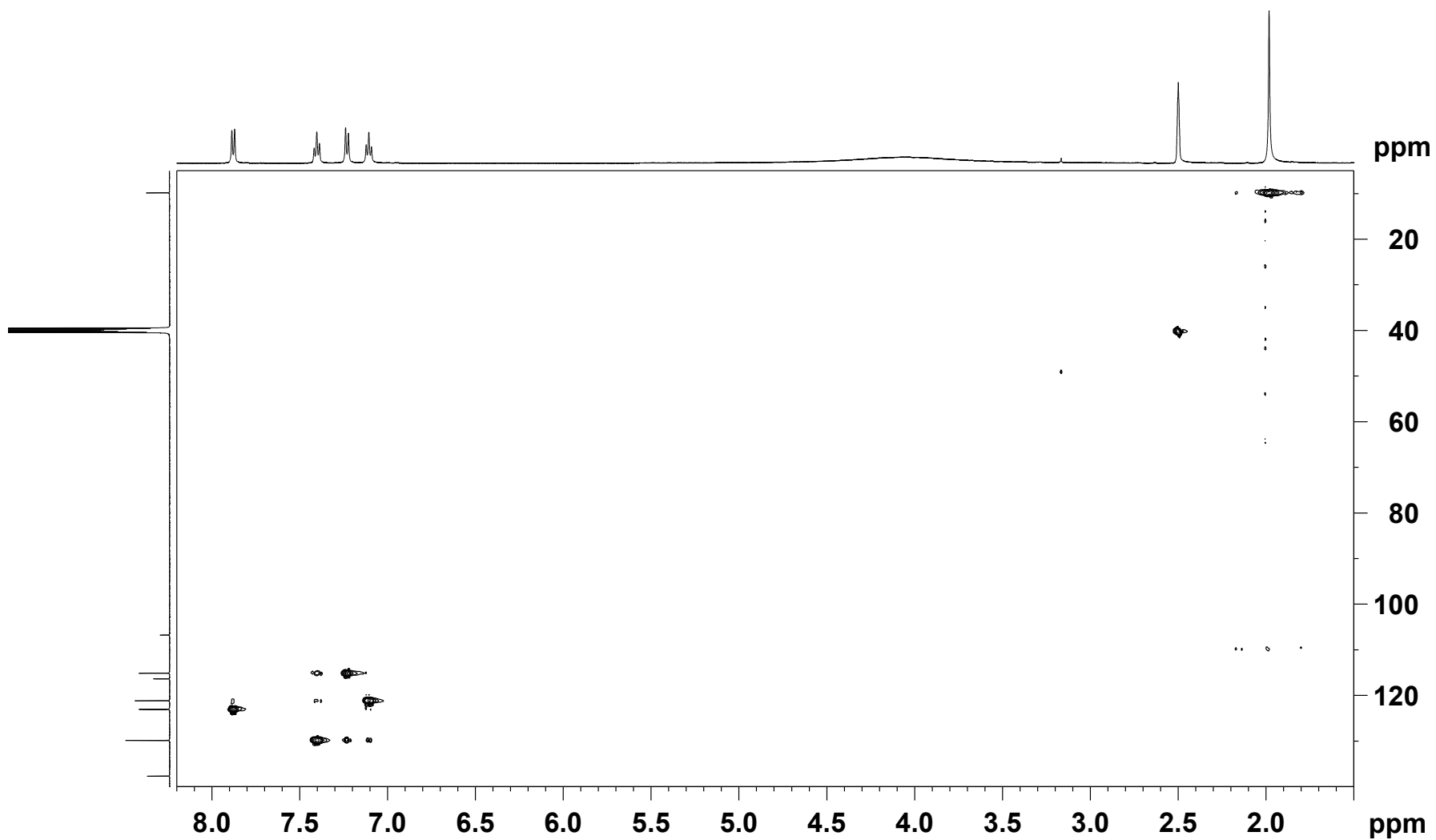


HSQC spectrum of natural **9** (500 MHz, 297 K, DMSO-*d*₆)

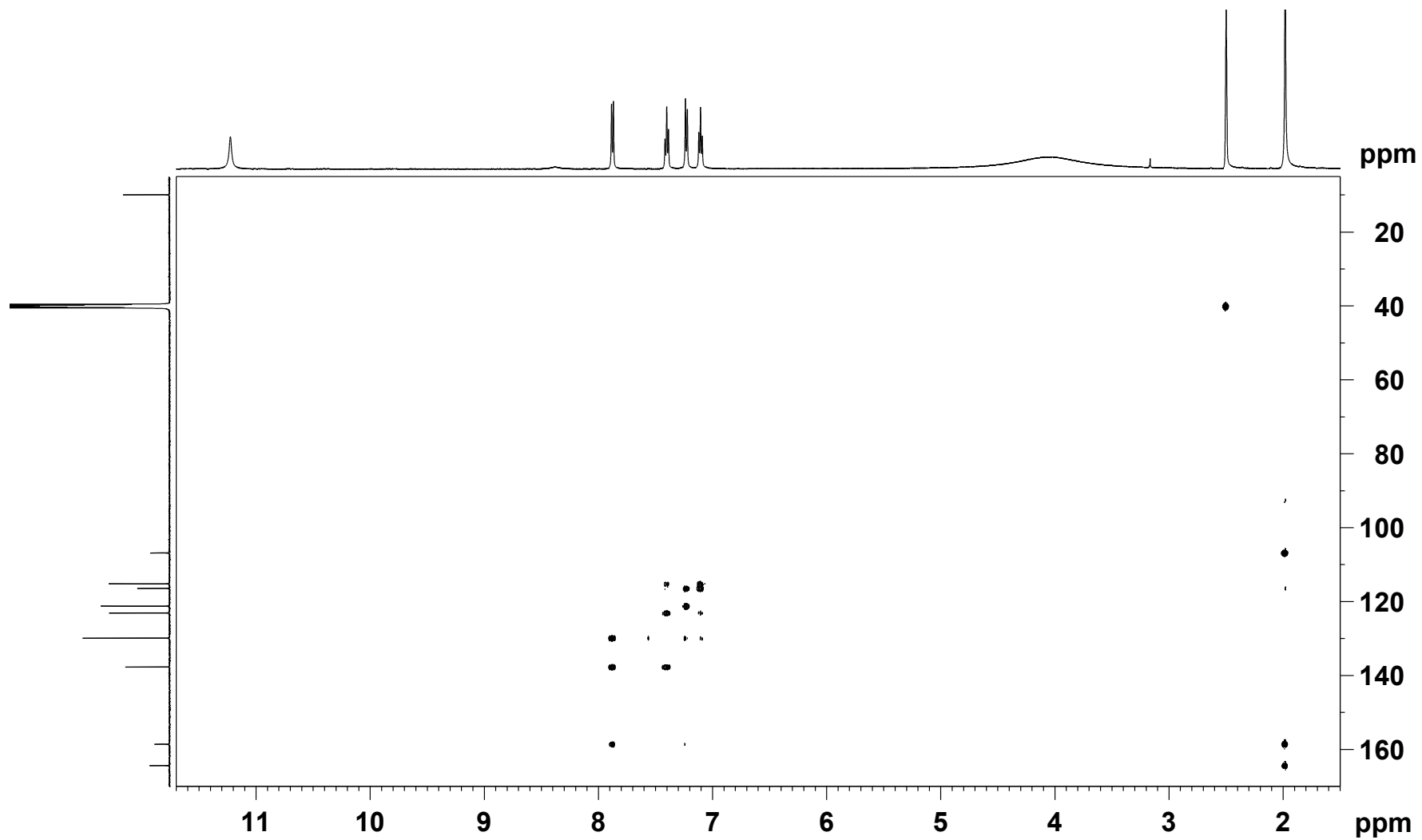


HMBC spectrum of natural **9** (500 MHz, 298 K, DMSO-*d*₆)

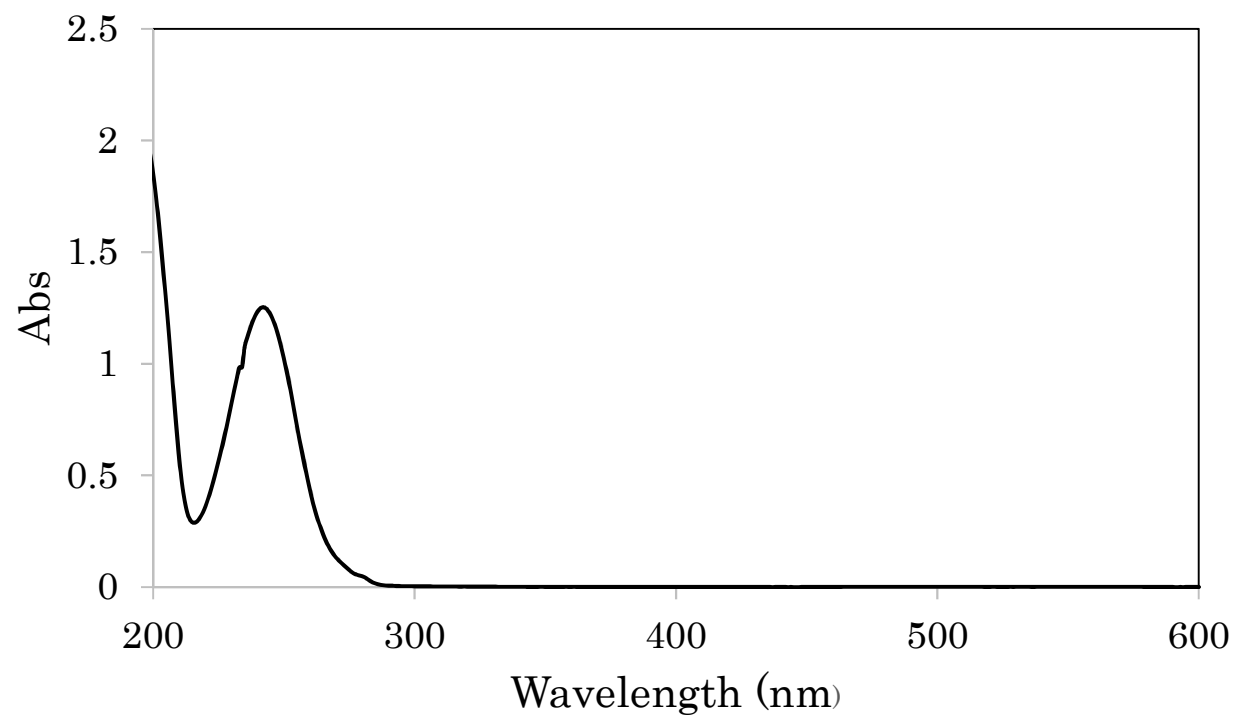




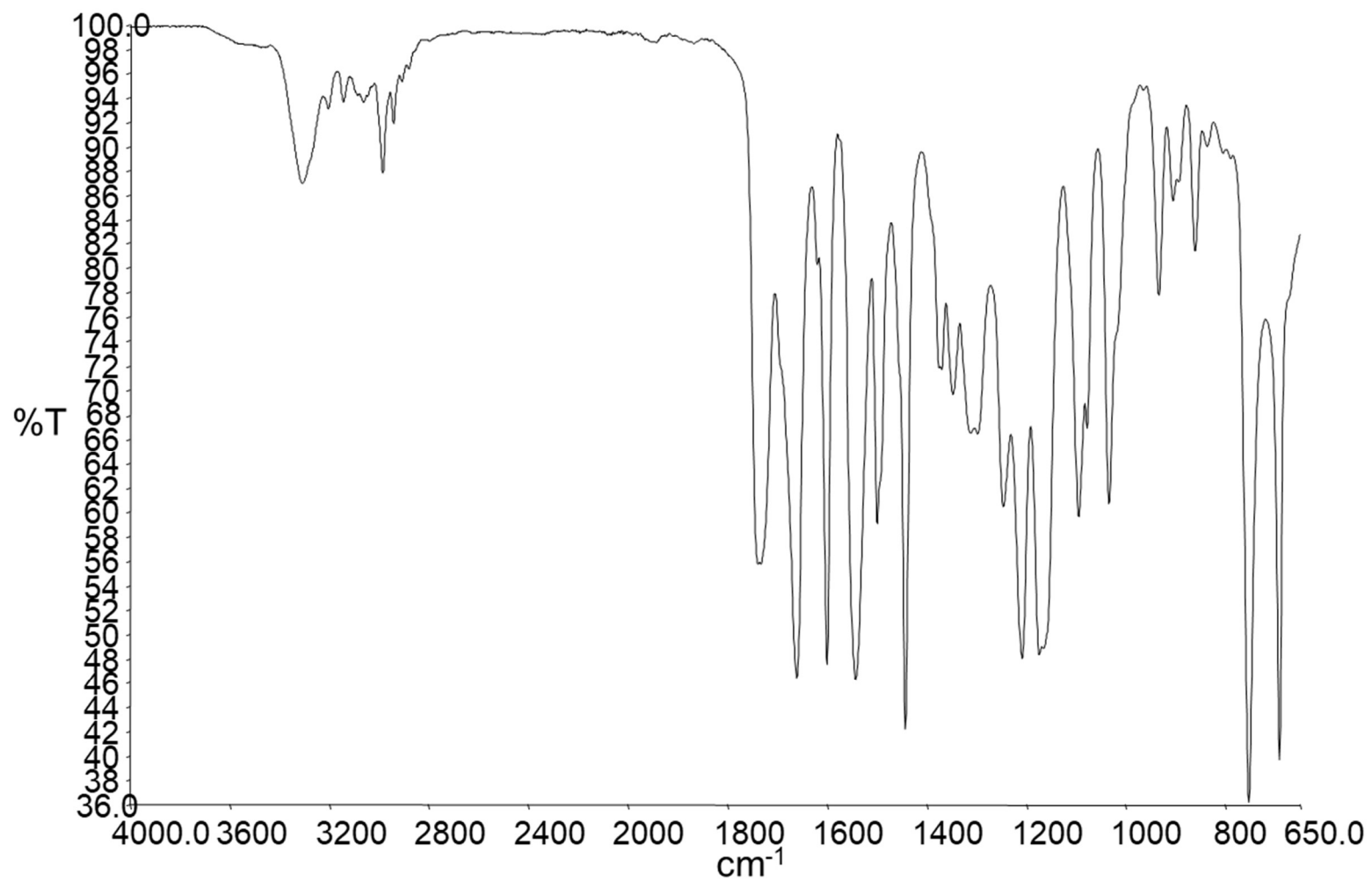
HSQC spectrum of synthetic **9** (500 MHz, 299 K, DMSO-*d*₆)



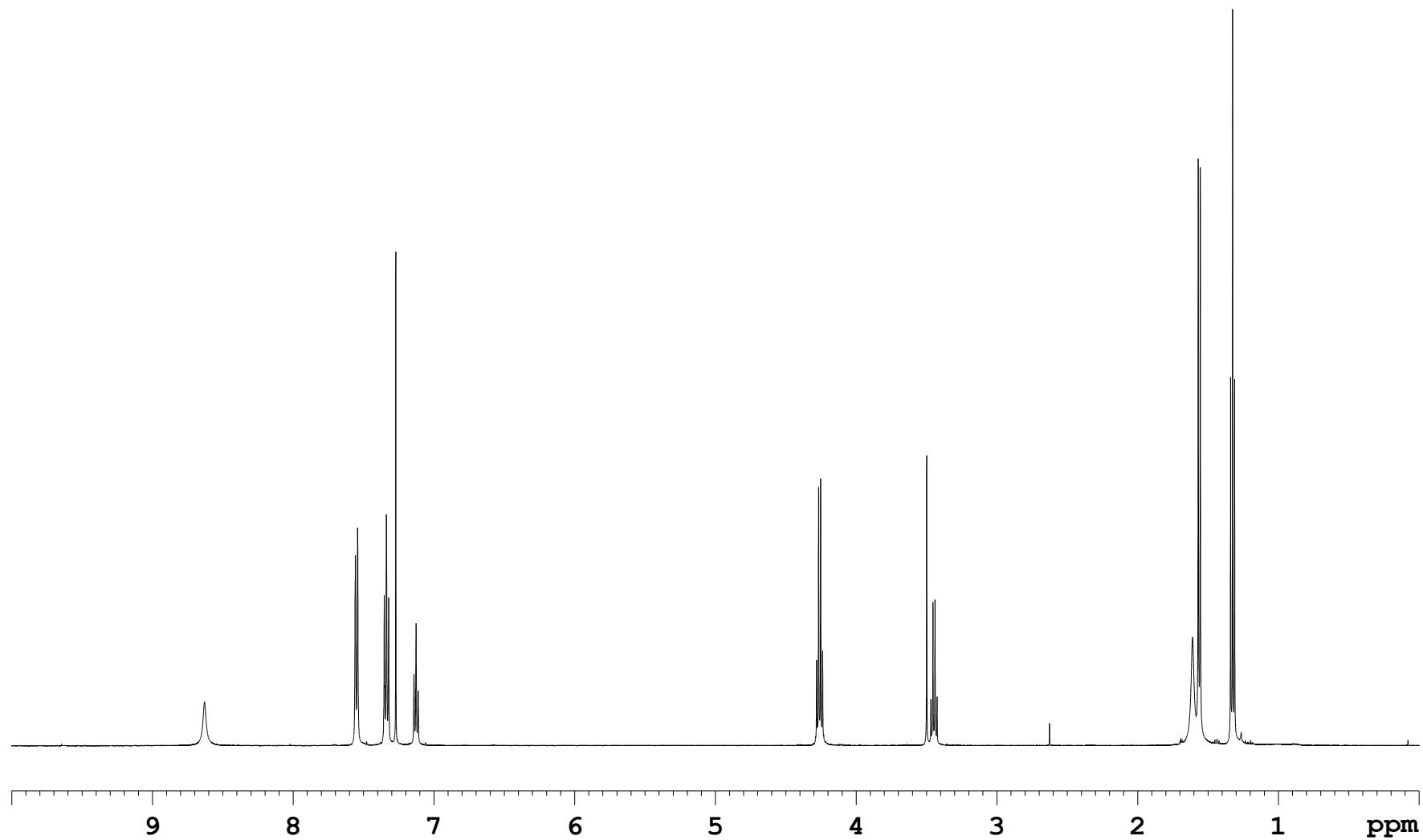
HMBC spectrum of synthetic **9** (500 MHz, 298 K, DMSO- d_6)



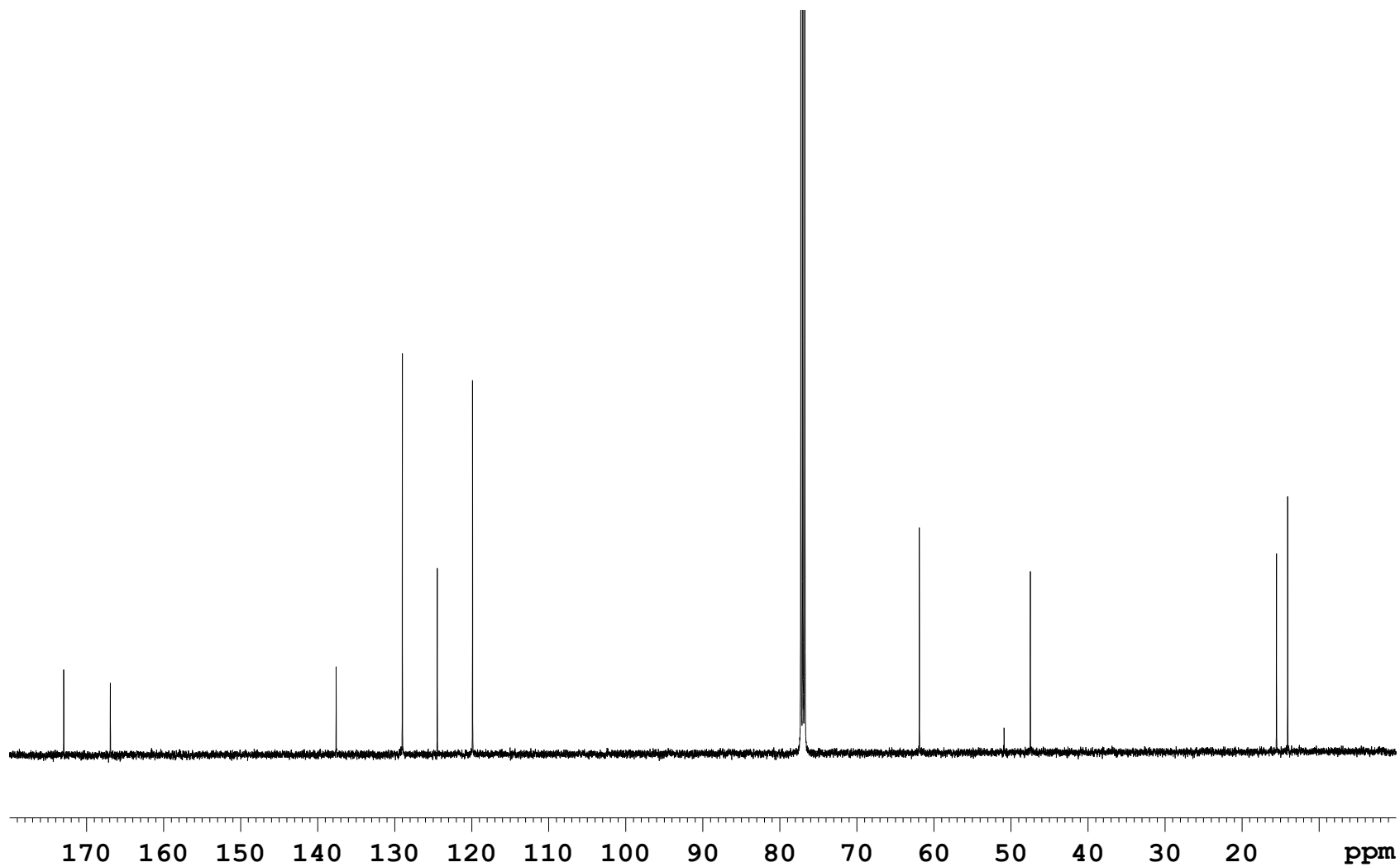
UV spectrum of ethyl 2-methyl-3-oxo-3-(phenylamino) propanoic acid



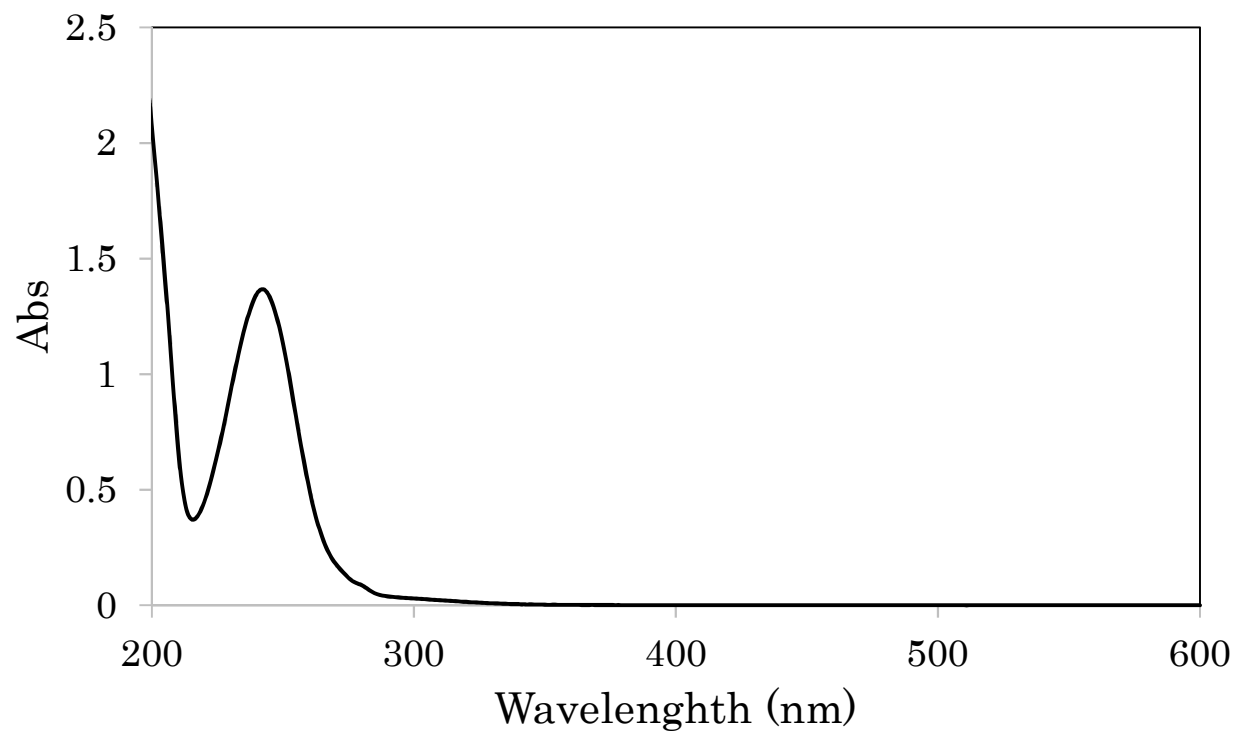
IR spectrum of ethyl 2-methyl-3-oxo-3-(phenylamino) propanoic acid



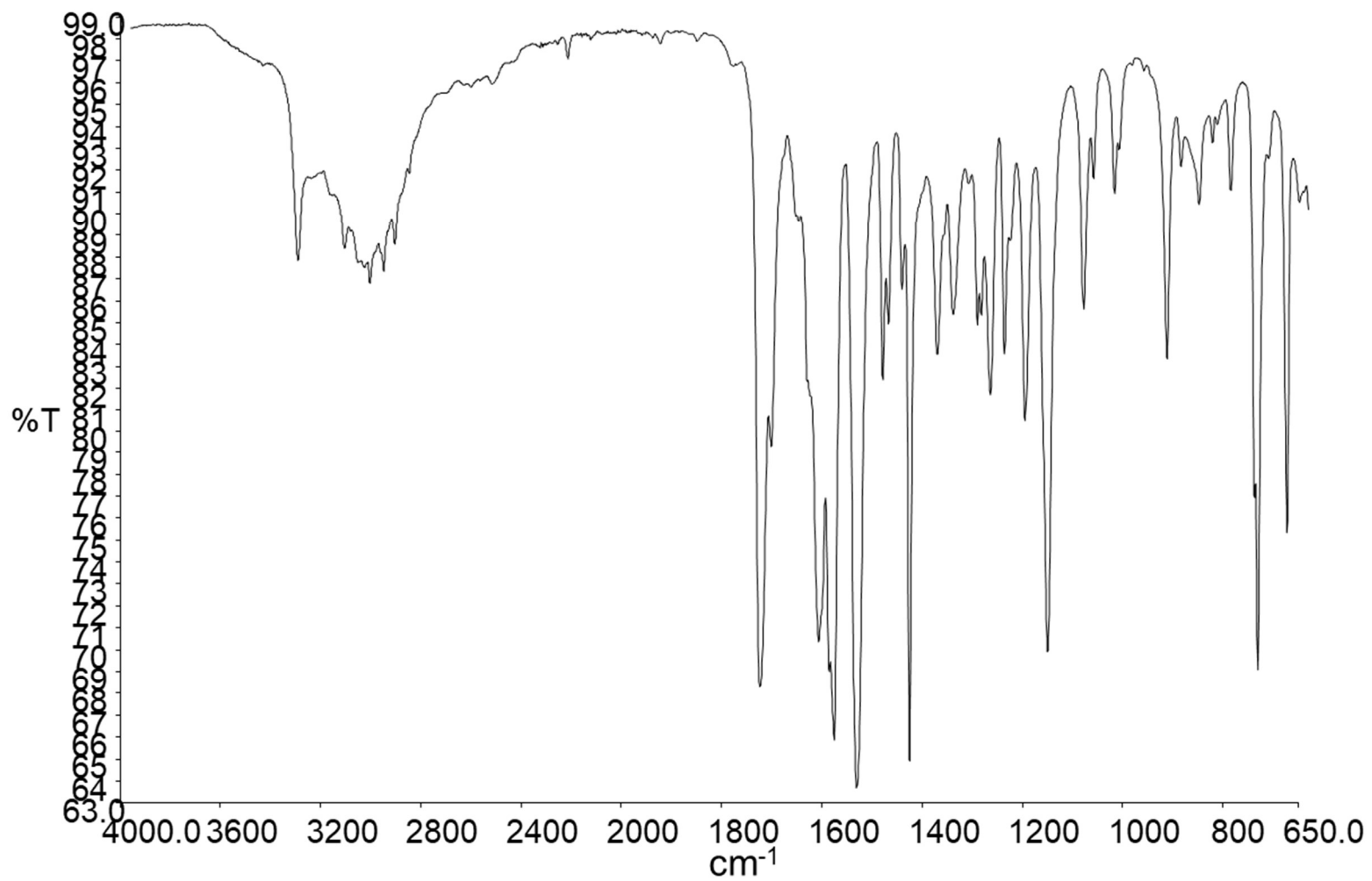
¹H NMR spectrum of ethyl 2-methyl-3-oxo-3-(phenylamino) propanoic acid (500 MHz, CDCl₃)



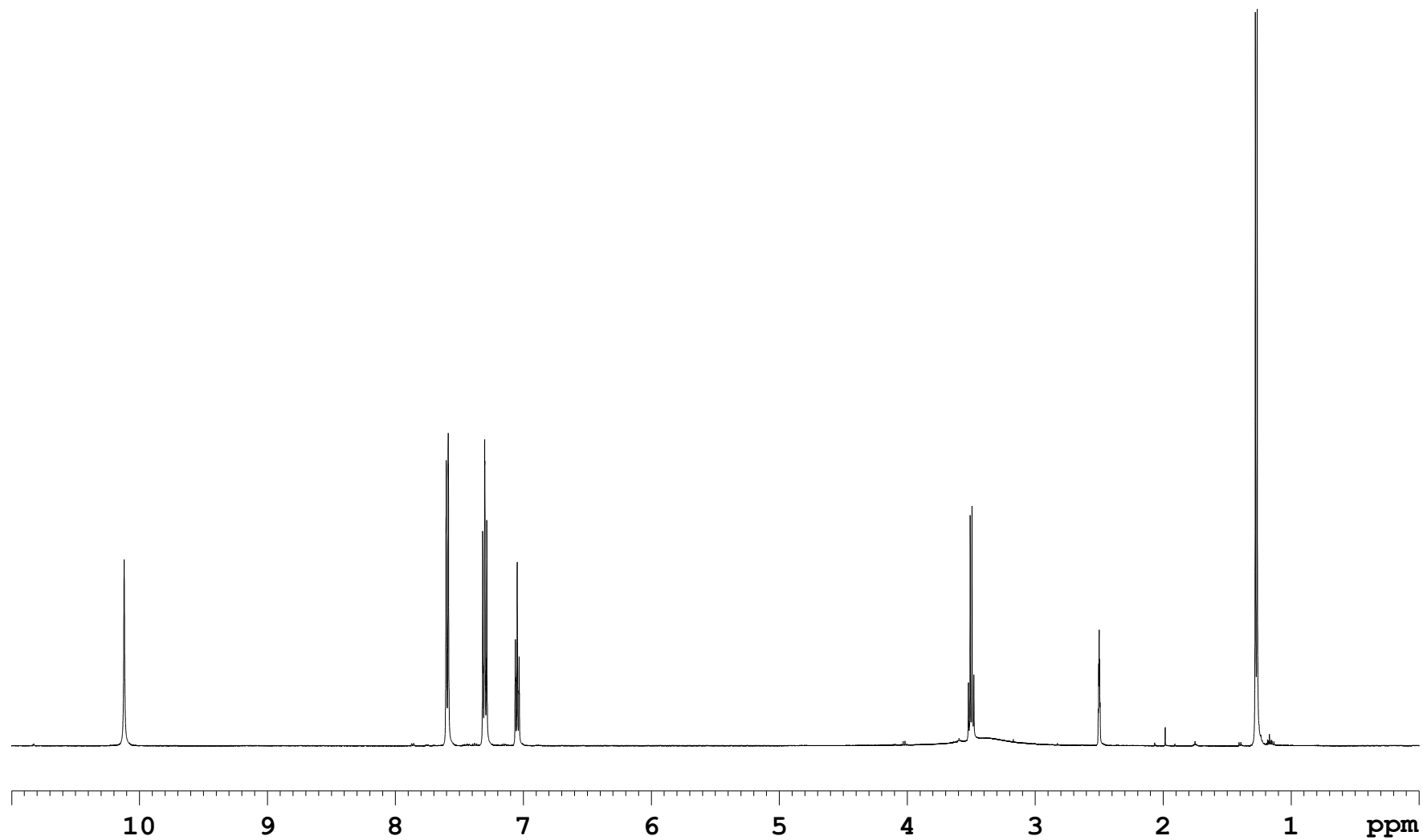
^{13}C NMR spectrum of ethyl 2-methyl-3-oxo-3-(phenylamino) propanoic acid (125 MHz, CDCl_3)



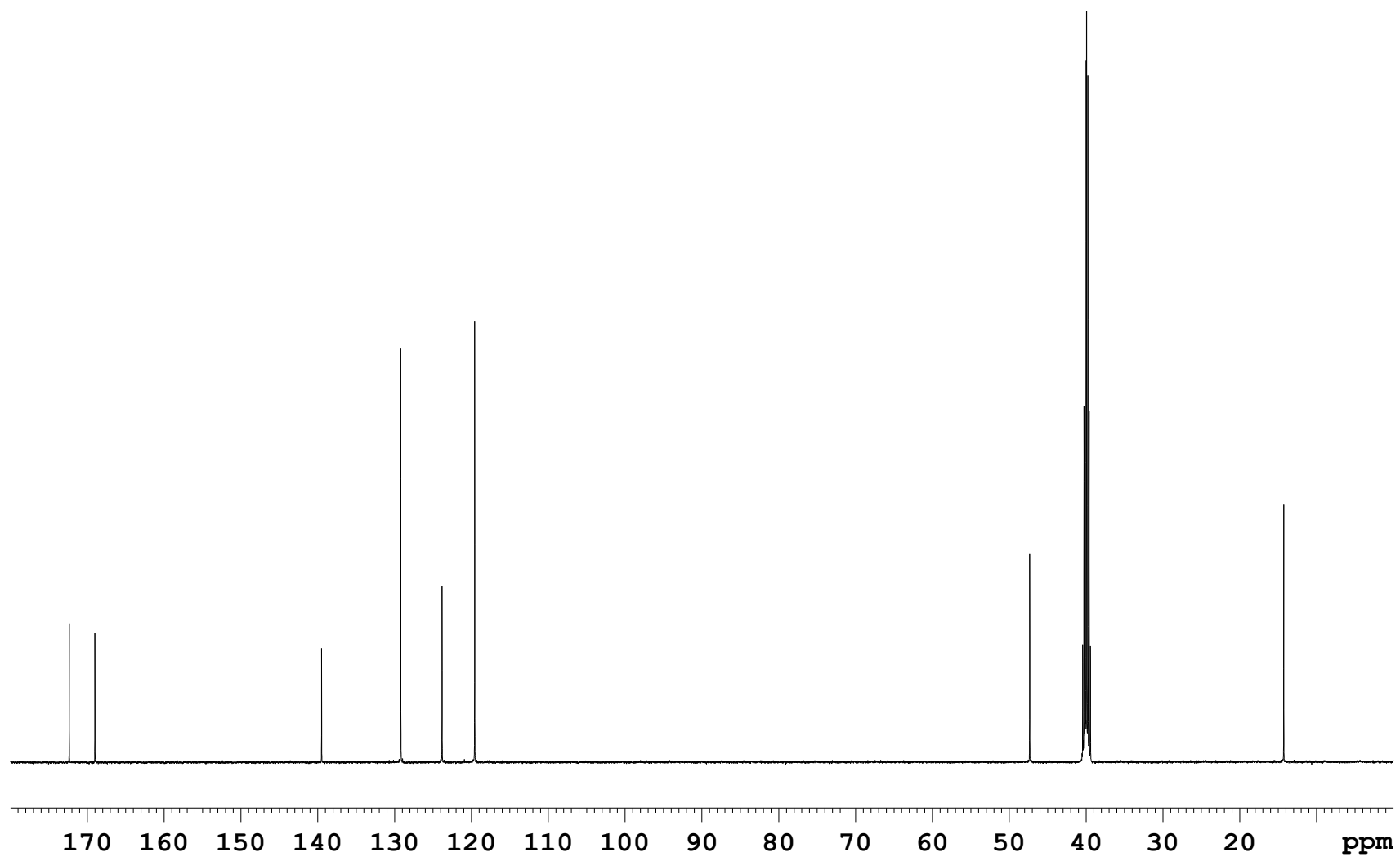
UV spectrum of *N*-phenyl-2-methylmalonamic acid



IR spectrum of *N*-phenyl-2-methylmalonic acid



¹H NMR spectrum of *N*-phenyl-2-methylmalonamic acid (500 MHz, DMSO-*d*₆)



^{13}C NMR spectrum of *N*-phenyl-2-methylmalonic acid (125 MHz, $\text{DMSO-}d_6$)

CHAPTER 4

Three new *O*-isocrotonyl-3-hydroxybutyric acid congeners produced by a sea anemone-derived marine bacterium of the genus *Vibrio*

4-1 Background

In Chapters 2 and 3, three new quinolone metabolites were isolated from two strains with different origins that belongs to the genus *Burkholderia*, a terrestrial taxon that contains many pathogenic species. The results substantiated the validity of targeting pathogenic bacteria for prospecting new bioactive molecules. To gain further support to this strategy, a strain from another pathogenic lineage, the genus *Vibrio*, indigenous to marine environments, was studied in this chapter.

In our laboratory, marine bacteria associated with invertebrates have been the focus of our research, because the number of new compounds from microorganisms associated with or symbiotic to the host invertebrates is quite small [1-4]. Recently, some new natural products were isolated from marine bacteria associated with invertebrates in our laboratory such as bulbimidazoles A–C, (6*E*,8*Z*)- and (6*E*,8*E*)-5-oxo-6,8-tetradecadienoic acids and (2*Z*,4*E*)-3-methyl-2,4-decadienoic acid [5-7]. The discovery further confirmed that marine bacteria associated with invertebrates are emerging source of new compounds. It is common knowledge that marine invertebrates, especially sedentary sea anemones, are evolved with rich sources of bioactive metabolites [8]. The related studies had clarified that the secondary metabolites produced from the associated microorganisms could transport into the sea anemone tissue [9]. Hence, exploitation of sea anemone-associated bacteria could solve the supply problem of raw materials. In this study, ten sea anemone-associated bacteria were collected.

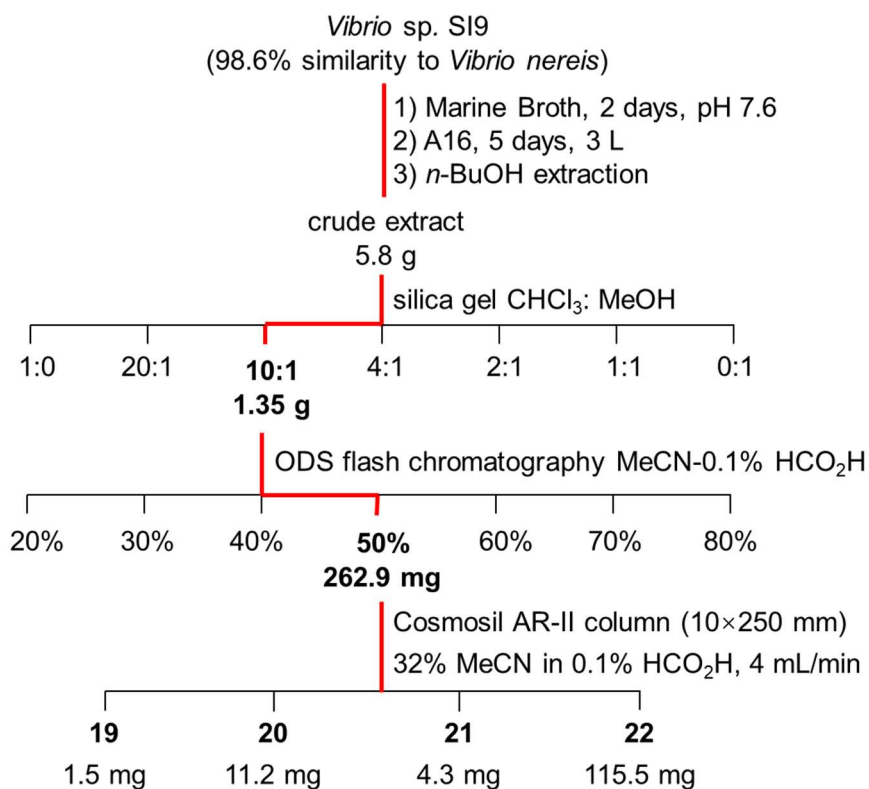
UV spectra are one of the useful traits to find a new natural compound. In this study, HPLC-UV screening was used to directly detect secondary metabolites from ten sea anemone-associated bacteria cultured in three types of fermentation media. The screening result showed that a sea anemone-derived marine bacterium SI9 of the genus *Vibrio* cultured in medium A16 was considered as promising because an extract isolated from SI9 had many absorption peaks at 210 nm and 230 nm. Even though this absorption spectrum of UV is not novel enough, a series of same absorption spectrum

appeared at the same time not identified in our laboratory.



Figure 4-1. *Vibrio* sp. SI9 on Marine Agar.

Thus, *Vibrio* SI9 was cultured, extracted and purified as described below to obtain three new *O*-isocrotonyl-3-hydroxybutyric acid **19-21** and one known 3-hydroxybutyric acid **22** (Scheme 4-1 and Figure 4-2).



Scheme 4-1. Isolation of **19-22** from *Vibrio* sp. SI9.

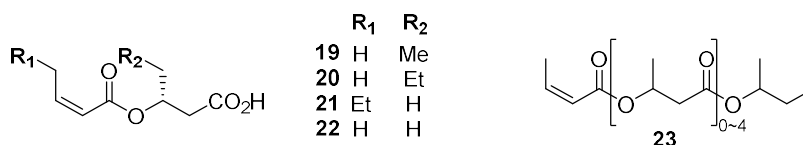


Figure 4-2. Structures of **19-22** and *O*-isocrotonyl-oligo(3-hydroxybutyrate).

4-2 Results and Discussion

4-2-1 Fermentation and isolation

The fermentation broth of strain SI9 was extracted with the same volume of *n*-BuOH, and then the concentrated butanol extract was purified by silica gel chromatography, ODS chromatography and reversed-phase HPLC to yield four acyloxy fatty acids **19** (1.5 mg), **20** (11.2 mg), **21** (4.3 mg) and **22** (135.5 mg) from the one of the mid-polar fractions.

4-2-2 Structure Determination

¹H NMR spectra of **19-22** showed the same splitting patterns (see Supporting Information and Tables 4-1) and a pair of mutually coupled double-doublet resonances. It implied that **19-22** share the same core structure. In addition, ¹³C NMR spectroscopic data indicated the presence of two carboxy, two olefinic, and one oxygenated carbon resonances (see Supporting Information). Meanwhile, additional analysis of a HSQC spectrum confirmed the presence of two methyl groups and one to three aliphatic methylene(s). Analysis of ESITOFMS ion peaks [M+Na]⁺ revealed that the molecular formula was C₉H₁₄O₄ for **19**, C₁₀H₁₆O₄ for **20** and **21**, and C₈H₁₂O₄ for **22**. The structural differences of **19-22** turned out to be attributed to the presence of one to two methylene unit. Thus, **19-22** were confirmed to be a series of acyclic compounds with varying length of aliphatic chains.

Table 4-1: NMR data for **19-22** in CDCl₃.

19				
No.	¹³ C	¹ H (J in Hz), integr.	COSY	HMBC ^a
3-hydroxy-4-methylbutyric acid				
1	175.0			
2	38.4	2.68, dd (7.3, 15.8), 1H	3	1, 3, 4
		2.61, dd (5.5, 15.9), 1H	3	1, 3, 4
3	70.8	5.22, brqui (6.3), 1H	2, 4	1, 2, 4, 5, 1'
4	26.9	1.71, m, 2H	3, 5	2, 3, 5
5	9.4	0.94, t (7.4), 3H	4	3, 4
isocrotonic acid				
1'	165.9			
2'	120.5	5.78, dq (11.5, 1.8), 1H	3'	1', 4'
3'	145.6	6.34, dq (11.5, 7.3), 1H	2', 4'	1', 4'
4'	15.4	2.13 dd (7.3, 1.8) 3H	3'	1', 2', 3'
20				
No.	¹³ C	¹ H (J in Hz), integr.	COSY	HMBC ^a
4-ethyl-3-hydroxybutyric acid				
1	176.2			
2	39.0	2.68, dd (7.2, 15.9), 1H	3	1, 3, 4
		2.60, dd (5.6, 15.8), 1H	3	1, 3, 4
3	69.5	5.25, m, 1H	2, 4	1, 2, 4, 5, 1'
4	36.1	1.61, m, 2H	3, 5	2, 3, 5, 6
5	18.4	1.35, m, 2H	4, 6	3, 4, 6
6	13.8	0.91, t (7.4), 3H	5	3, 4, 5
isocrotonic acid				
1'	165.8			
2'	120.5	5.74, qd (11.4, 1.8), 1H	3'	1', 4'
3'	145.5	6.30, m, 1H	2', 4'	1', 4'
4'	15.4	2.10, dd (7.3, 1.6), 3H	3'	1', 2', 3'

21				
No.	¹³ C	¹ H (J in Hz), integr.	COSY	HMBC ^a
3-hydroxybutyric acid				
1	175.6			
2	40.5	2.73, dd (7.2, 15.9), 1H	3	1, 3, 4
		2.56, dd (5.7, 15.9), 1H	3	1, 3, 4
3	66.5	5.30, brsep (6.3), 1H	2, 4	1, 2, 4, 1'
4	19.9	1.35, d (6.2), 3H	3	2, 3
(Z)-2-hexenoic acid				
1'	165.6			
2'	109.6	5.73, dt (11.6, 1.6), 1H	3'	1', 4'
3'	150.9	6.23, dt (11.5, 7.5), 1H	2', 4'	1', 4', 5'
4'	31.0	2.61, qd (7.4, 1.6), 2H	3', 5'	2', 3', 5', 6'
5'	22.3	1.46, sex (7.4), 2H	4', 6'	3', 4', 6'
6'	13.7	0.94, t (7.3), 3H	5'	4', 5'

22				
No.	¹³ C	¹ H (J in Hz), integr.	COSY	HMBC ^a
3-hydroxybutyric acid				
1	175.4			
2	40.5	2.73, dd (7.1, 15.9), 1H	3	1, 3, 4
		2.56, dd (5.5, 15.9), 1H	3	1, 3, 4
3	66.5	5.32, brsep (6.3), 1H	2, 4	1, 2, 4, 1'
4	19.9	1.35, d (6.3), 3H	3	2, 3
(Z)-2-hexenoic acid				
1'	165.6			
2'	120.5	5.76, dt (11.5, 1.6), 1H	3'	1', 4'
3'	145.5	6.33, dq (11.5, 7.3), 1H	2', 4'	1', 4'
4'	15.4	2.13, dd (7.2, 1.9), 3H	3'	2', 3'

^aHMBC correlations from proton to indicated carbons.

Based on the analysis of a COSY spectrum, the smallest congener **22** was consisted of two C₃ fragments, 2-propene (H2'-H3'-H4') and 2-methylethylenoxy (H2-H3-H4) groups. The geometry of double bond was determined to be *Z*-configured, based on a vicinal coupling constant (11.5 Hz, Table 4-2). Both fragments showed HMBC correlations to the same carboxy carbon C1 (δ_c 165.6), revealing an intervening ester linkage, which was in accordance with IR absorbance at 2641 cm⁻¹. Finally, the HMBC spectrum showed correlations from the methylene proton H₂ and an oxymethine proton H₃ to the other carboxy carbon C1 (δ_c 175.3), placing a carboxylic acid functionality on the methylene group. This structure of **22** was determined to be *O*-

isocrotonyl-3-hydroxybutyric acid (Figure 4-2).

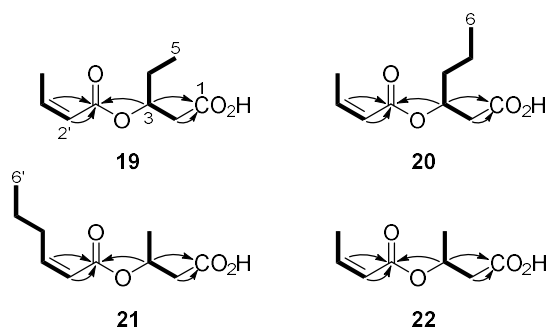


Figure 4-3. COSY (bold lines) and selected HMBC (arrows) correlations for **19-22**.

Based on the similar NMR spectra between **19-21** and **22** (Tables 4-1 and 4-2), the same sequence of structure analysis established the structure **19-21**. The molecular formula $C_9H_{14}O_4$ of **19** implied extra extension C_1 on the butyric acid units. The same specification happened to **20** with extra extensions C_2 in the same positions, while in **21**, an extra C_2 extension occurred on the isocrotonyl group, as shown by the connectivity established by the analysis of COSY spectra in Figure 2. Thus, compounds **19-21** were confirmed as *O*-isocrotonyl-3-hydroxypentanoic acid, *O*-isocrotonyl-3-hydroxyhexanoic acid, and *O*-(*Z*)-2-hexenoyl-3-hydroxybutyric acid, respectively (Figure 4-2).

4-2-3 Absolute Configuration

Fatty acid **22** was first isolated as colorless oil from *Vibrio* sp. C-984 by Kikuchi et al [10], although, the absolute configuration of the chiral carbons was not determined and spectroscopic data have not been assigned. In order to determine the absolute configuration of C3 in **19-22**, the (*S*)- or (*R*)-phenylglycine methyl ester (PGME) was used [11]. Compounds **19-22** and (*S*)- or (*R*)-PGME were mixed and reacted by the action of *N*, *N'*-diisopropylcarbodiimide (DIC) and *N*, *N*-dimethylaminopyridine (DMAP) in CH_2Cl_2 , followed by purification by reversed phase HPLC to yield the respective (*S*)- or (*R*)-PGME amides **19a**, **19b**, **20a**, **20b**, **21a**, **21b**, **22a**, and **22b**.

Chemical shift differences for each proton were calculated by subtraction (Figure 4-4).

In the β,β -substituted carboxylic acids, the PGME anisotropy group is flipped upside down due to the insertion of an extra methylene group [12]. The sign distribution of $\Delta\delta_{(S-R)}$ values is opposite to those of α,α -substituted counterparts. Thus, according to the distribution of positive and negative number on both sides of C_3 , the absolute configuration of C_3 in all four compounds **19-22** was determined to be *R*.

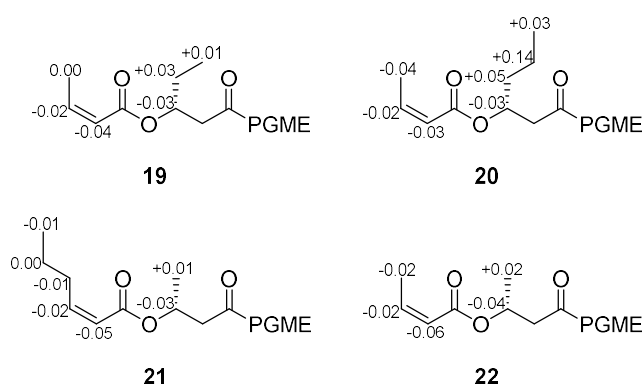


Figure 4-4. Distribution of positive (red) and negative (blue) $\Delta\delta_{(S-R)}$ values (in ppm) calculated from ^1H NMR chemical shifts of (*S*)- and (*R*)-PGME amides of **19-22**.

Polyhydroxyalkanoates (PHAs) are the energy reserve substances for eubacteria and some species of archaea [13], which are mainly composed of 3-hydroxybutyric acid and 3-hydroxyhexanoic acid. Compounds **19-22** are structurally closely related to PHAs and component fatty acids in both groups are all (*R*)-configured [14]. In addition, except for the *O*-isocrotonyl-oligo(3-hydroxybutyrate) [10], the degrees of polymerization as low as **19-22** and dehydrative modification are unprecedented.

PHAs are biodegradable and can be produced by renewable bioresources. Their material properties are close to the conventional petroleum-derived plastics. At the era of growing plastic waste crisis, some companies are seeking industrial production of PHA [15, 16]. *Vibrio* are perhaps the first to be known as producers of PHAs among marine microbes [17], and still be isolated predominantly in the screening of PHA

productivity [18]. Intriguingly, addition of the poly(3-hydroxybutyrate) to food has been reported to improve survival rate of aquatic farmed animals than those not fed upon challenge by pathogenic *Vibrio* species, which implied the potential application of PHAs as a biocontrol agent [19]. None of them showed cytotoxicity against 3Y1 rat embryonic fibroblastic cells below 50 µg/mL. The inhibitory activities against *Tenacibaculum maritimum* are marginal with MIC values of 25, 50, 50, and 25 µg/mL, respectively.

4-4 Experimental

4-3 Conclusion

In summary, three new acyloxy fatty acids with different alkyl chain lengths, *O*-isocrotonyl-3-hydroxypentanoic acid (**19**), *O*-isocrotonyl-3-hydroxyhexanoic acid (**20**), and *O*-(*Z*)-2-hexenoyl-3-hydroxybutyric acid (**21**), along with one known *O*-isocrotonyl-3-hydroxybutyric acid (**22**) were isolated from a selective sea anemone-derived bacterium of the genus *Vibrio*. The planar structure of compounds **19-21** were determined by NMR and MS data. The chiral centers of compounds **19-22** were determined to have *R*-configurations by the PGME chiral analysis.

Among marine bacteria, *Vibrio* appears to be the first known as PHAs producers. The structural similarity between **19-22** and PHA suggest the same biosynthetic origin of these molecules. Moreover, dehydration would be also possible at the hydroxy-terminus of PHA in analogy with **19-22**.

Compounds **19-22** were not cytotoxic but weakly active against a fish pathogen *T. maritimum*. Based on the biodegradable PHA and renewable capacity, the discovery of new compounds **19-22** will offer a clue to alter the property of these promising biomaterials.

4-4-1 General experimental procedures

Optical rotations were recorded on a JASCO DIP-3000 polarimeter. Hitachi U-3210 and Perkin Elmer Spectrum 100 were chosen for UV and IR analysis, respectively. NMR spectra (500 MHz for ^1H , 125 MHz for ^{13}C) were obtained on a Bruker AVANCE 500 spectrometer and solvent peaks were referenced at $\delta_{\text{H}}/\delta_{\text{C}}$ 7.26/77.0 ppm for CDCl_3 . HR-ESI-TOF-MS spectra were measured using a Bruker micrOTOF focus mass spectrometer. Absorbance of formazan solution at 540 nm was measured on a ThermoFisher Scientific Multiskan Sky microplate reader.

4-4-2 Biological material

The sea anemone sample, *Radianthus crispus*, was obtained from an aquarium vendor in Nagasaki, Japan. Strain SI1-SI10 was isolated according to the method described previously [20]. After screening of HPLC-DAD for crude extract from ten strains in three media above, strain SI9 was chosen for further study. Strain SI9 was identified as a member of genus *Vibrio* on basis of 98.6% similarity in the 16S rRNA gene sequence (1458 nucleotides; DDBJ accession number LC498627) to *Vibrio nereis* DSM 19584^T (accession number LHPJ01000025).

4-4-3 Fermentation and isolation of 19-22

Vibrio SI9 recovered on Marine Agar plates were transferred onto a 500 mL K-1 flask containing 100 mL Marine Broth (0.5% peptone and 0.1% yeast extract in 3 L seawater, pH 7.6) at 30 °C at 200 rpm for 2 days of seed culture. Then 3 L A16 production medium (2% glucose, 1% Pharmamedia, 0.5% CaCO_3 and 1% Diaion HP-20 in natural seawater) was prepared and 500 mL K-1 flask each containing 100 mL production medium and 3 mL seed culture were incubated at 30 °C at 200 rpm. After 5 days fermentation on a shaker, *n*-butanol was added to K-1 flask as a ratio 1:1 shaking for 1 h. Then the butanol layer was collected and concentrated to give crude extract 5.8 g after centrifugation at 6000 rpm for 10 min. This material was first fractionated on a

silica gel column chromatography eluting with CHCl₃-MeOH (1:0, 20:1, 10:1, 4:1, 2:1, 1:1, and 0:1 v/v). The concentrated fraction 3 (1.35 g) was further purified by ODS column chromatography eluting with MeCN-0.1% HCOOH (2:8, 3:7, 4:6, 5:5, 6:4, 7:3, and 8:2 v/v). Finally, the pure fatty acid **19-22** were isolated from fraction 4 (5:5) by the preparative HPLC (Cosmosil AR-II column, 1 × 25 cm) with 32% MeCN-0.1% HCOOH eluting at 9.8 min (**22**, 135.6 mg), 16.1 min (**19**, 1.5 mg), 17.6 min (**20**, 11.2 mg) and 18.3 min (**21**, 4.3 mg), respectively.

(*R*)-*O*-Isocrotonyl-3-hydroxypentanoic acid (**19**): colorless amorphous solid; $[\alpha]_D^{24}$ -53 (*c* 0.10, MeOH); UV (MeOH) λ_{\max} (log ϵ) 208 (3.67) nm; IR (ATR) ν_{\max} : 2973, 2938, 2641, 1716, 1646, 1438, 1415, 1368, 1179, 1135, 1057, 1033, 997, 927, 815 cm⁻¹; ¹H and ¹³C NMR data see Table 1; HRESITOFMS *m/z* 209.0784 [M+Na]⁺ (calcd for C₉H₁₄O₄Na, 209.0784).

(*R*)-*O*-Isocrotonyl-3-hydroxyhexanoic acid (**20**): colorless amorphous solid; $[\alpha]_D^{24}$ -67 (*c* 0.10, MeOH); UV (MeOH) λ_{\max} (log ϵ) 207 (4.15) nm; IR (ATR) ν_{\max} : 2962, 2937, 1717, 1646, 1438, 1415, 1178, 1009, 970, 815 cm⁻¹; ¹H and ¹³C NMR data see Table 1; HRESITOFMS *m/z* 223.0941 [M+Na]⁺ (calcd for C₁₀H₁₆O₄Na, 223.0941).

(*R*)-*O*-(*Z*)-2-Hexenoyl -3-hydroxybutyric acid (**21**): colorless amorphous solid; $[\alpha]_D^{24}$ -38 (*c* 0.10, MeOH); UV (MeOH) λ_{\max} (log ϵ) 209 (4.17) nm; IR (ATR) ν_{\max} : 2962, 2934, 2874, 1717, 1640, 1456, 1414, 1178, 1059, 816 cm⁻¹; ¹H and ¹³C NMR data see Table 2; HRESITOFMS *m/z* 223.0941 [M+Na]⁺ (calcd for C₁₀H₁₆O₄Na, 223.0941).

(*R*)-*O*-Isocrotonyl-3-hydroxybutyric acid (**22**): colorless oil; $[\alpha]_D^{23}$ -43 (*c* 0.10, MeOH); UV (MeOH) λ_{\max} (log ϵ) 208 (4.07) 274 (2.47) nm; IR (ATR) ν_{\max} : 2985, 2937, 2643, 1710, 1644, 1435, 1414, 1291, 1175, 1057, 970, 815 cm⁻¹; ¹H and ¹³C NMR data see Table 2; HRESITOFMS *m/z* 195.0627 [M+Na]⁺ (calcd for C₈H₁₂O₄Na, 195.0628).

4-4-4 Preparation of (*S*)- and (*R*)-Phenylglycine Methyl Ester

Amides

10 μmol of compound **22** was first dissolved in 0.5 mL of anhydrous CH_2Cl_2 in a dried vial and then 16.4 μmol of (*S*)-phenylglycine methyl ester (PGME), 10 μmol of DMAP and 19.5 μmol of DIC were added into the above mixture. After the stirring for 30 min at room temperature, the reaction product was checked by thin layer chromatography (TLC) developed by ethyl acetate /*n*-hexane (1:1) followed by heating with phosphomolybdic acid. Then the mixture was dried and purified by HPLC on a Cosmosil π -NAP column (10 x 250 mm) eluted by a gradient method (MeCN-0.1% HCOOH) at 4 mL/min with monitoring at 254 nm to give (*S*)-PGME amide **22a** (2.9 mg, 93%) as colorless oil.

(*S*)-PGME amide of **22** (**22a**): ^1H NMR (500 MHz, CDCl_3) δ 7.34 (4H, m), 6.75 (1H, d), 6.31 (1H, m), 5.70 (1H, qd), 5.57 (1H, d), 5.25 (1H, m), 3.72 (3H, s), 2.54 (2H, m), 2.09 (3H, dd), 1.34 (3H, d); HRESITOFMS m/z 342.1312 (calcd for $\text{C}_{17}\text{H}_{21}\text{NO}_5\text{Na}$ 342.1312).

Other PGME amides **19a**, **19b**, **20a**, **20b**, **21a**, **21b**, and **22b** were prepared by the same manner with replacing the starting material and chiral reagent.

(*S*)-PGME amide of **19** (**19a**): ^1H NMR (500 MHz, CDCl_3) δ 7.34 (4H, m), 6.75 (1H, d), 6.33 (1H, t), 5.57 (1H, d), 5.56 (1H, qd), 5.25 (1H, m), 5.14 (1H, t), 3.72 (3H, s), 2.11 (3H, d), 1.70 (2H, m), 0.92 (3H, t), ; HRESITOFMS m/z 356.1468 [$\text{M}+\text{Na}$] $^+$ (calcd for $\text{C}_{18}\text{H}_{23}\text{NO}_5\text{Na}$, 356.1468).

(*R*)-PGME amide of **19** (**19b**): ^1H NMR (500 MHz, CDCl_3) δ 7.34 (4H, m), 6.75 (1H, d), 6.35 (1H, t), 5.57 (1H, d), 5.56 (1H, qd), 5.25 (1H, m), 5.17 (1H, t), 3.72 (3H, s), 2.11 (3H, d), 1.67 (2H, m), 0.91 (3H, t); HRESITOFMS m/z 356.1495.

(*S*)-PGME amide of **20** (**20a**): ^1H NMR (500 MHz, CDCl_3) δ 7.34 (4H, m), 6.75 (1H, d), 6.34 (1H, m), 5.75 (1H, m), 5.57 (1H, d), 5.25 (1H, m), 5.23 (1H, m), 3.72 (3H, s), 2.13 (3H, m), 1.51 (2H, m), 1.35 (2H, overlapped), 0.93 (3H, t); HRESITOFMS m/z

370.1625 [M+Na]⁺ (calcd for C₁₉H₂₅NO₅Na, 370.1625).

(*R*)-PGME amide of **20** (**20b**): ¹H NMR (500 MHz, CDCl₃) δ 7.34 (4H, m), 6.75 (1H, d), 6.36 (1H, m), 5.79 (1H, m), 5.26 (1H, m), 5.25 (1H, m), 5.57 (1H, d), 3.72 (3H, s), 2.13 (3H, m), 1.49 (2H, m), 1.35 (2H, overlapped), 0.91 (3H, t); HRESITOFMS *m/z* 370.1625 [M+Na]⁺.

(*S*)-PGME amide of **21** (**21a**): ¹H NMR (500 MHz, CDCl₃) δ 7.34 (4H, m), 6.75 (1H, d), 6.24 (1H, m), 5.72 (1H, d), 5.57 (1H, d), 5.27 (1H, m), 5.25 (1H, m), 3.72 (3H, s), 2.62 (2H, m), 1.73 (3H, m), 1.49 (2H, m), 0.95 (3H, m); HRESITOFMS *m/z* 370.1625 [M+Na]⁺.

(*R*)-PGME amide of **21** (**21b**): ¹H NMR (500 MHz, CDCl₃) δ 7.34 (4H, m), 6.75 (1H, d), 6.26 (1H, m), 5.77 (1H, d), 5.57 (1H, d), 5.30 (1H, m), 5.25 (1H, m), 3.72 (3H, s), 2.63 (2H, m), 1.68 (3H, m), 1.49 (2H, m), 0.96 (3H, m); HRESITOFMS *m/z* 370.1625 [M+Na]⁺.

(*S*)-PGME amide of **22** (**22b**): ¹H NMR (500 MHz, CDCl₃) δ 7.34 (4H, m), 6.75 (1H, d), 6.31 (1H, m), 5.70 (1H, qd), 5.57 (1H, d), 5.25 (1H, m), 3.72 (3H, s), 2.54 (2H, m), 2.09 (3H, dd), 1.34 (3H, d); HRESITOFMS *m/z* 342.1312 (calcd for C₁₇H₂₁NO₅Na 342.1312).

4-4-5 Antibacterial Assay

Paper disk assay was used to evaluate the inhibited activity for the pathogen *T. maritimum* NBRC16015, *R. radiobacter* NBRC14554, *R. solanacearum* SUPP1541, *S. aureus* FDA209P JC-1, *C. albicans* NBRC0197 and *S. cerevisiae* S100, respectively. Paper-disk method was described in our previous research [21]. MIC method was the same except for 1/100 reduction of the seeding density of *T. maritimum*.

4-4-6 Cytotoxicity Assay

In this assay, low-glucose DMEM medium (L-glutamine and phenol red

supplemented with 10% fetal bovine serum, 100 units/mL penicillin, 100 µg/mL streptomycin, 0.25 µg/mL amphotericin B, and 100 µg/mL gentamicin sulfate) was used to maintain 3Y1 rat embryonic fibroblastic cells. 96-well culture plate was used to culture cells to make sure the density of each well coming up to 2500 cells. Doxorubicin hydrochloride as a positive control and **19-22** were serially diluted 1:3.16 (half-log dilution) by the same medium in a different microtiter plate. After culturing cells in the 95% air and 5% CO₂ saturated with H₂O for 12 h at 37°C, the solutions of **19-22** and doxorubicin hydrochloride were transferred into above 96-well culture plate culturing cells to reach 200 µL of each well. The concentration of MeOH or DMSO solvents in well cannot exceed 0.5 v/v % to allow normal growth of cells. After incubation for 84 h, 100 µL of medium containing MTT 1 mg/mL were added into the test plate, and the test plate was further incubated for 4 h. Then the medium was removed by aspiration and 150 µL DMSO was added to dissolve the remaining formazan-dye at the bottom. A microplate reader was used to detect the respiration of live cells at 540 nm. The assay was repeat three times and the inhibition of cell growth at each concentration were recorded to calculate the GI₅₀ values of the test compounds **19-22** on a single logarithmic chart.

References

1. Leal, M. C., Calado, R., Sheridan, C.; Alimonti, A., Osinga, R. *Trends Biotechnol.* **2013**, *31*, 555–561.
2. Bibi, F., Faheem, M., Azhar, E. I., Yasir, M., Alvi, S. A., Kamal, M. A., Ullah, I., Nasser, M. I. *Curr. Drug Metab.* **2016**, *17*, 1–6.
3. Blockley, A., Elliott, D., Roberts, A., Sweet, M. *Diversity* **2017**, *9*, 49.
4. Rizzo, C., Giudice, A. L. *Diversity* **2018**, *10*, 52.
5. Sharma, A. R., Harunari, E., Zhou, T., Trianto, A., Igarashi, Y. *Beilstein J. Org. Chem.* **2019**, *15*, 2327–2332.
6. Sharma, A. R., Harunari, E., Oku, N., Matsuura, N., Trianto, A., Igarashi, Y. *Beilstein J. Org. Chem.* **2020**, *16*, 297–304.
7. Karim, Md. R., Harunari, E., Oku, N., Akasaka, K., Igarashi, Y. *J. Nat. Prod.* **2020**, *83*, 1295–1299.
8. Williams, G. P., Babu, S., Ravikumar, S., Kathiresan, K., S. Prathap, A., Chinnapparaj, S., Marian, M. P., Alikhan, L. S. *JEB.* **2007**, *28*, 789-793.
9. Kushmaro, A., Y. Loya, M. *Nature*, **1996**, *380*, 396.
10. Kikuchi, K., Chen, C., Takadera, T., Nishijima, M., Araki, M., Adachi, K., Sano, H. New 3-hydroxybutyric acid oligomer and their preparation. J. P. Patent 104, 991, Jan. 18 1998.
11. Nagai, Y., Kusumi, T. *Tetrahedron Lett.* **1995**, *36*, 1853-1856.
12. Yabuuchi, T., Kusumi, T., *J. Org. Chem.* **2000**, *65*, 397-404.
13. Rehn, B. H. A. *Biochem J.* **2003**, *376*, 15-33.

14. Kaunzinger, A., Podebrad, F.; Liske, Rüd.; Maas, B.; Dietrich, A.; Mosandl, A. *J. High Resolt. Chromatogr.* **1995**, *18*, 49–53.
15. Choi, S. Y., Rhie, M. N., Kim, H. T., Joo, J. C., Cho, I. J., Son, J., Jo, S. Y., Sohn, Y. J., Baritugo, K. A. Pyo, J., Lee, Y., Lee, S. Y., Park, S. J. *Metab. Eng.* **2020**, *58*, 47-81.
16. Alexander H. Tullo. PHA: A biopolymer whose time has finally come. *Chem. Eng. News*, **2019**, *97*, 20-21.
17. Baumann, P., Baumann, L., Mandel, M. *J. Bacteriol.* **1971**, *107*, 268-294.
18. Kavitha, G., Ramasamy Rengasamy, R., Inbakandan, D. *Int. J. Biol. Macromol.* **2018**, *111*, 102-108.
19. Laranja, J. L. Q., Bossier, P. Poly-beta-hydroxybutyrate (PHB) and infection reduction in farmed aquatic animals. In *Health Consequences of Microbial Interactions with Hydrocarbons, Oils, and Lipids*; Goldfine, H., Ed.; Springer International Publishing: Cham, Switzerland, 2019; pp. 1-27
20. Raj Sharma, A., Zhou, T., Harunari, E., Oku, N., Trianto, A., Igarashi, Y. *J. Antibiot.* **2019**, *72*, 634–639.
21. Oku, N., Matsumoto, M., Yonejima, K., Tansei, K., Igarashi, Y. *Beilstein J. Org. Chem.* **2014**, *10*, 1808-1816.

4-5 Spectral data

Table of contents

(R)-*O*-Isocrotonyl-3-hydroxypentanoic acid (**19**)

- Figure S1 UV spectrum
- Figure S2 IR spectrum
- Figure S3 ¹H NMR spectrum (CDCl₃, 500 MHz)
- Figure S4 ¹³C NMR spectrum (CDCl₃, 125 MHz)
- Figure S5 COSY spectrum (CDCl₃, 500 MHz)
- Figure S6 HSQC spectrum (CDCl₃, 500 MHz)
- Figure S7 HMBC spectrum (CDCl₃, 500 MHz)
- Figure S8 ¹H NMR spectrum of (*S*)-PGME amide (**19a**) (CDCl₃, 500 MHz)
- Figure S9 ¹H NMR spectrum of (*R*)-PGME amide (**19b**) (CDCl₃, 500 MHz)

(R)-*O*-Isocrotonyl-3-hydroxyhexanoic acid (**20**)

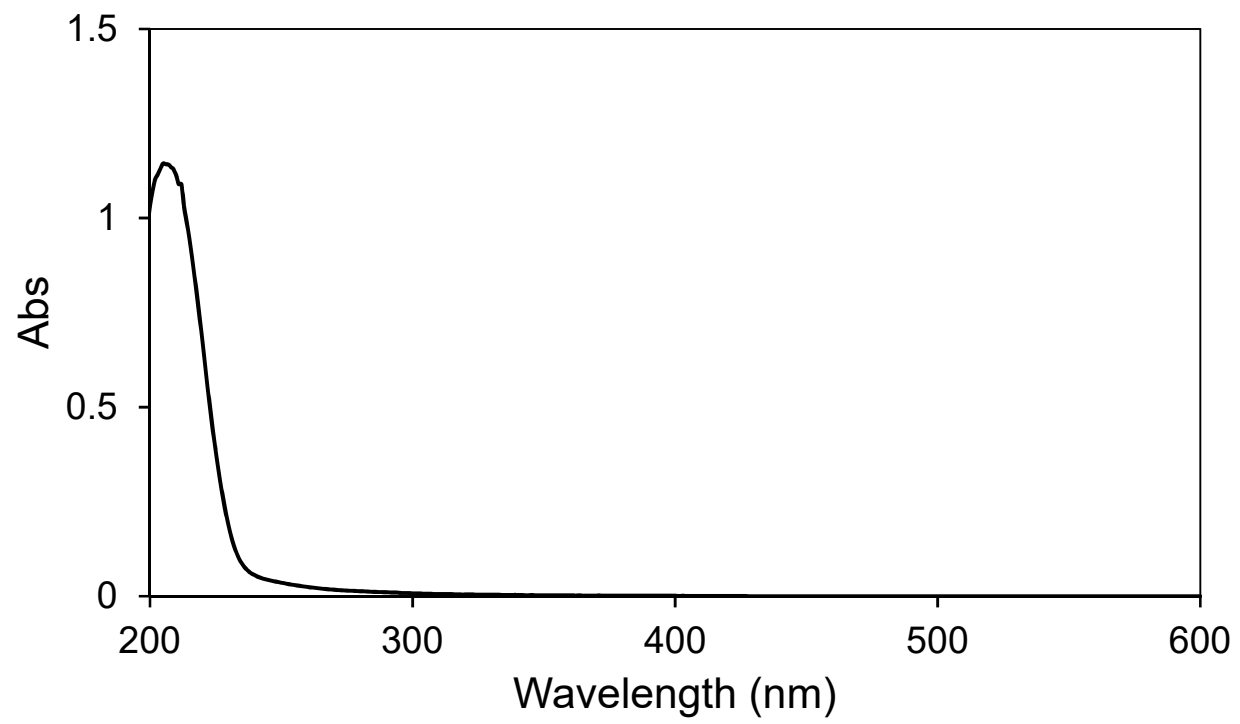
- Figure S10 UV spectrum
- Figure S11 IR spectrum
- Figure S12 ¹H NMR spectrum (CDCl₃, 500 MHz)
- Figure S13 ¹³C NMR spectrum (CDCl₃, 125 MHz)
- Figure S14 COSY spectrum (CDCl₃, 500 MHz)
- Figure S15 HSQC spectrum (CDCl₃, 500 MHz)
- Figure S16 HMBC spectrum (CDCl₃, 500 MHz)
- Figure S17 ¹H NMR spectrum of (*S*)-PGME amide (**20a**) (CDCl₃, 500 MHz)
- Figure S18 ¹H NMR spectrum of (*R*)-PGME amide (**20b**) (CDCl₃, 500 MHz)

(R)-*O*-4-Ethylisocrotonyl-3-hydroxybutyric acid (**21**)

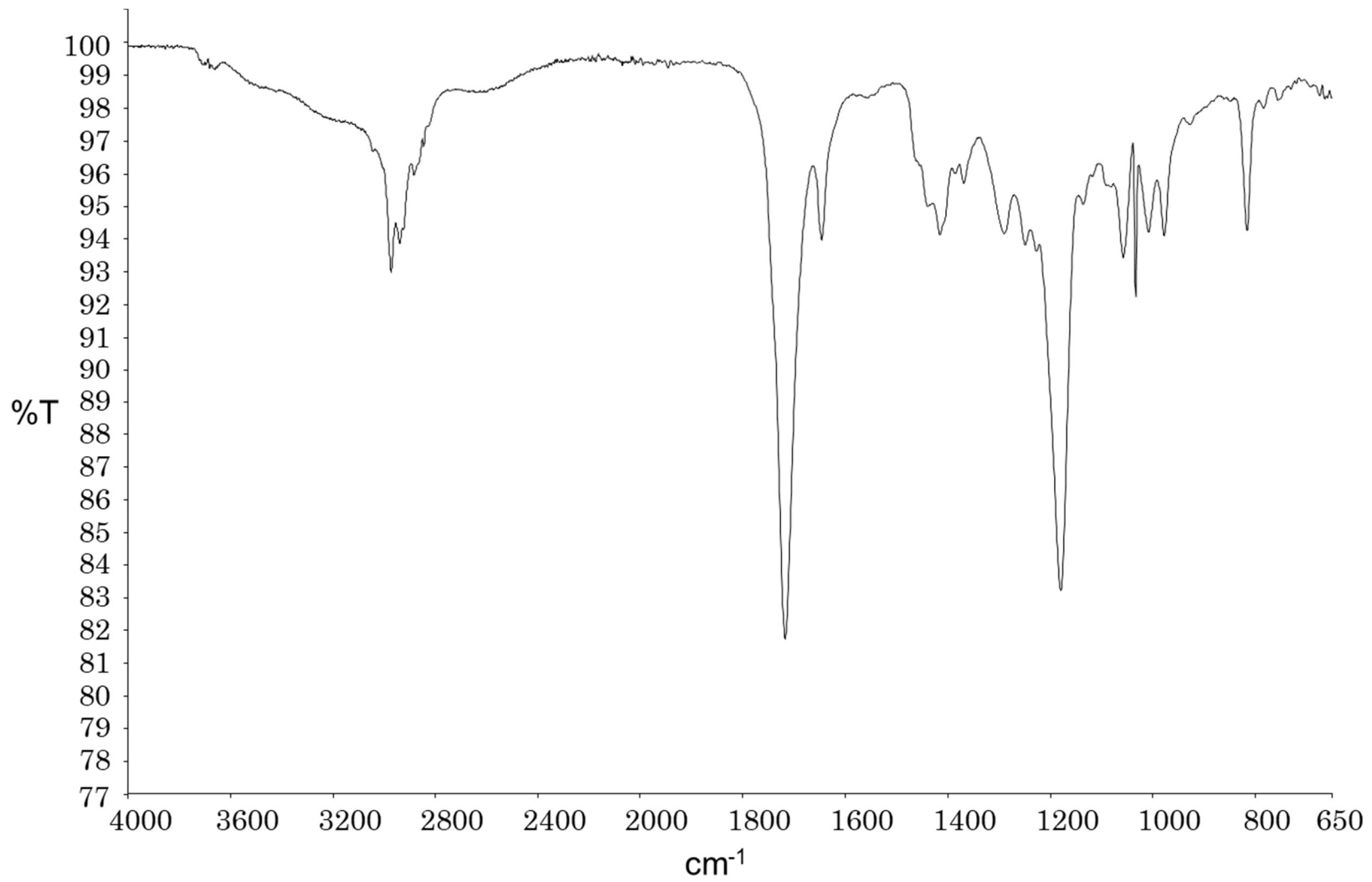
- Figure S19 UV spectrum
- Figure S20 IR spectrum
- Figure S21 ¹H NMR spectrum (CDCl₃, 500 MHz)
- Figure S22 ¹³C NMR spectrum (CDCl₃, 125 MHz)
- Figure S23 COSY spectrum (CDCl₃, 500 MHz)
- Figure S24 HSQC spectrum (CDCl₃, 500 MHz)
- Figure S25 HMBC spectrum (CDCl₃, 500 MHz)
- Figure S26 ¹H NMR spectrum of (*S*)-PGME amide (**21a**) (CDCl₃, 500 MHz)
- Figure S27 ¹H NMR spectrum of (*R*)-PGME amide (**21b**) (CDCl₃, 500 MHz)

(R)-*O*-Isocrotonyl-3-hydroxybutyric acid (**22**)

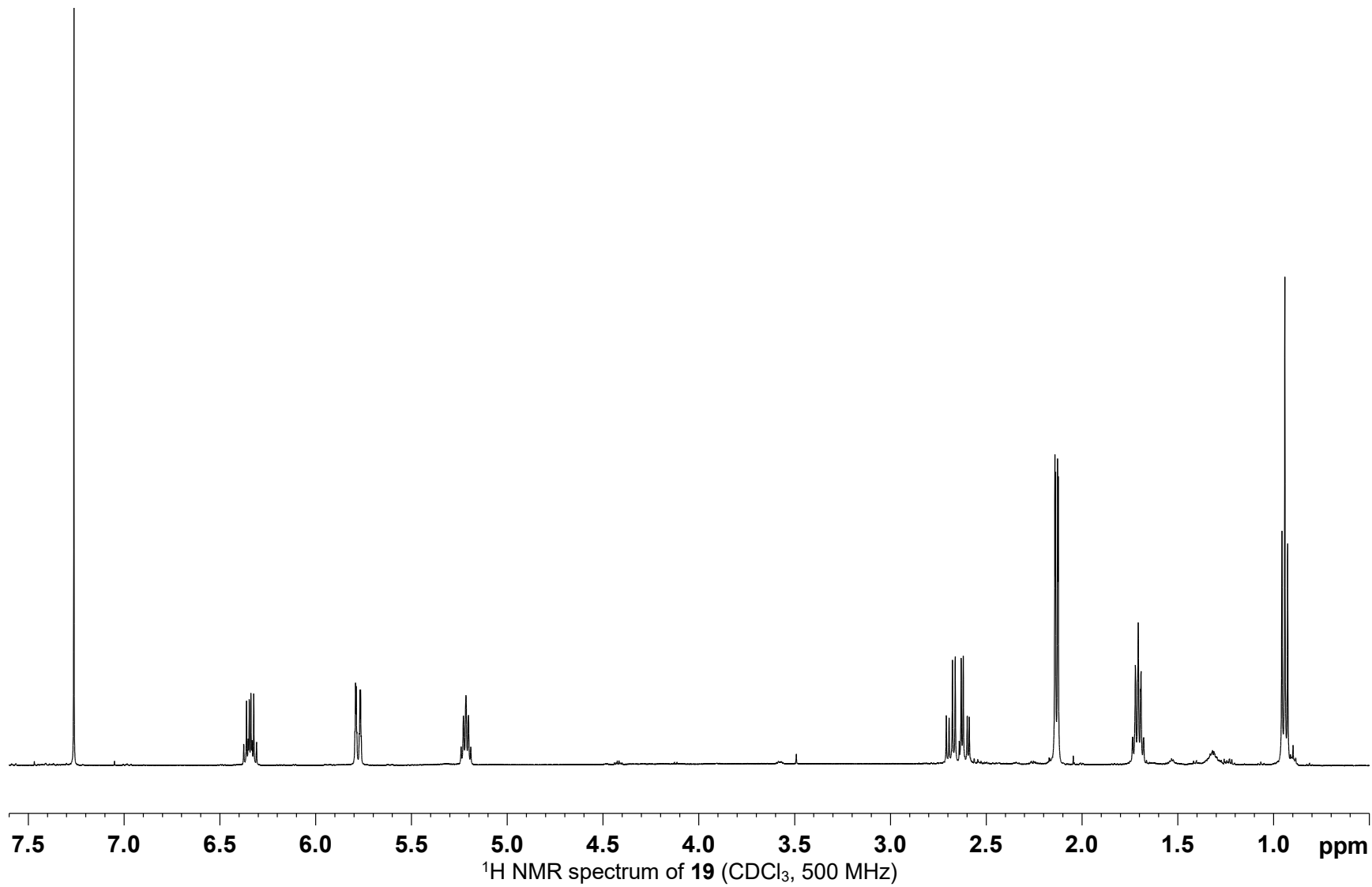
- Figure S28 UV spectrum
- Figure S29 IR spectrum
- Figure S30 ¹H NMR spectrum (CDCl₃, 500 MHz)
- Figure S31 ¹³C NMR spectrum (CDCl₃, 125 MHz)
- Figure S32 COSY spectrum (CDCl₃, 500 MHz)
- Figure S33 HSQC spectrum (CDCl₃, 500 MHz)
- Figure S34 HMBC spectrum (CDCl₃, 500 MHz)
- Figure S35 ¹H NMR spectrum of (*S*)-PGME amide (**22a**) (CDCl₃, 500 MHz)
- Figure S36 ¹H NMR spectrum of (*R*)-PGME amide (**22b**) (CDCl₃, 500 MHz).

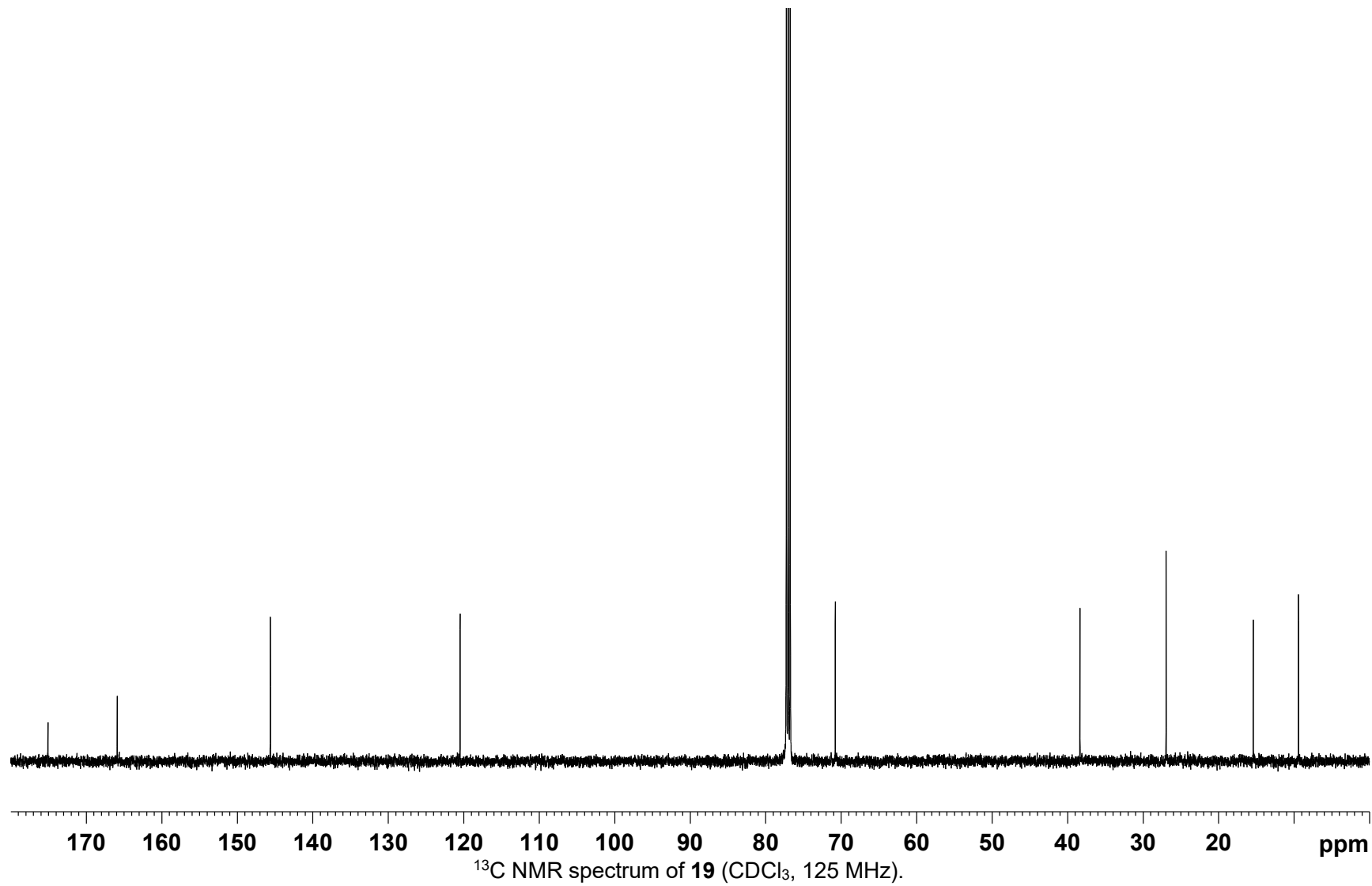


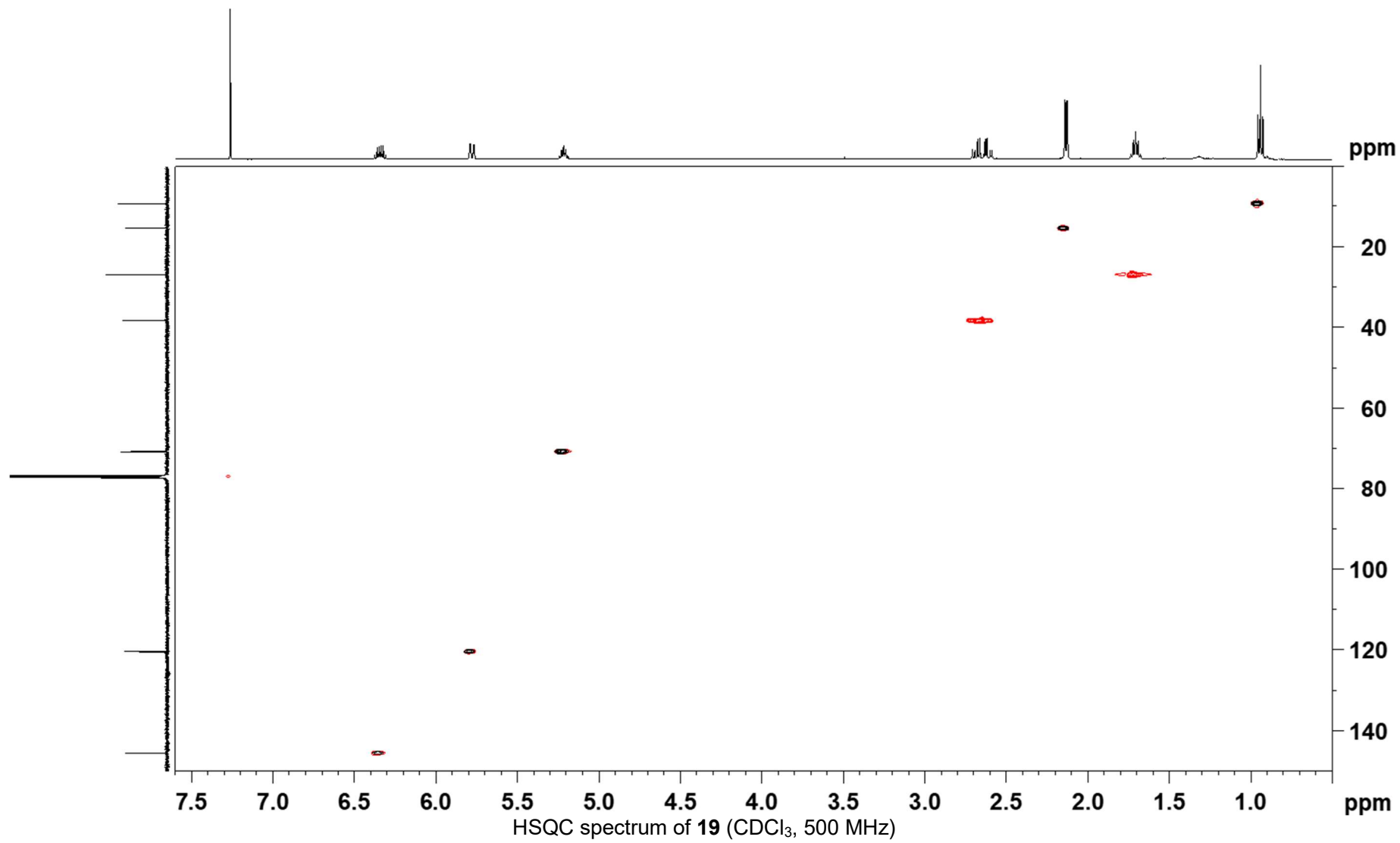
UV spectrum of **19**

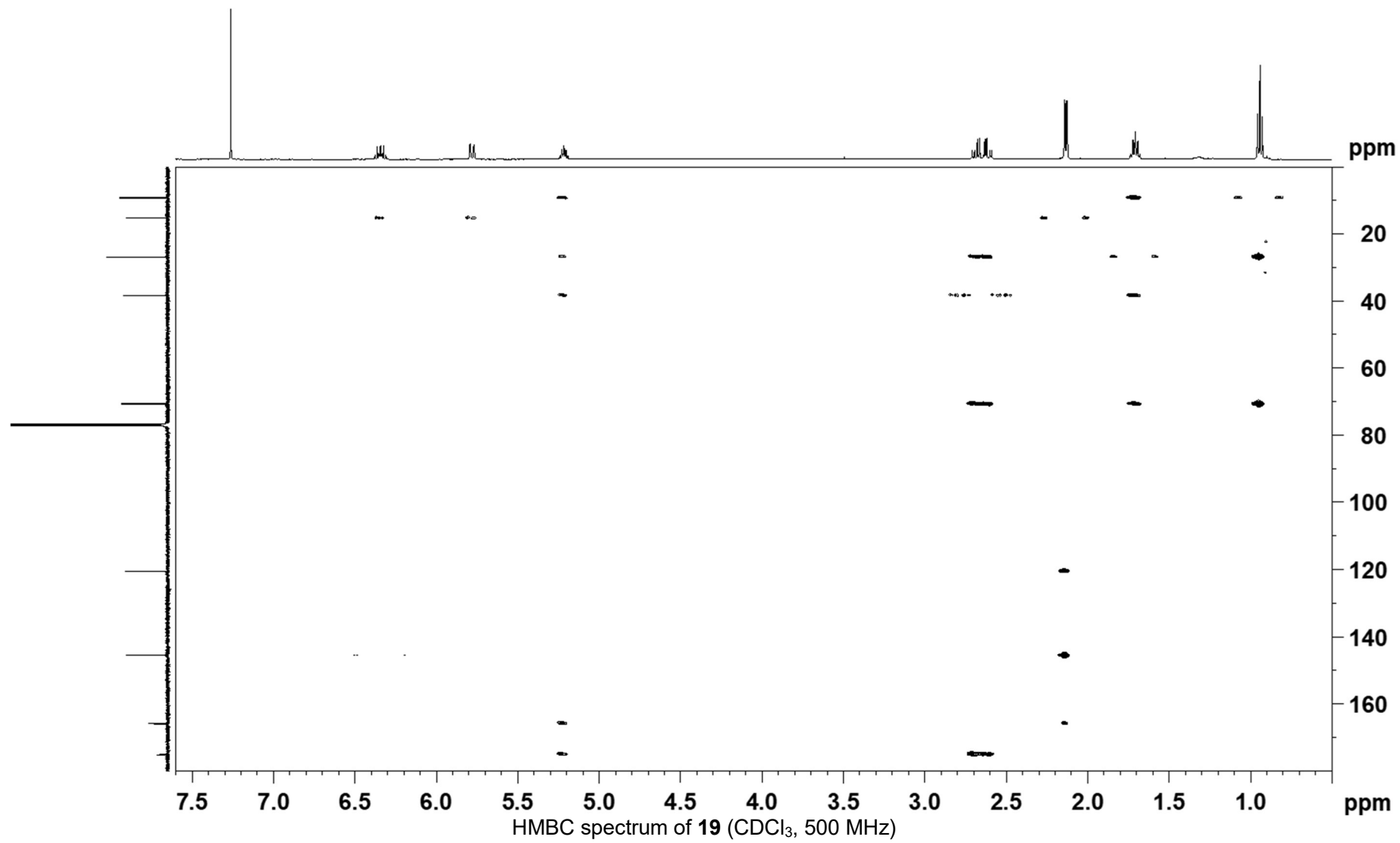


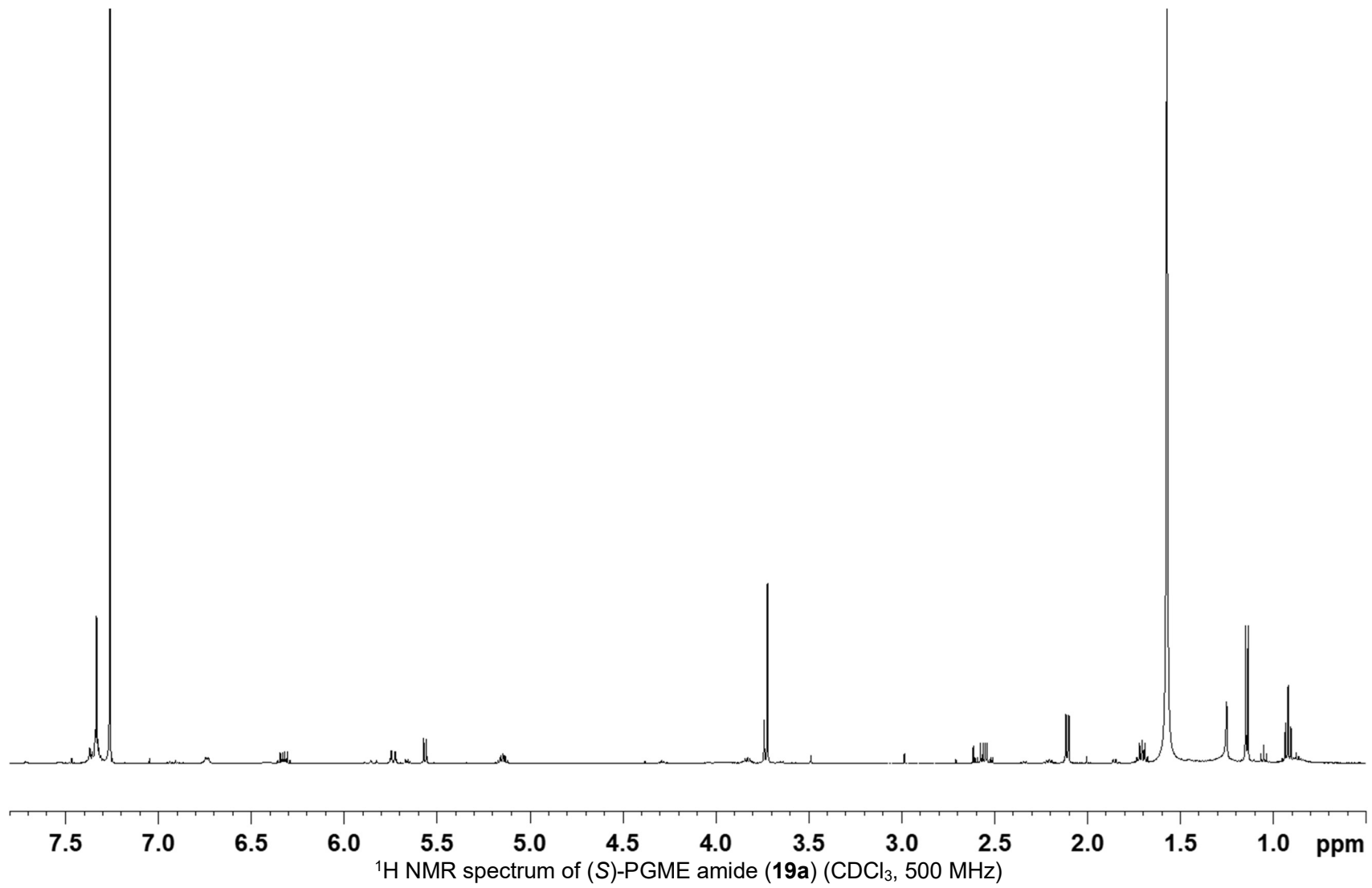
IR spectrum of **19**

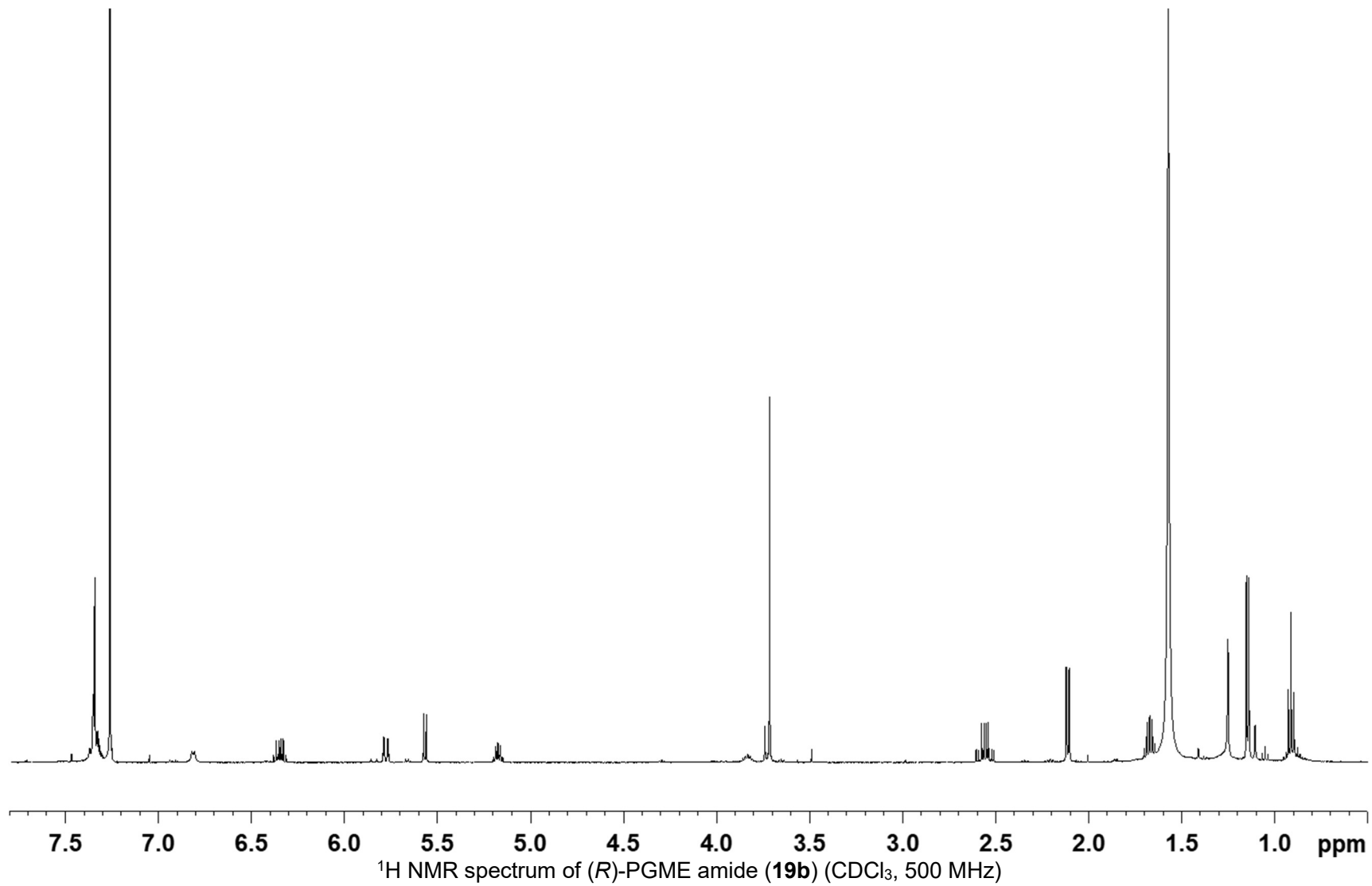


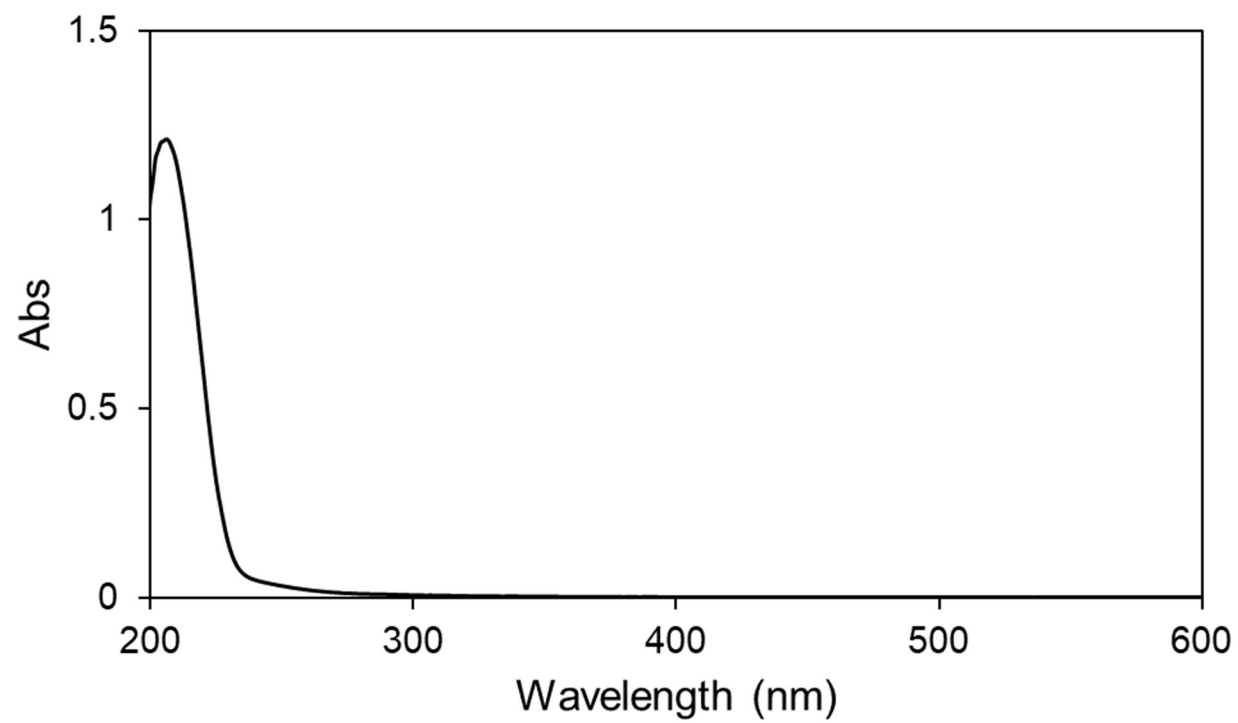




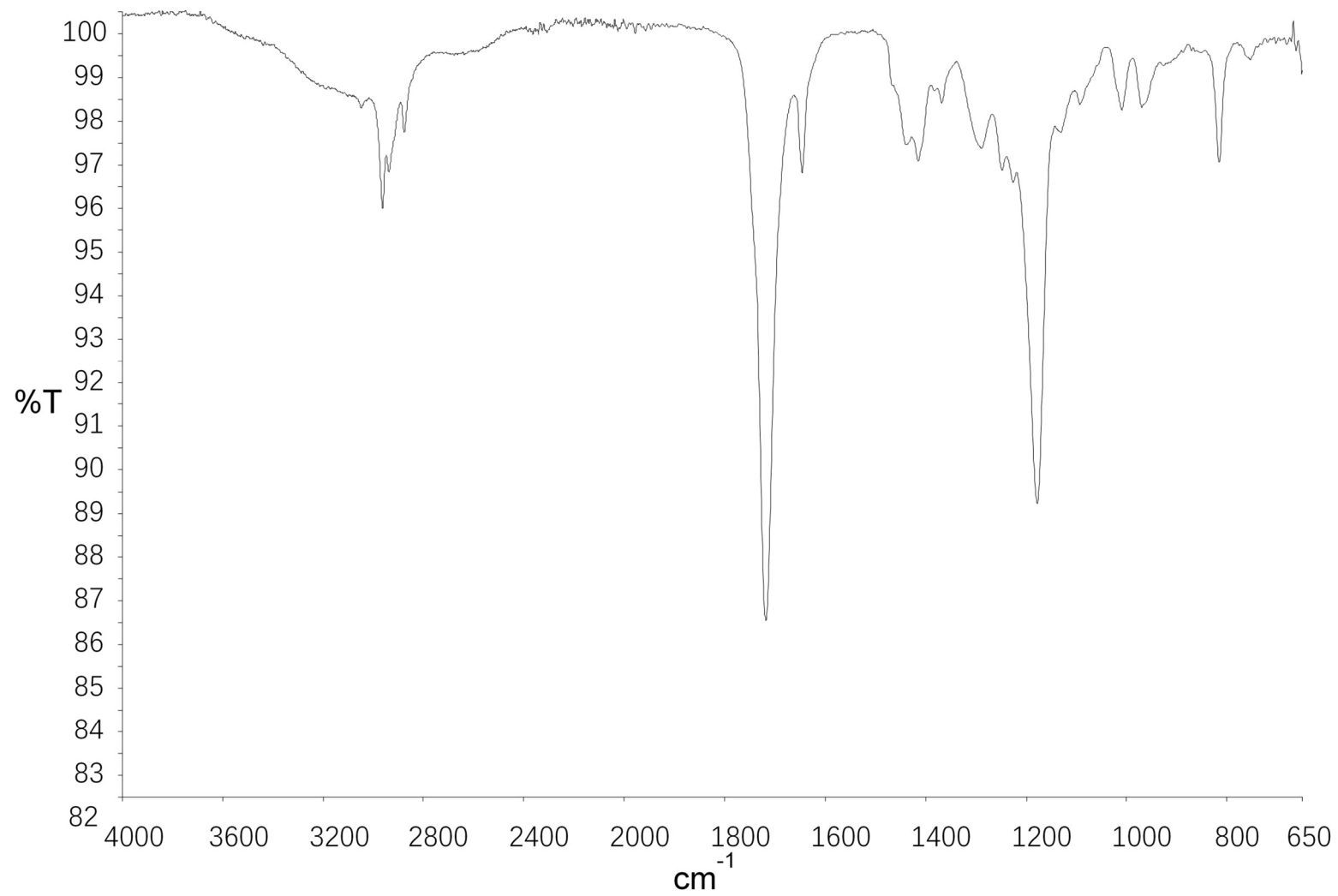




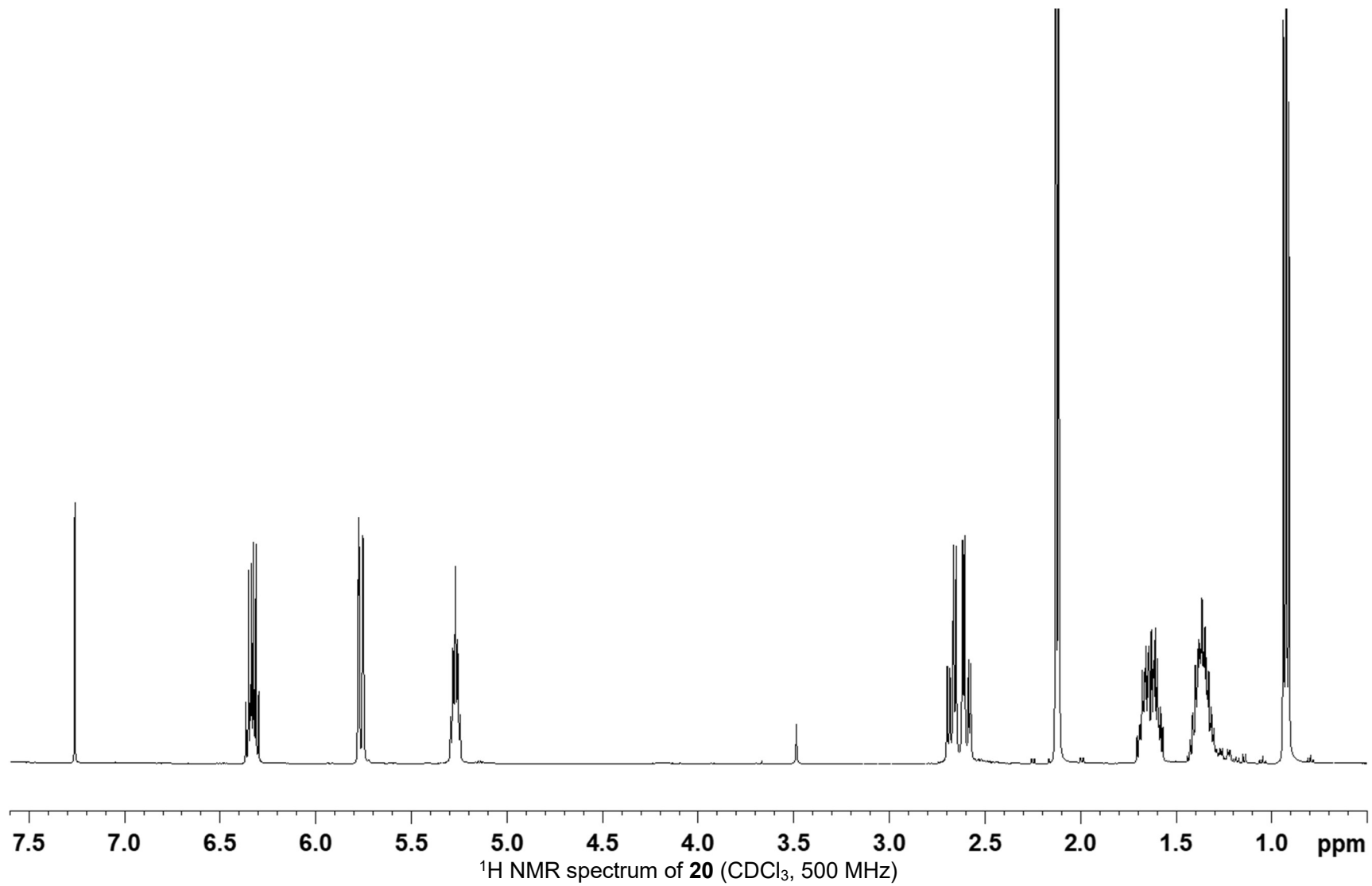


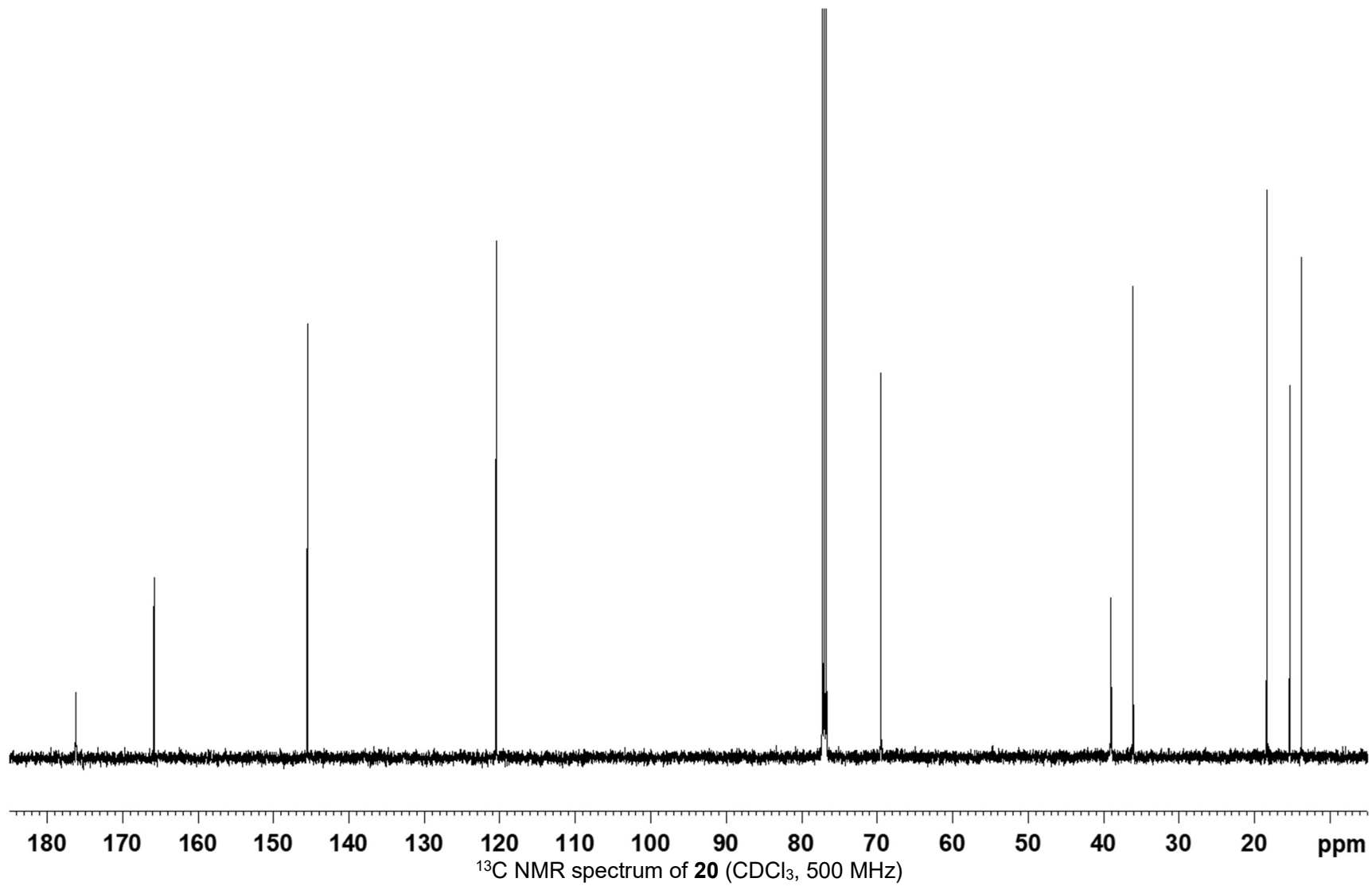


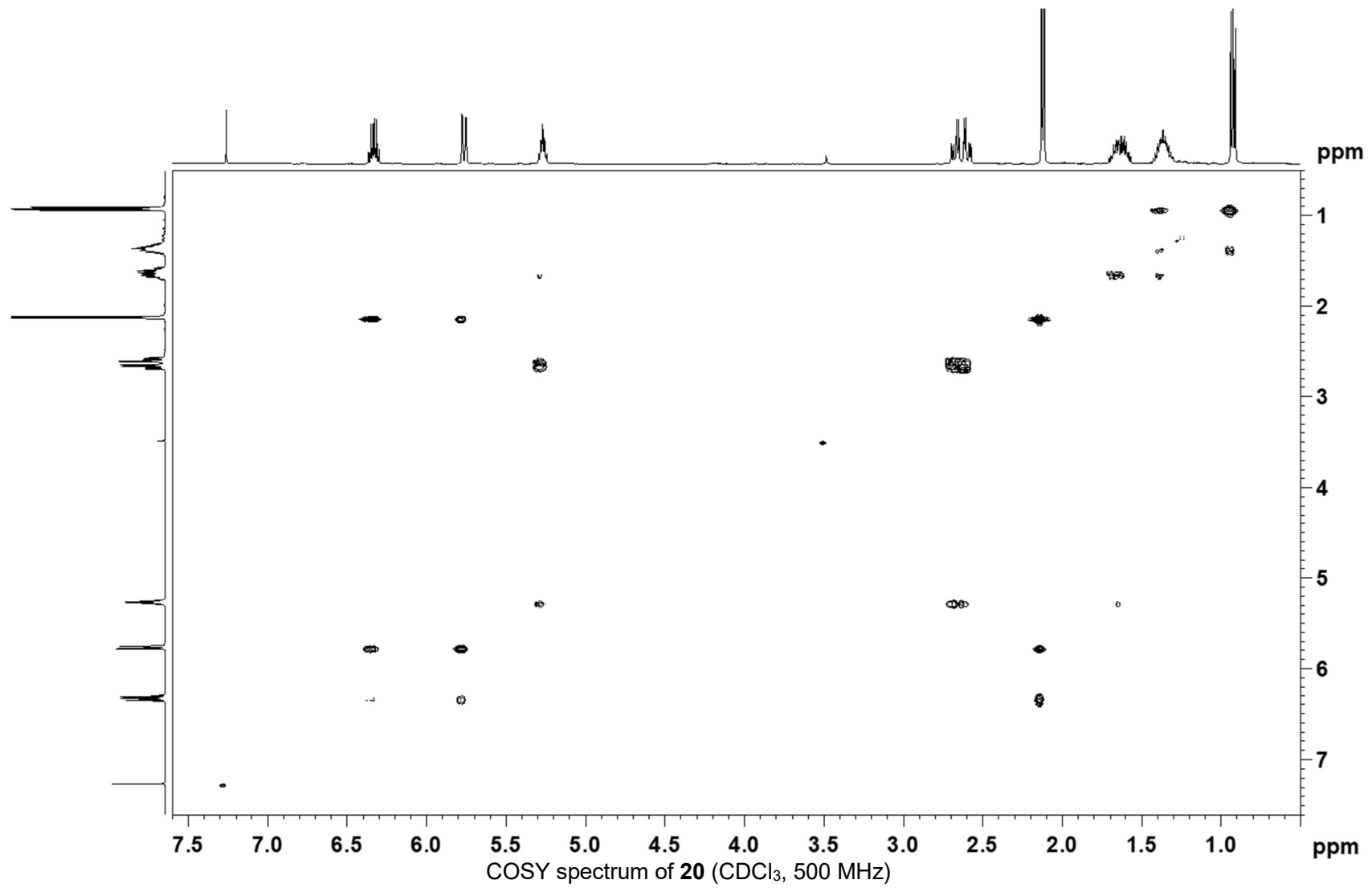
UV spectrum of **20**

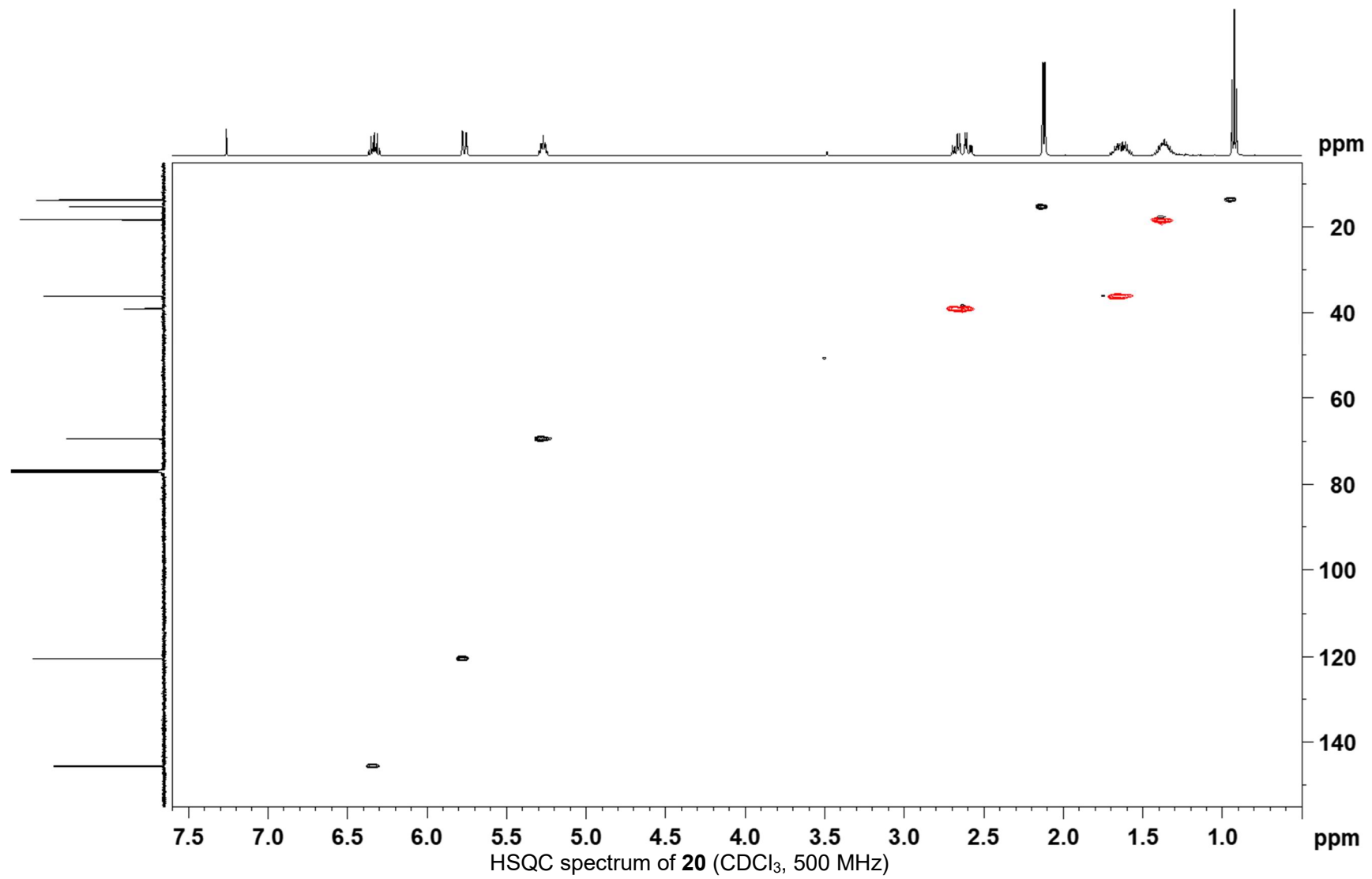


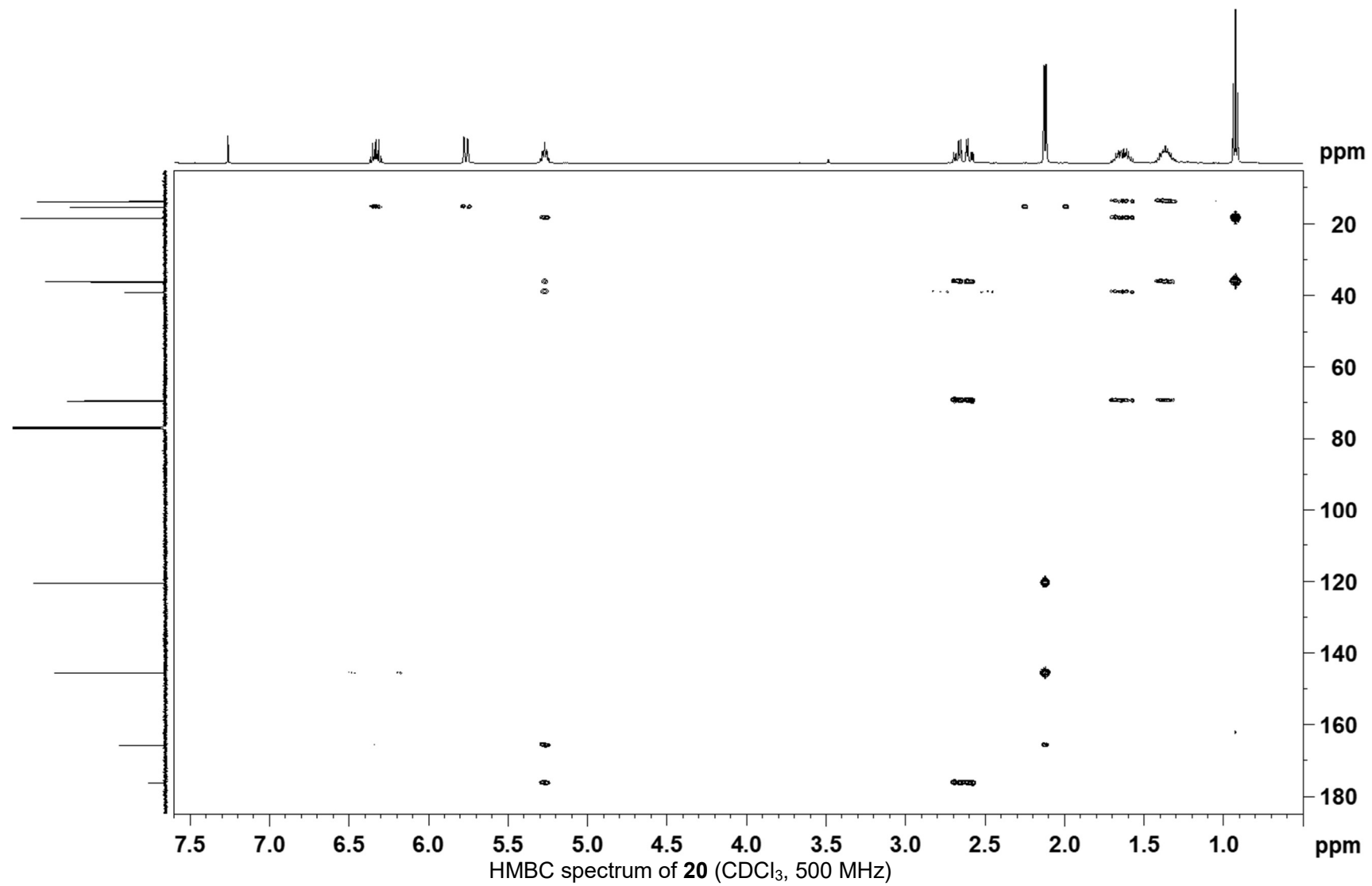
IR spectrum of **20**

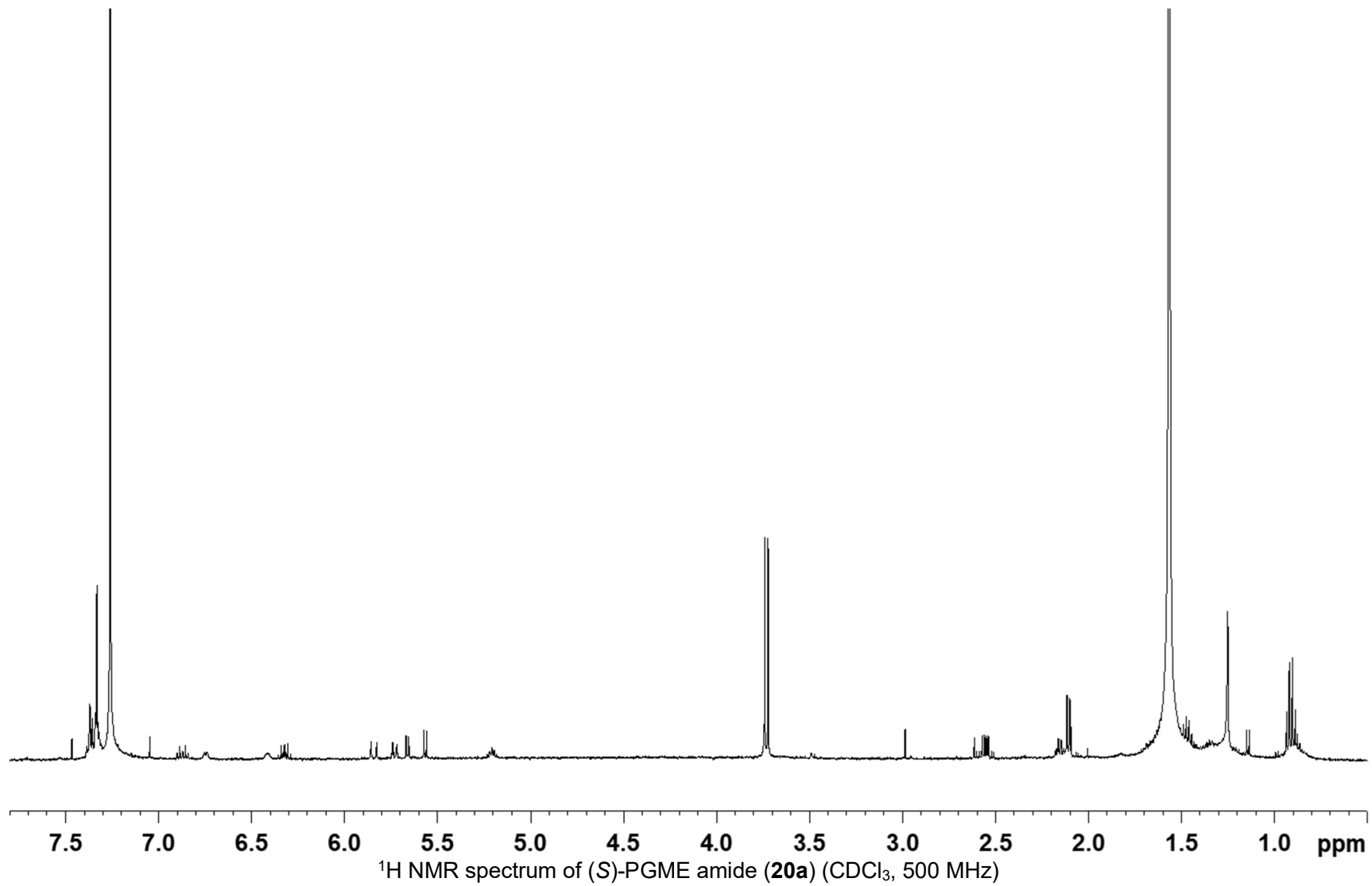


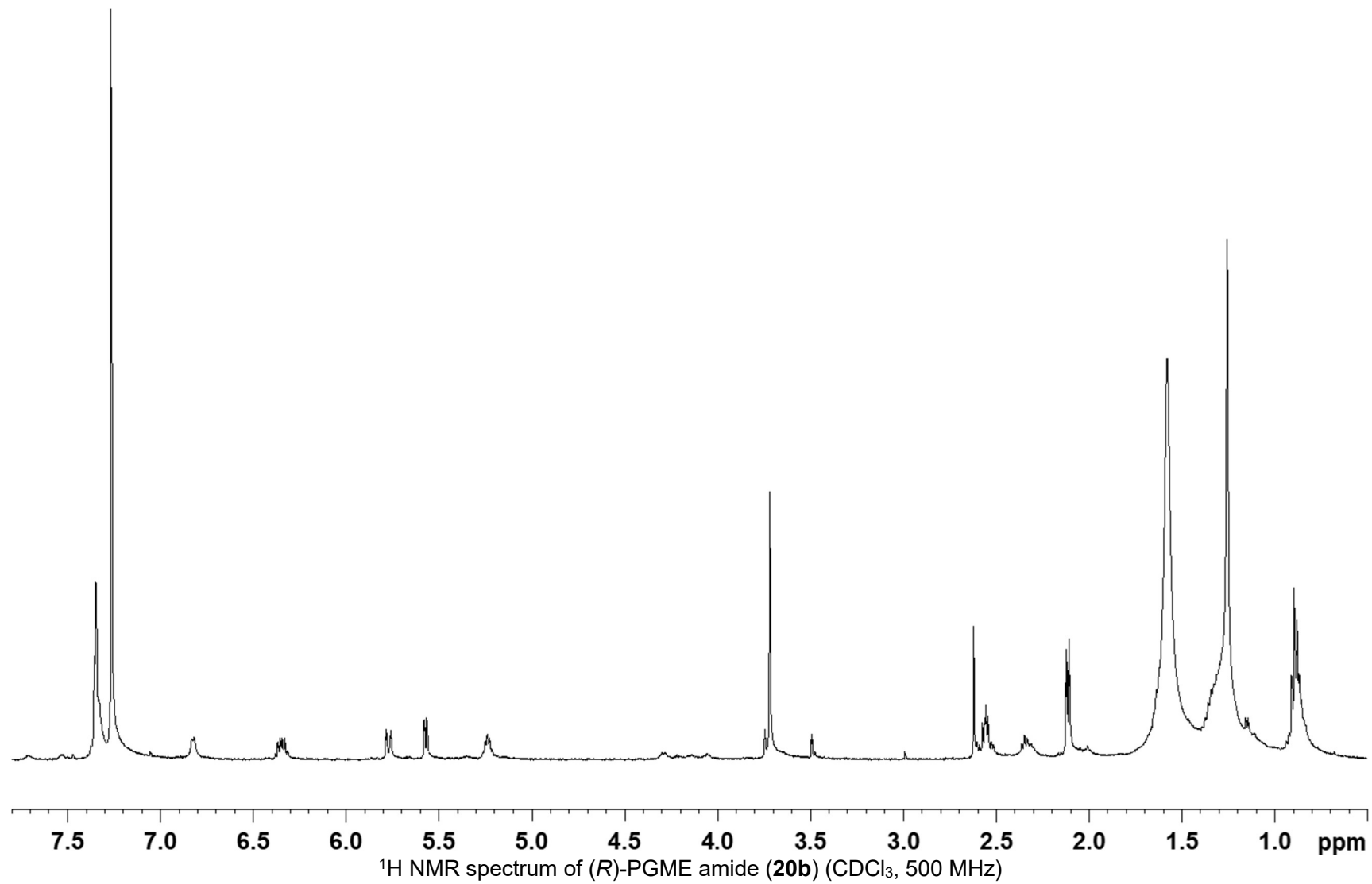


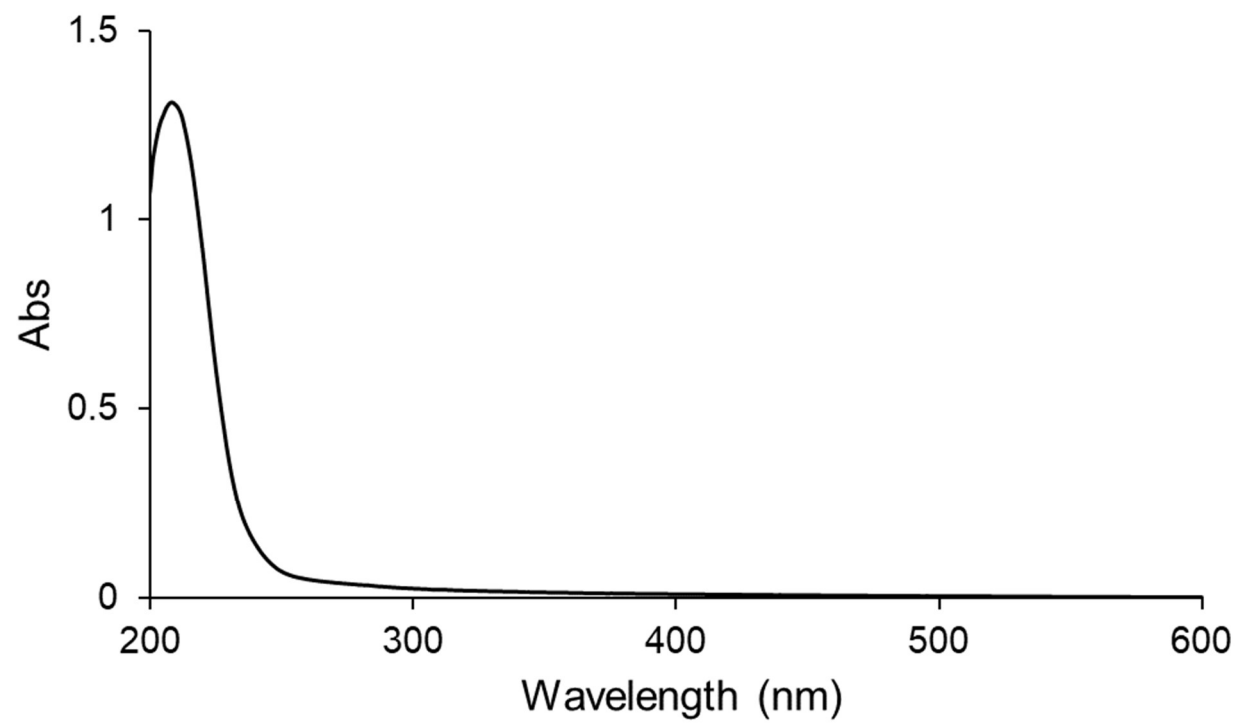




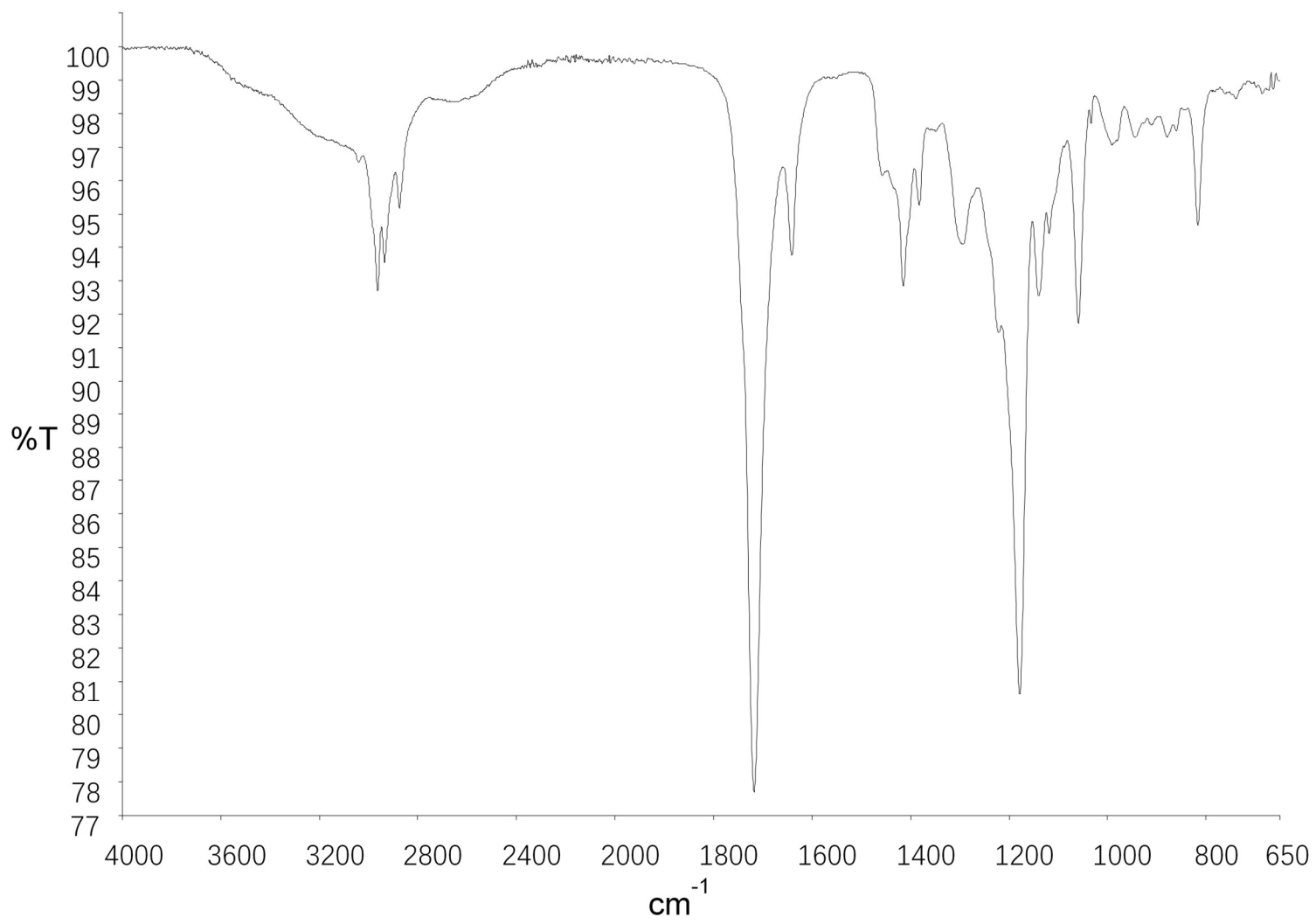




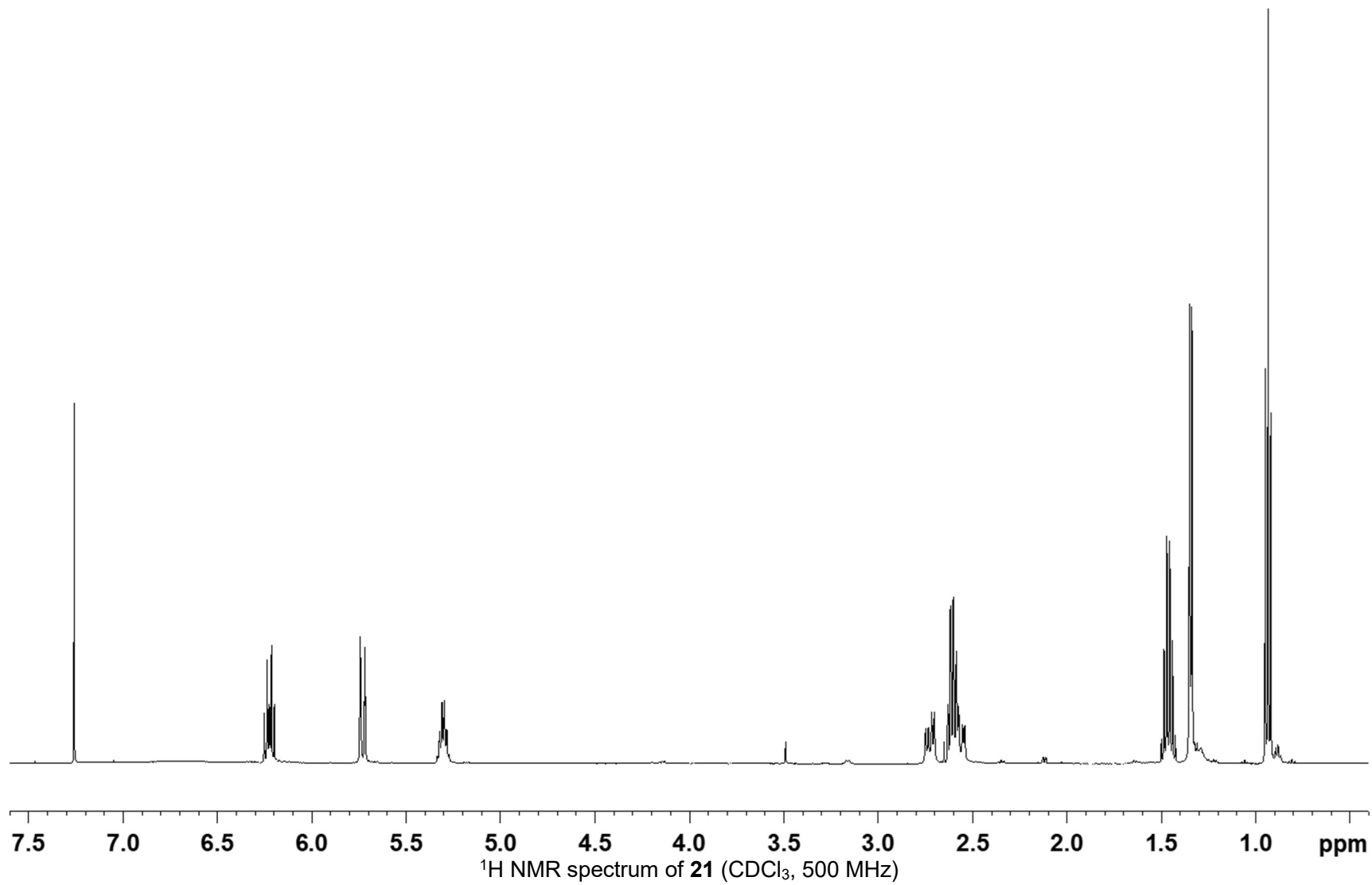


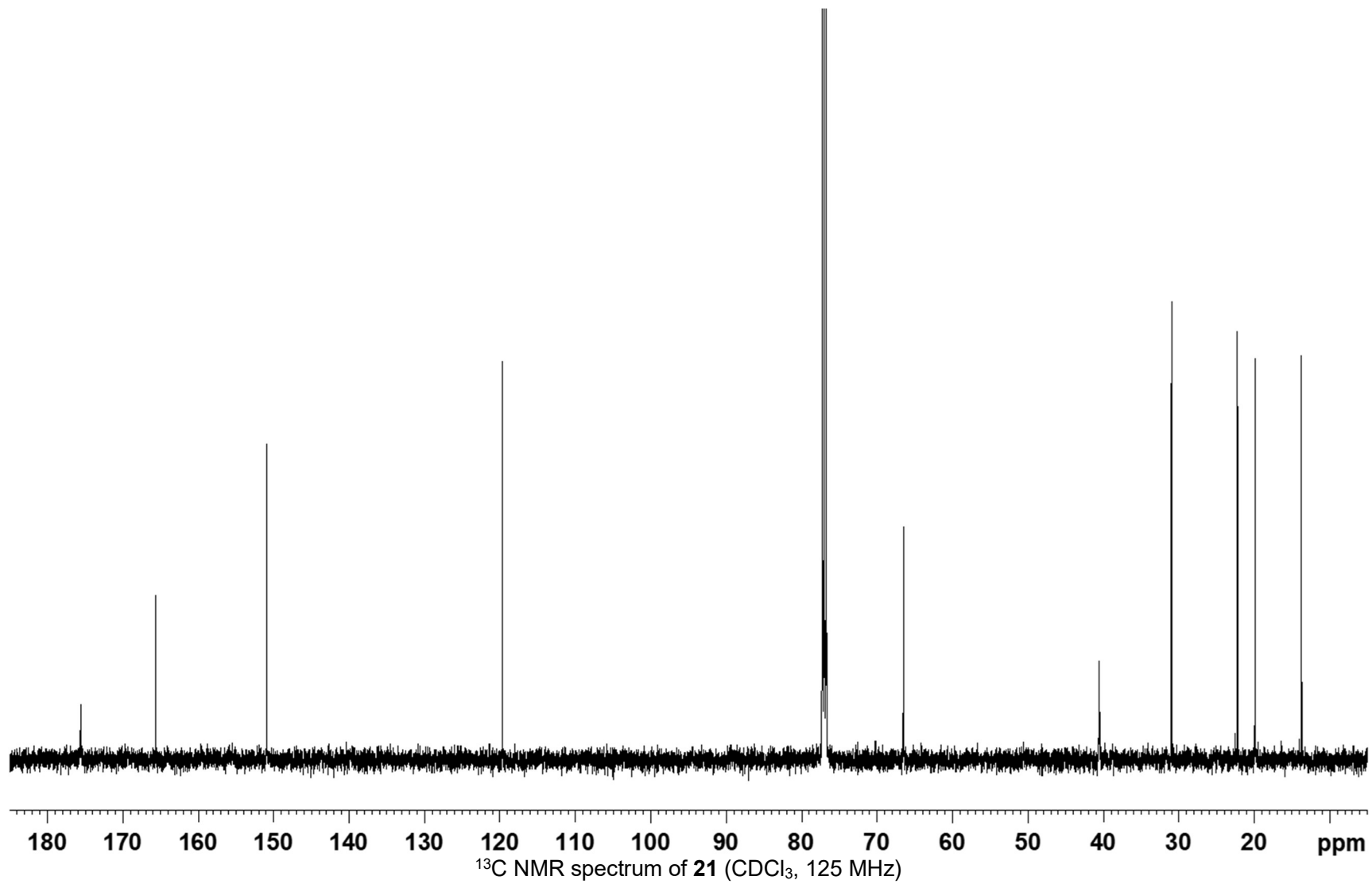


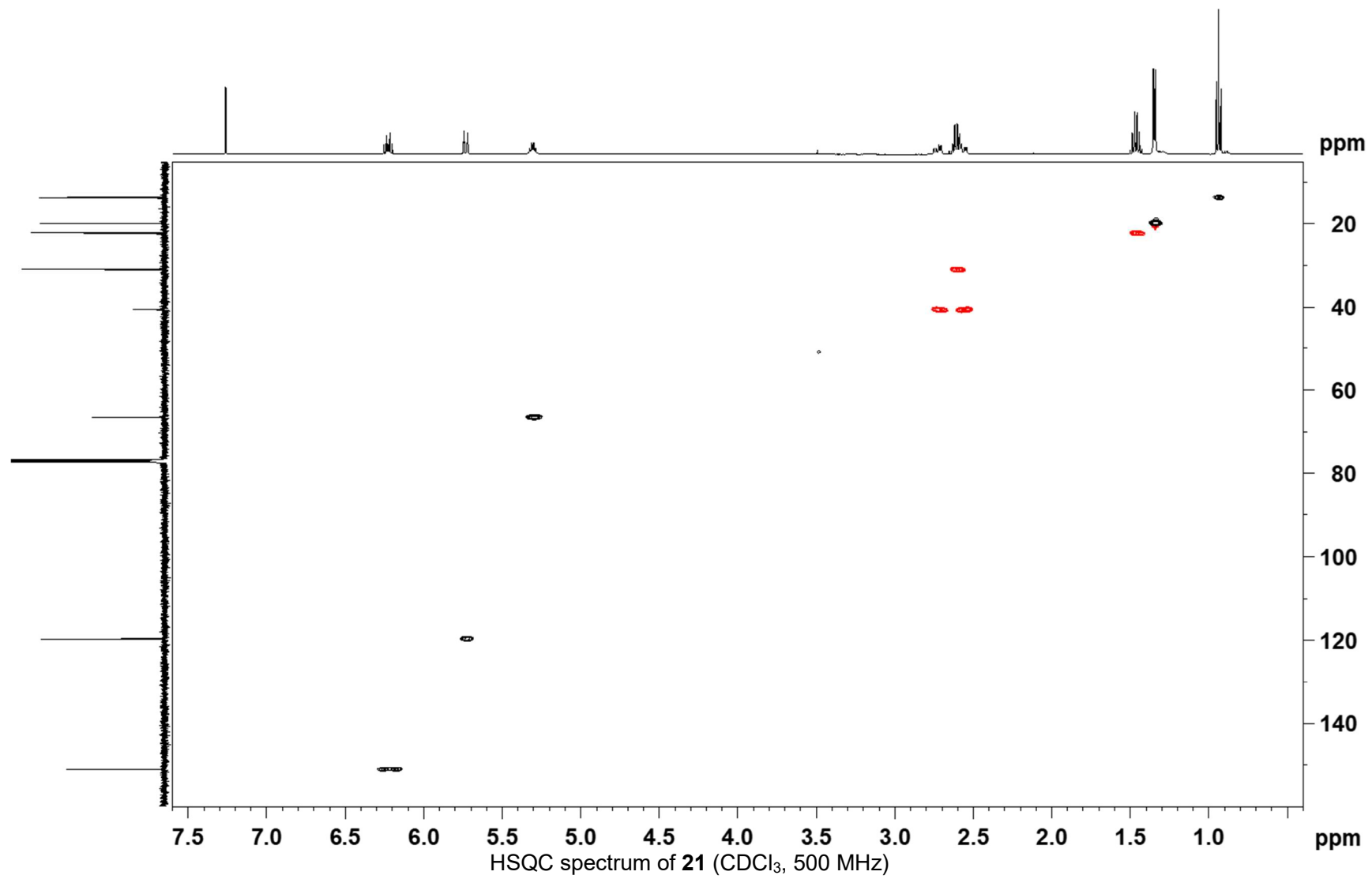
UV spectrum of **21**

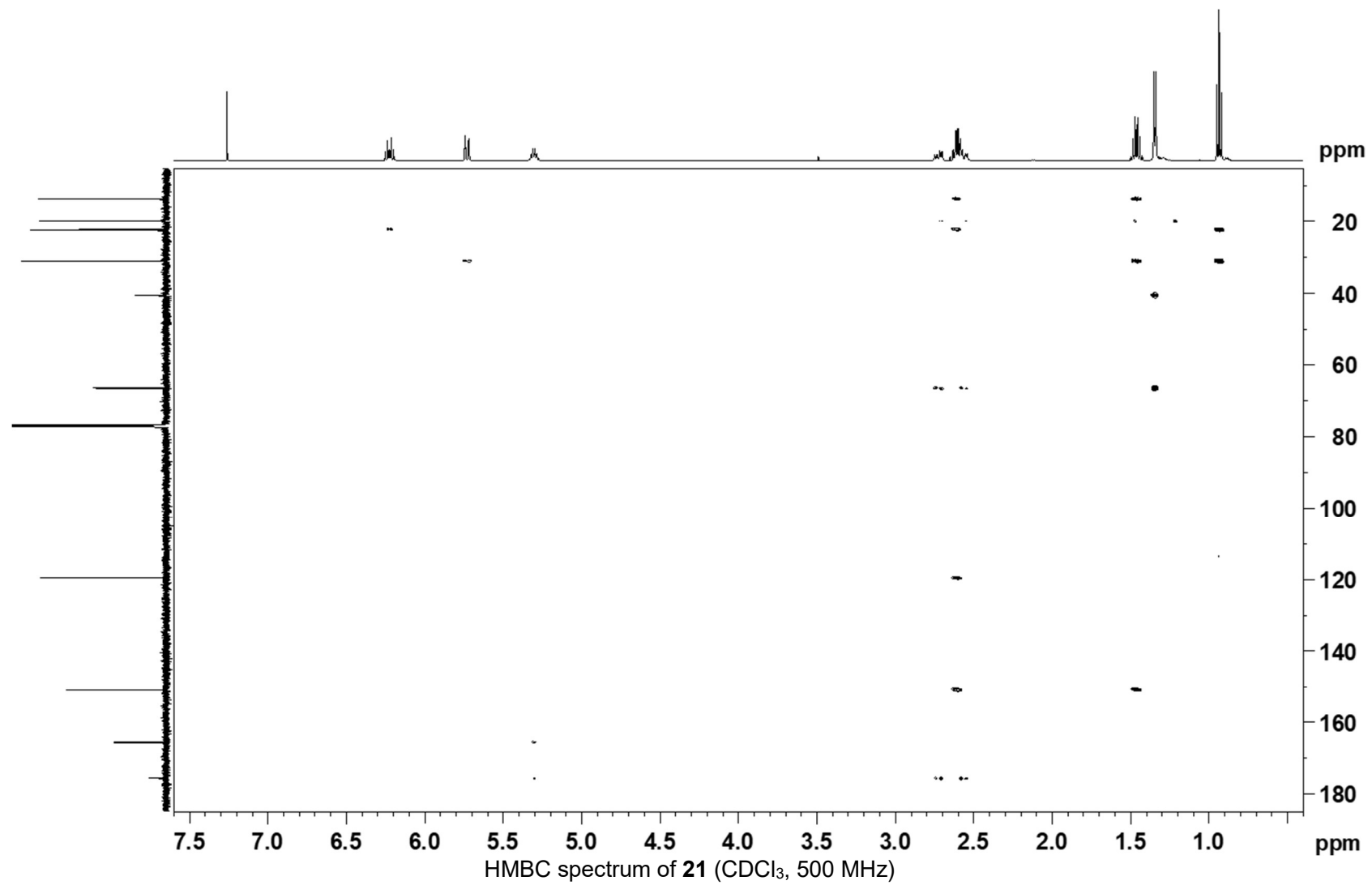


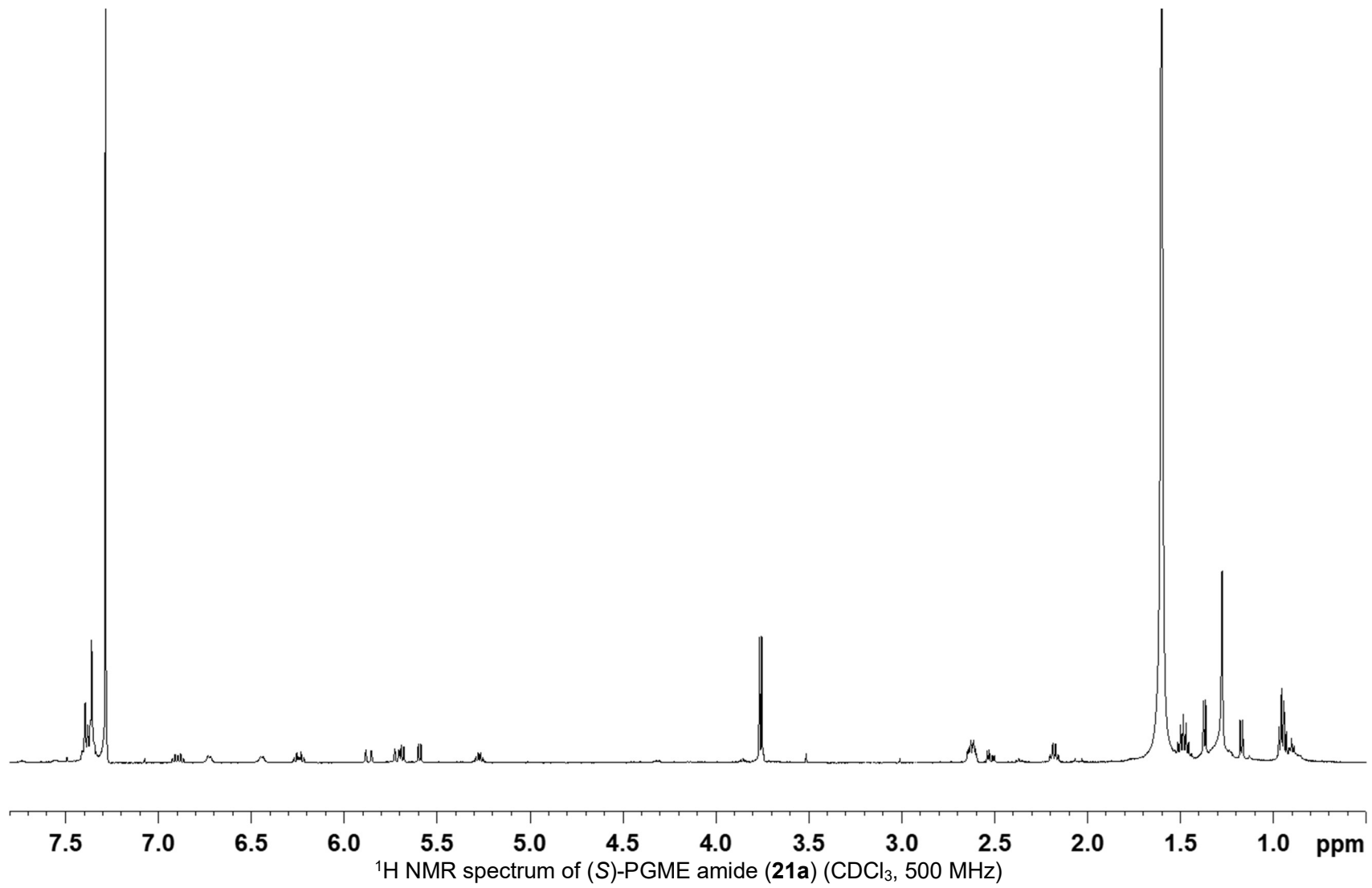
IR spectrum of **21**

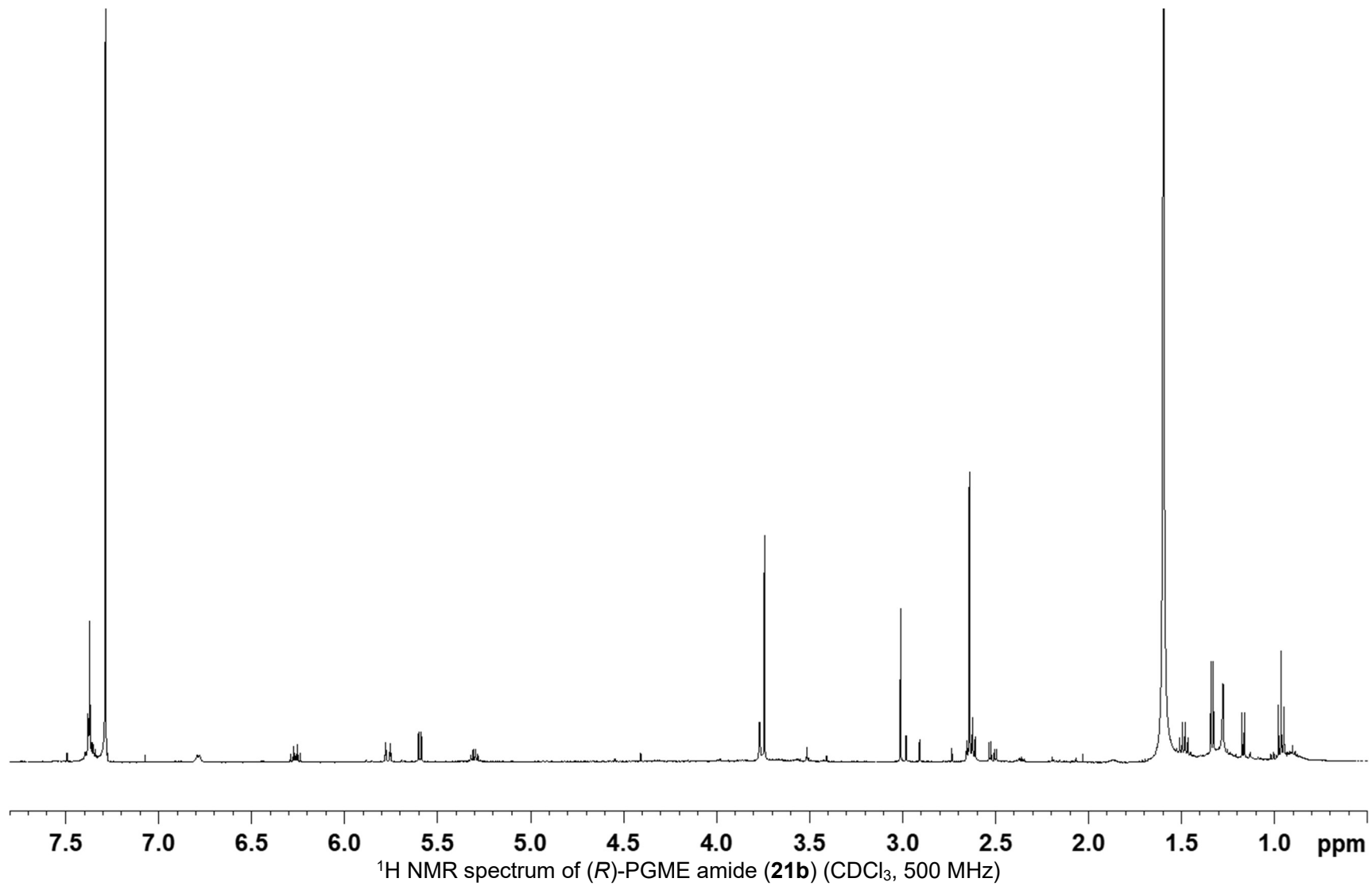


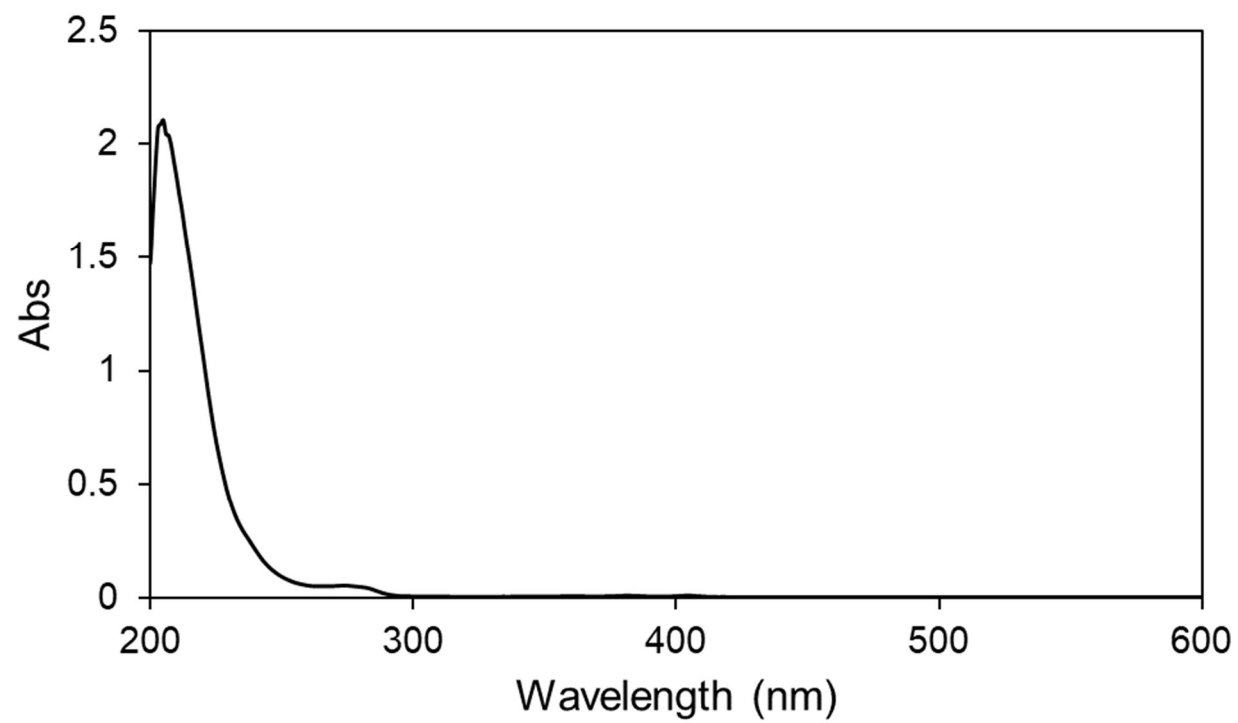




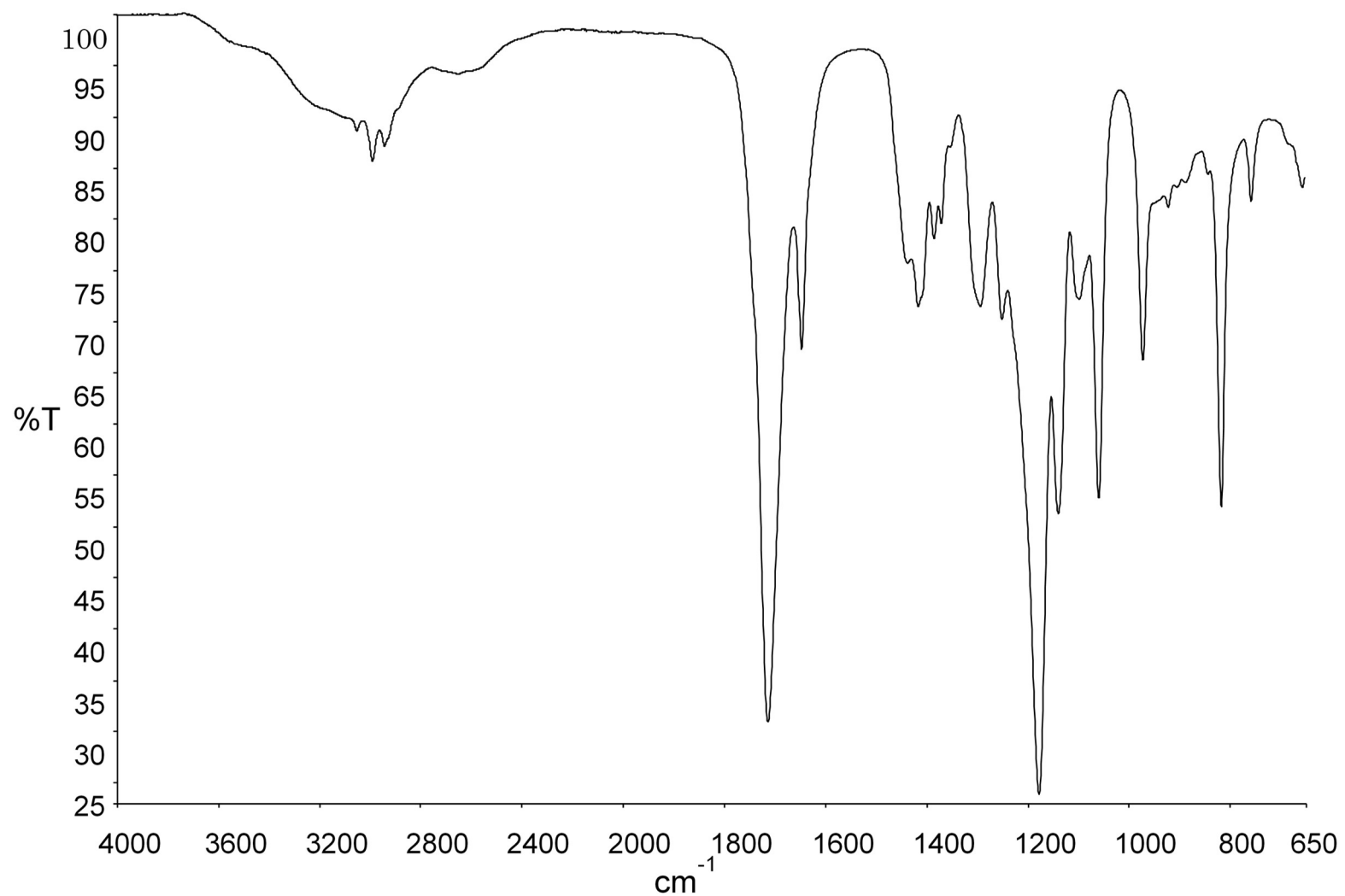




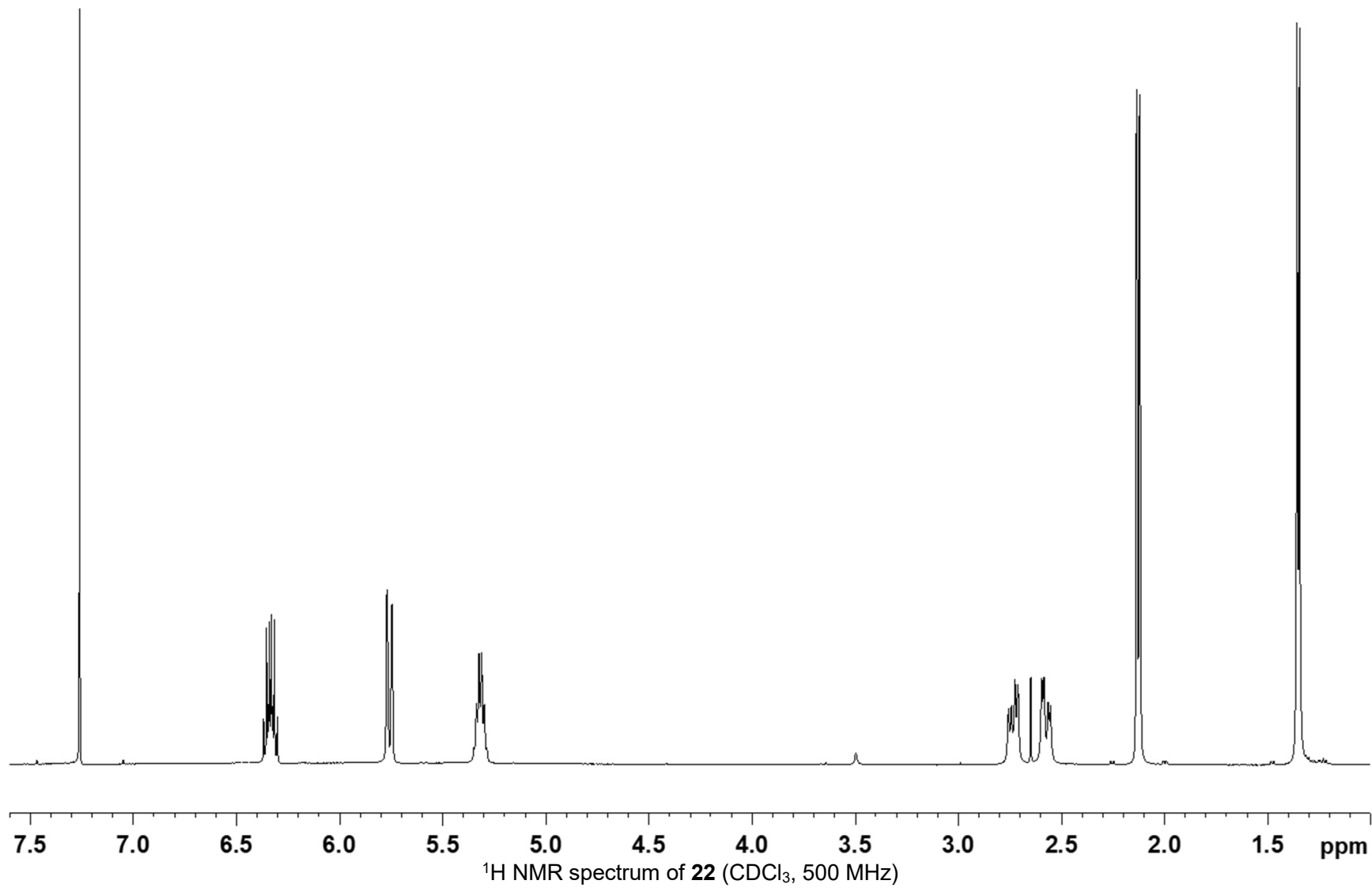


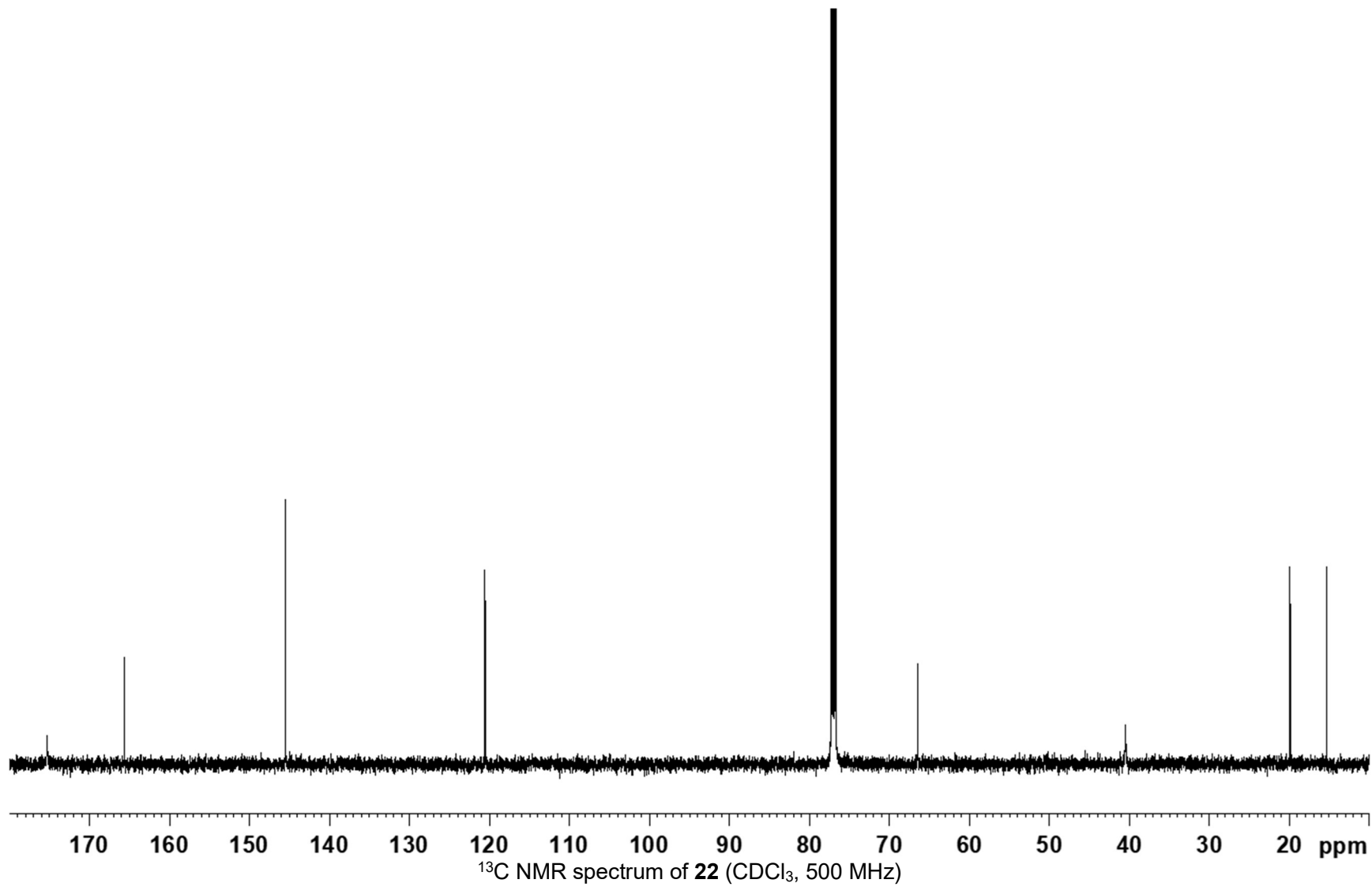


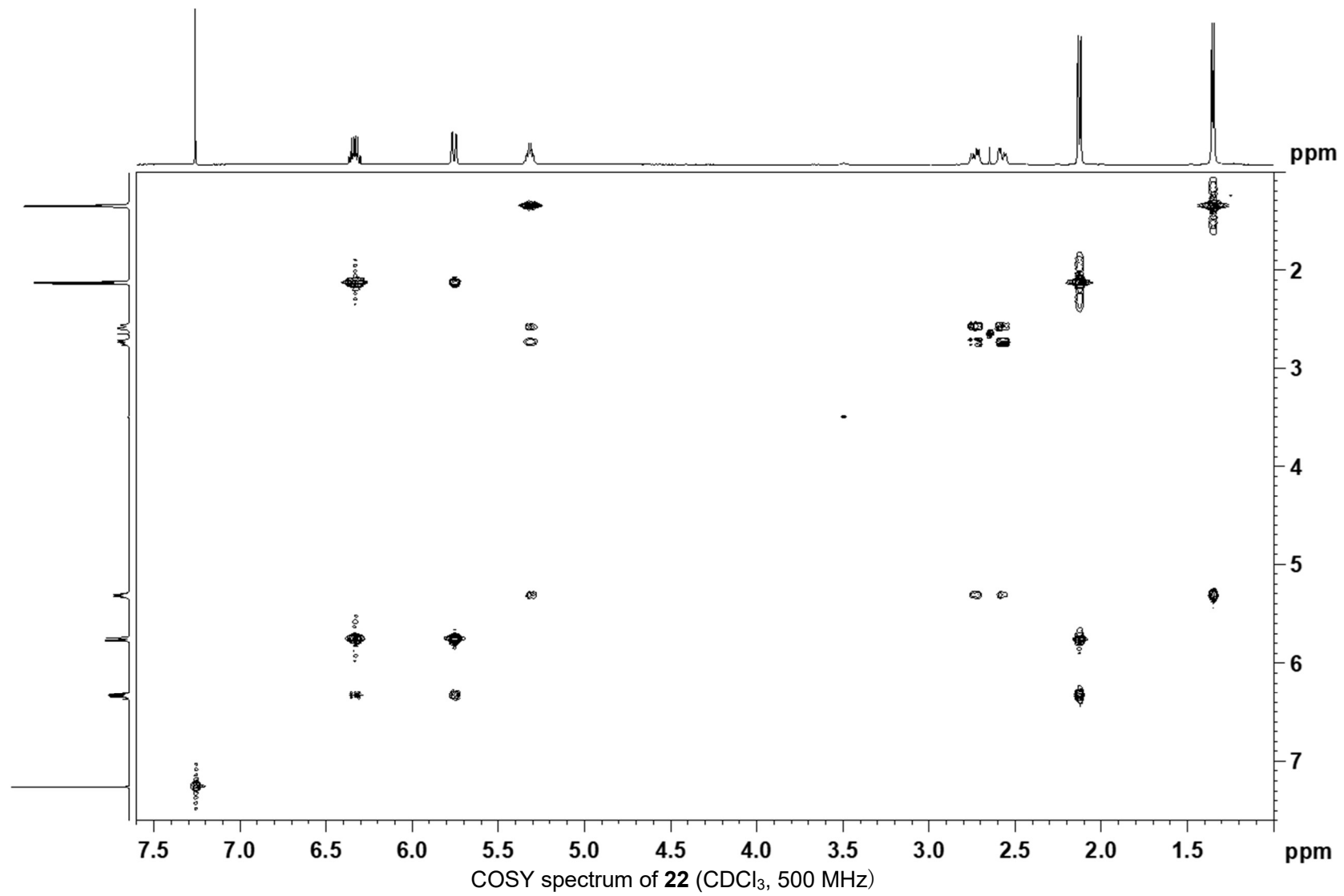
UV spectrum of **22**

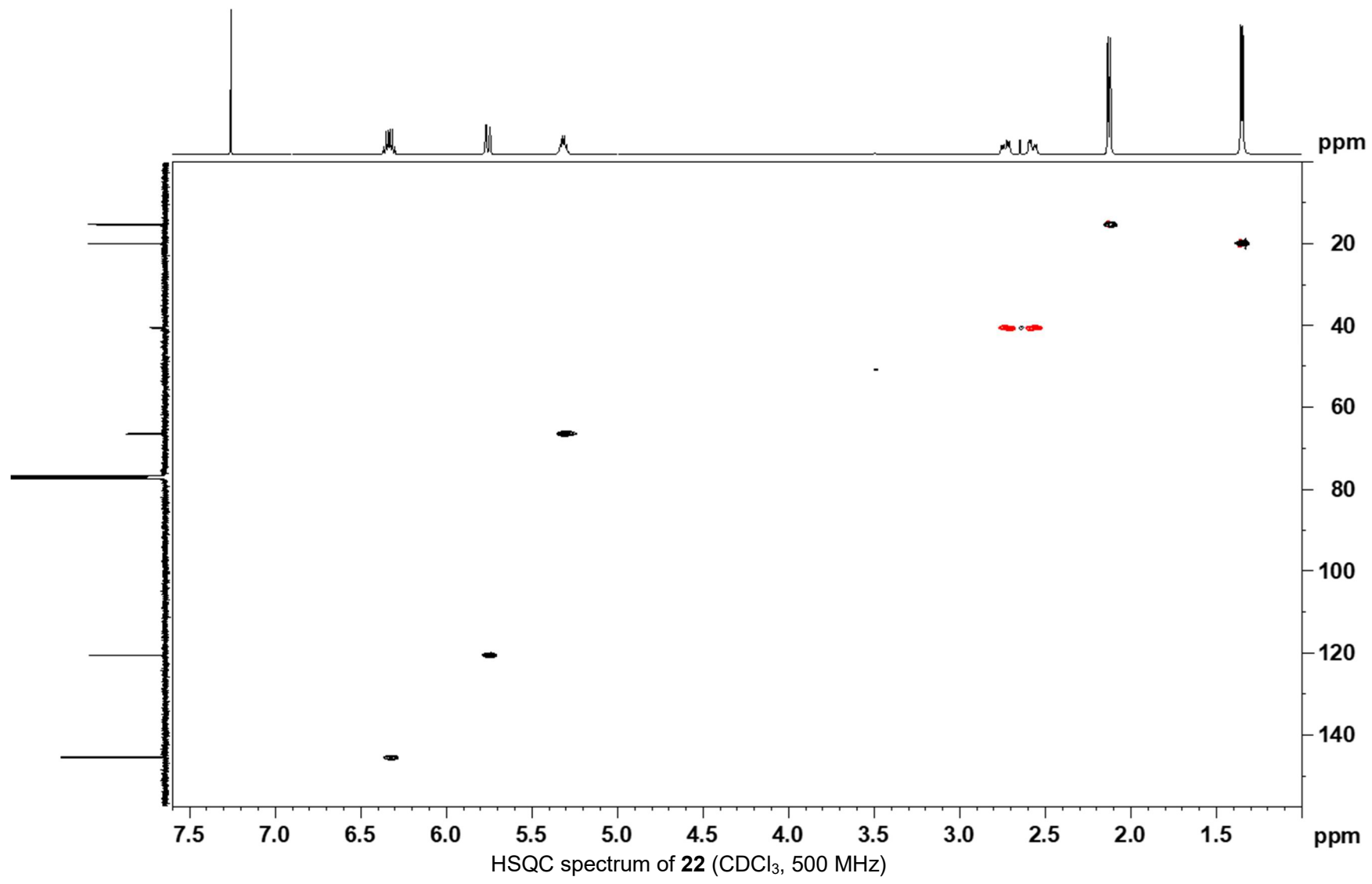


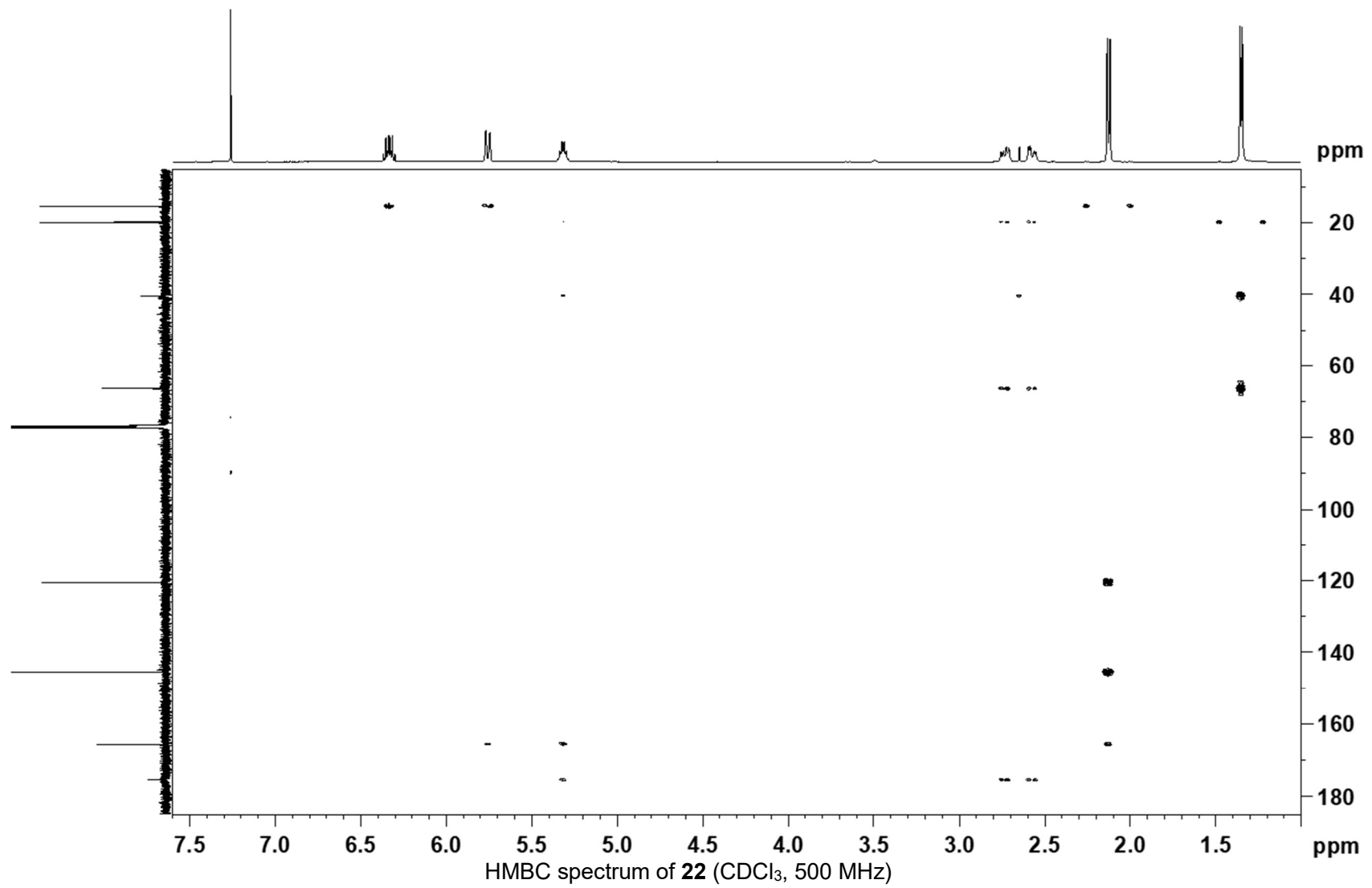
UV spectrum of **22**

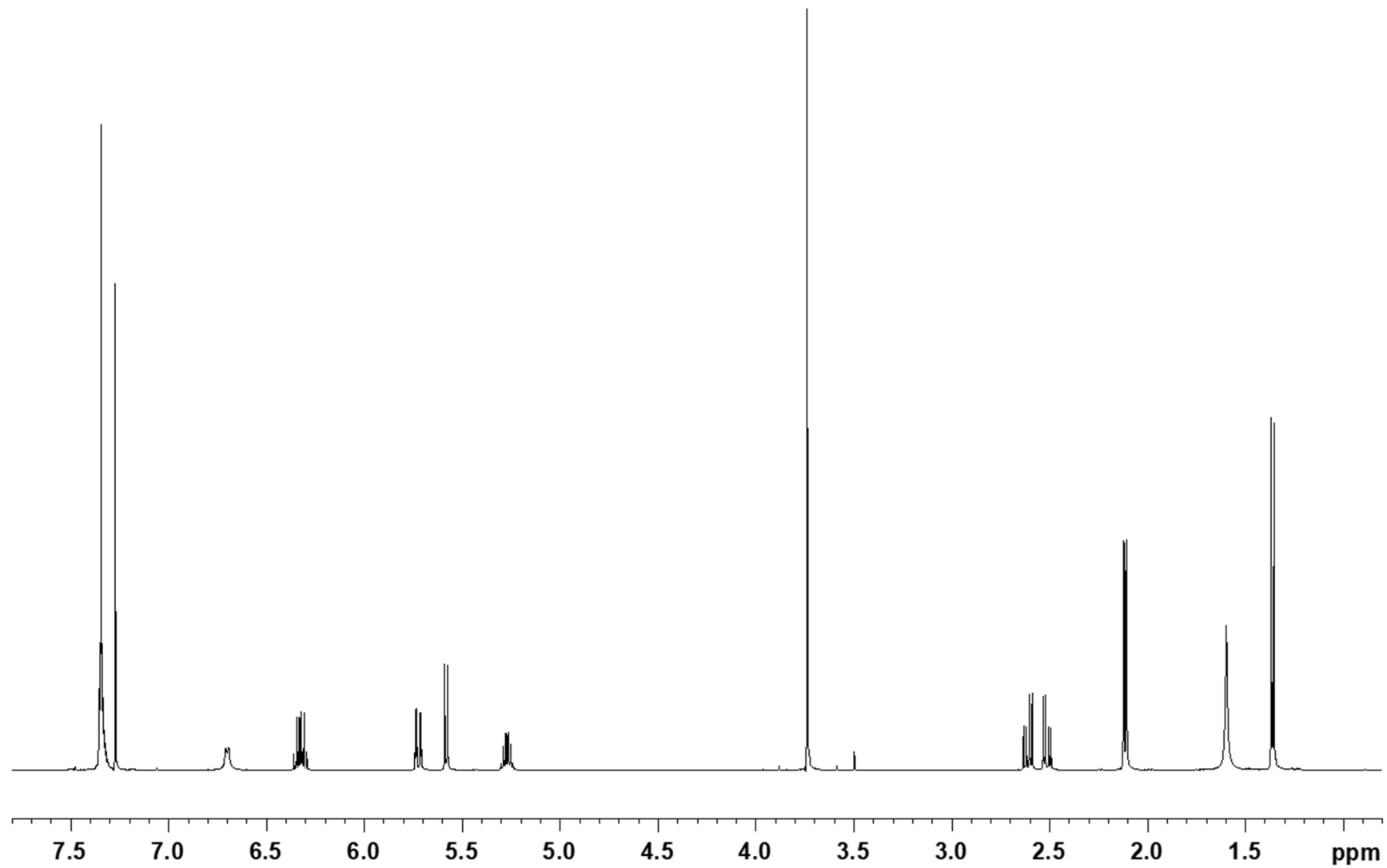


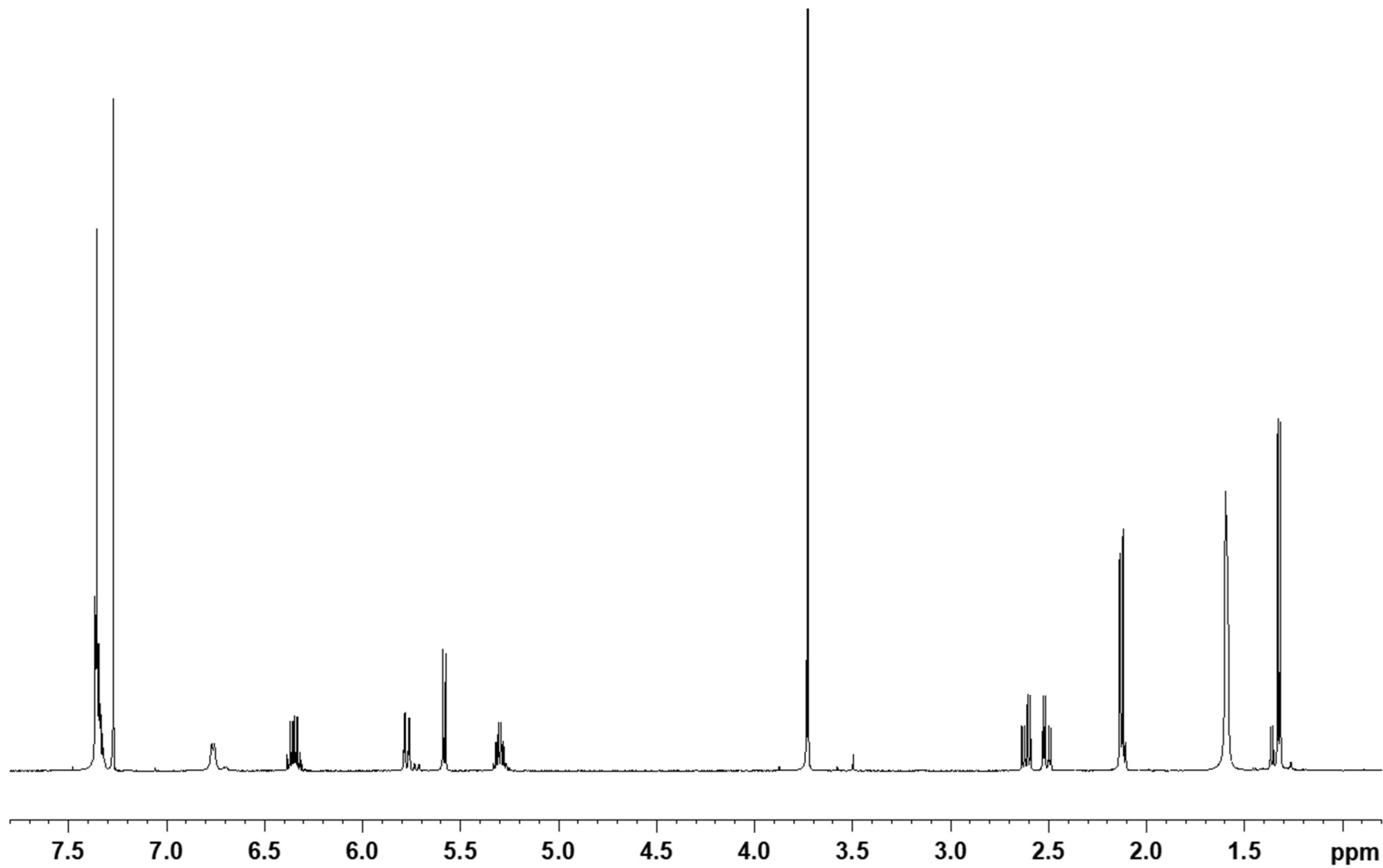












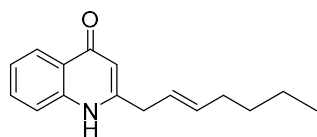
CHAPTER 5

Conclusion

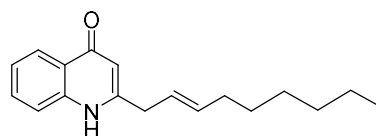
Actually, many bacterial in pathogenic lineages developed unique machineries to detect and approach host organisms, interconvert their life forms between free-living and infectious phases, disable host immune system for successful infection, and ward off competitors to monopolize host nutrients. These machineries are often regulated by small signaling molecules, as exemplified by autoinducer 2 from *Escherichia coli*, *N*-3-oxo-C₁₂-homoserine lactone and 2-heptyl-3-hydroxy-4-quinolone from *Pseudomonas aeruginosa*. These facts indicate that pathogenic (symbiotic) bacteria are prolific producer of metabolites, and the potentially can substitute for those previously exploited species.

The aim of this dissertation is to validate the prospect of bacteria in pathogenic lineages as a new source of natural product-based drug discovery through the study of metabolites produced by *Burkholderia* and *Vibrio*, as representatives of these kind of bacteria from terrestrial and marine habitats, respectively. Specifically, three strains, two from *Burkholderia*, isolated from soil samples, and one from *Vibrio*, isolated from a sea anemone, were chosen and subjected to metabolite analysis.

In Chapter 2, the first strain, *Burkholderia* sp. MBAF 1239, was chosen for chemical study after an antimicrobial screening of 144 culture broths obtained by fermentation of 38 isolates in 4 different media, which were isolated from the rhizosphere of welsh onion (*Allium fistulosum*) in the experimental field of Mie University. A 16S rRNA gene sequence analysis revealed that strain MBAF 1239 belongs to *Burkholderia cepacia* complex, one of the major clades in the family *Burkholderiaceae* that includes several species pathogenic to plants and human. Because strain MBAF 1239 potently inhibited the growth of *Tenacibacrium maritimum* NBRC16015 (fish skin ulcer bacterial pathogen), and *Rhizopus. oryzae* NBRC4705 (a fungal pathogen of rice seeding blight), the responsible constituents were pursued, which resulted in the isolation of two new antimicrobial 2-alkyl-4-quinolones, (*E*)-2-(hept-2-en-1-yl)quinolin-4(1*H*)-one (**3**) and (*E*)-2-(non-2-en-1-yl)quinolin-4(1*H*)-one (**7**) along with 6 known compounds. Detection of **3** and **7** by LC-MS has previously been reported several times, but not rigorously characterized until this work. All isolated compounds inhibited the growth of *T. maritimum* with different extents. Because *T. maritimum* is one of the major etiologies for fatal skin ulcers in marine fish, all isolated compounds offer novel scaffolds to develop new therapeutic modalities for this economically devastating epizootic.

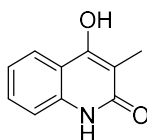


(E)-2-(hept-2-en-1-yl)quinolin-4(1H)-one (3)



(E)-2-(non-2-en-1-yl)quinolin-4(1H)-one (7)

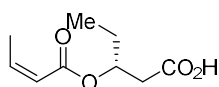
In Chapter 3, *Burkholderia* sp. 3Y-MMP, isolated by an enrichment culture under Zn^{2+} load from the soil of a rice pad in Toyama, was subjected to metabolite analysis. This strain was 99.9% identical to *B. cepacia* based on the 16S rDNA sequence similarity. Fermentation and subsequent extraction, fractionation, and chromatographic separation led to the isolation of 4-hydroxy-3-methyl-2(1H)-quinolone (**9**). Compound **9** is an old synthetic molecule and recently discovered from dyer woad (*Isatis tinctoria*, family *Brassicaceae*) without providing sufficient evidence for this structure. Because another tautomeric structure, 2, 4-dihydroxyquinoline, was also possible, and in fact, several previous publications adopted the latter structure, a careful literature survey on the chemical shifts of the related structures was made. As a result, the chemical shifts of ring junction carbon were found to be useful for structure diagnosis, which supported the quinolone structure for **9**. Based on this diagnostic criterion, structures of two compounds reported by other researchers, proposed to have the 2, 4-dihydroxyquinoline motif, were corrected. Thus, I have for the first time gave the complete NMR assignment on structure **9** and also offered a convenient NMR-based diagnosis to distinguish 4-hydroxy-2-quinolone structure from tautomeric 2, 4-dihydroxyquinoline. Compound **9** was not growth-inhibitory to *T. maritimum*, but was found to extinct hydroxy radical-catalyzed luminol chemoluminescence by 86% at 10 μM , suggesting that **9** works as an antioxidant to counteract reactive oxygen species-based immune response in the cells of plant hosts.



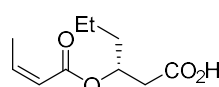
4-hydroxy-3-methyl-2(1H)-quinolone (9)

In Chapter 4, *Vibrio* sp. SI9, isolated from the sea anemone, *Radianthus crispus*,

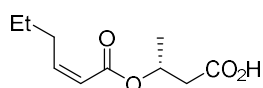
was chosen as the subject of metabolite analysis. This strain was obtained from an aquarium vendor in Nagasaki, Japan, and showed 98.6% identity to *Vibrio nereis* DSM 19584TM. From the fermentation extract of this strain were isolated a series of new acyloxy fatty acids, *O*-isocrotonyl-3-hydroxypentanoic acid (**19**), *O*-isocrotonyl-3-hydroxyhexanoic acid (**20**), and *O*-(*Z*)-2-hexenoyl-3-hydroxybutyric acid (**21**), along with the known *O*-isocrotonyl-3-hydroxybutyric acid (**22**). The planar structures of **19-22** were determined by NMR analysis, and the absolute configuration were determined to be an *R*-configuration by an anisotropy-based chiral analysis. Compounds **19-22** showed weak growth inhibitory activity against *T. maritimum* with MIC values of 25, 50, 50, and 25 µg/mL, respectively. Among marine bacteria, *Vibrio* seems to be the first known as a producer of polyhydroxyalkanoates (PHA), a bacterial storage substance used as bioplastics. The structural similarity between **19-22** and PHA suggests the same biosynthetic origin of these compounds. Moreover, dehydrative modification at the hydroxy-terminus of PHA is implied. Thus, the findings of new compounds **19-21** will offer a clue to alter the property of these promising biomaterials.



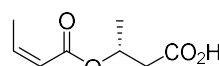
O-isocrotonyl-3-hydroxypentanoic acid (**19**)



O-isocrotonyl-3-hydroxyhexanoic acid (**20**)



O-(*Z*)-2-hexenoyl-3-hydroxybutyric acid (**21**)



O-isocrotonyl-3-hydroxybutyric acid (**22**)

In summary, as part of work to exploit new drug discovery resource from microbes in the Laboratory of Microbial Engineering at Toyama Prefectural University, three bacterial strains in two pathogenic lineages, the genera *Burkholderia* (class *Betaproteobacteria*) and *Vibrio* (class *Gammaproteobacteria*), were chemically examined. Chromatographic separation of fermented products and NMR-based structure analysis resulted in the discovery of six new bioactive compounds, including two antimicrobial 2-alkylquinolones **3** and **7** and hydroxylated quinolone **9** with the antioxidant activity from *Burkholderia* spp. isolated from soil samples, and three new antibacterial compounds **19-21** and a related known metabolite **22** from *Vibrio* sp. SI9

obtained from the sea anemone *Radianthus crispus*. These results verify the usefulness of bacteria in pathogenic lineages as a source of new bioactive natural products and warrant further studies toward the development of microbial metabolite-based drugs. The isolation of **1-9** and **19-22** also helps promote mechanistic understanding of the pathogenicity of pathogens.

Acknowledgements

I would like to express my sincere appreciation for my Supervisor Professor Yasuhiro Igarashi, Toyama Prefectural University, for his valuable advice and warm encouragement throughout the course of this work.

I also would like to express my deepest gratitude to Lecturer Naoya Oku, Toyama Prefectural University, for his valuable guidance, supervision and encouragement throughout the course of this work.

In addition, I greatly appreciate Assistant Professor Enjuro Harunari, Toyama Prefectural University, for his warm encouragement and help throughout the course of this work.

And I also greatly appreciate all members of the Laboratory of Microbial Engineering, Biotechnology Center, Toyama Prefectural University.

Acknowledgements are also made to co-authors: Associate Professor Masafumi Shimizu at Gifu University for providing MBAF 1239 and other rhizobacterial isolates, Associate Professor Yukiko Shinozaki at National Institute of Technology, Toyama College for isolation of *Burkholderia* sp. 3Y-MMP, Lecturer Yoichi Kurokawa at Fukui Prefectural University for testing with luminol chemiluminescence extinction assay, Ms. Atsumi Hasada of this laboratory for broth screening of *Burkholderia* strains and Dr. Tao Zhou for experimental help.

Finally, I am grateful to my parents and my family members for their inspiration, support, and patience.

Publication List

1. Two new 2-alkylquinolones, inhibitory to a fish skin ulcer pathogen *Tenacibaculum maritimum*, produced by a rhizobacterium of the genus *Burkholderia* sp.

Dandan Li, Naoya Oku, Atsumi Hasada, Masafumi Shimizu, and Yasuhiro Igarashi

Beilstein Journal of Organic Chemistry **2018**, *14*, 1446-1451.

2. 4-Hydroxy-3-methyl-2 (1*H*)-quinolone, originally discovered from a *Brassicaceae* plant, produced by a soil bacterium of the genus *Burkholderia* sp.: determination of a preferred tautomer and antioxidant activity

Dandan Li, Naoya Oku, Yukiko Shinozaki, Yoichi Kurokawa, and Yasuhiro Igarashi

Beilstein Journal of Organic Chemistry **2020**, *16*, 1489-1494.

3. Three new *O*-isocrotonyl-3-hydroxybutyric acid congeners produced by a sea anemone-derived marine bacterium of the genus *Vibrio*

Dandan Li, Enjuro Harunari, Tao Zhou, Naoya Oku, and Yasuhiro Igarashi

Beilstein Journal of Organic Chemistry **2020**, *16*, 1869-1874.